Advances in Computational Mathematics (2023) 49:30
https://doi.org/10.1007/s10444-023-10028-0

An extrapolated Crank-Nicolson virtual element scheme for the nematic liquid crystal flows

Guang-an Zou[1,2] · Xuyang Wang[1] · Jian Li[3]

Received: 16 September 2022 / Accepted: 14 March 2023 / Published online: 11 May 2023

Abstract
In this paper, we consider the numerical approximations of the Ericksen-Leslie system for nematic liquid crystal flows, which can be used to describe the dynamics of low molar-mass nematic liquid crystal in certain materials. The main numerical challenge to solve this system lies in how to discretize nonlinear terms so that the energy stability can be held at the discrete level. This paper address this numerical problem by constructing a fully discrete virtual element scheme with second-order temporal accuracy, which is achieved by combining the extrapolated Crank-Nicolson (C-N) time-stepping scheme for the nonlinear coupling terms and the convex splitting method for the Ginzburg-Landau term. The unconditional energy stability and unique solvability of the fully discrete scheme are rigorously proved, we further prove the optimal error estimates of the developed scheme. Finally, some numerical experiments are presented to demonstrate the accuracy, energy stability, and performance of the proposed numerical scheme.

Keywords Nematic liquid crystal flows · Virtual element method · Crank-Nicolson scheme · Unconditional energy stability · Error estimates

Mathematics Subject Classification (2010) 35Q35 · 65M12 · 65M15 · 65M60

Communicated by: Long Chen

✉ Guang-an Zou
zouguangan@henu.edu.cn

✉ Jian Li
jiaaanli@gmail.com

1 School of Mathematics and Statistics, Henan University, Kaifeng 475004, People's Republic of China

2 Henan Engineering Research Center for Artificial Intelligence Theory and Algorithms, Henan University, Kaifeng 475004, People's Republic of China

3 School of Mathematics and Data Science, Shaanxi University of Science and Technology, Xi'an 710021, People's Republic of China

1 Introduction

Liquid crystals are substances, which exhibit a phase of matter that has properties between a conventional liquid and a solid crystal. For instance, a liquid crystal may flow like a liquid, but has the molecules in the liquid arranged or oriented in a crystal-like way. One of the simplest liquid crystal phases is called the nematic phase. It is characterized by a high degree of long range orientational order but no translational order. Molecules in a nematic phase spontaneously order with their (for calamitic molecules) long axes roughly parallel. Readers can refer to [37] for a review on dynamic phenomena in liquid crystal materials.

To describe the liquid crystal flows we need not only the orientation, as represented by the director field $\boldsymbol{d}$, but also a macroscopic motion, represented by the velocity field $\boldsymbol{u}$. Ericksen and Leslie derived a hydrodynamic model for nematic liquid crystals [23, 24, 37]. To understand the Ericksen-Leslie theory from the analysis point of view, Lin [26] proposed a simplified system which retained most mathematical and physical significance of the original model for liquid crystal flows. The Ericksen-Leslie system also emphasized the special coupling between the director and the flow field. We refer to [18, 24, 26, 28] and the references therein for the derivation of the above system and further physical background on the continuum theory of liquid crystals. In addition to the well-known barriers for analyzing the Navier–Stokes equations, the non-convex side constraint $|\boldsymbol{d}| = 1$ causes further difficulties (see [15]) for both analytically and numerically, and is a main source for possible formation of defects of the system at finite times. Hence, a widely used approach is to approximate the constraint $|\boldsymbol{d}| = 1$ by a penalty function such as the Ginzburg-Landau approximation.

Considering the boundary condition for the director vector $\boldsymbol{d}$ to be time-independent and for any fixed ε, Lin and Liu [27] proved the global existence of weak solution and local existence of classical solution for the regularized Ericksen-Leslie system. The numerical studies for the regularized Ericksen-Leslie system were firstly proposed by Liu and Walkington [30, 31], but the uniform discrete energy law is not available for the numerical solutions. In [29], Lin and Liu presented two linear finite element schemes, the first was using a backward Euler approximation in time and the second using a characteristic method, but the discrete energy law and error estimates of these schemes are not proved. In [5], the authors proposed two fully discrete finite element methods, the first scheme for the regularized Ericksen-Leslie system was unconditionally stable and convergent to the original problem, and the second scheme based on direct discretization for the original problem was conditionally stable, however, the convergence orders of numerical scheme are missing. In [21], Guillén-González and Gutiérrez-Santacreu investigated a fully discrete mixed scheme based on continuous finite elements, but the error estimate for the pressure is not given. In [32, 45–47], the authors developed the linear, first-order or second-order energy stable numerical schemes for the nematic liquid crystal flows, but the algorithms only consider the time semi-discrete version assuming continuous space.

The main purpose of this paper is to develop and analyze a fully discrete virtual element scheme for the regularized Ericksen-Leslie system. As a generalization of the standard finite element method that allows for general polytopal meshes, the virtual element method (VEM) was first proposed and analyzed in [6]. The VEM has some advantages over the standard finite element method. For example, it can handle general polygons (including non-convex elements, very distorted elements and curved elements [14]) and build the high-order methods without complex integration. In addition, by using the degrees of freedom and the construction of some operators involved in the discretization of the problem, the VEM not only avoids an explicit expression of a local basis function, but also introduces a non-polynomial virtual element discrete space that includes (but is not limited to) standard polynomials. These characteristics of the VEM guarantee its accuracy and efficiency. Until now, there have developed many conforming and nonconforming VEMs for the parabolic problems [1, 35, 41], second-order elliptic problems [2, 6, 10, 17], linear and nonlinear elasticity problems [7, 9, 19], the Stokes [16, 33] and Navier–Stokes equations [13, 20, 34, 36], and so on. In short, the main advantages of VEM include an extension of the classical finite element method (FEM) to general polygonal and polyhedral meshes, and also as a generalization of the mimetic finite difference method to arbitrary degrees of accuracy and arbitrary continuity properties. We also mention that, compared with the standard FEM for the nematic liquid crystal flows, the VEM can help us achieve higher order approximations to gain better accuracy for the orientation vector $\boldsymbol{d}$, which can be confirmed by the numerical examples.

However, to our best knowledge, how to use the VEM for solving the hydrodynamic model of nematic liquid crystal flows has not been resolved successfully, this is by no means an easy task due to the highly nonlinear terms and the couplings among the velocity, pressure and orientation vector of liquid crystals. The main contribution of this paper is to develop an extrapolated Crank-Nicolson virtual element scheme with second-order temporal accuracy for the nematic liquid crystal flows. Furthermore, we rigorously prove the unconditional energy stability, unique solvability and optimal error estimates for the proposed scheme, especially for the pressure. Through a set of benchmarking simulations, we further demonstrate the stability, accuracy and effectiveness of the proposed schemes thereafter.

The rest of paper is organized as follows. In the next section, we establish the hydrodynamics system for the nematic liquid crystal flows, and derive the unconditional energy stability in the continuous level. In Section 3, we propose a fully discrete virtual element scheme and derive some properties of the numerical scheme, i.e., the unique solvability, and the discrete energy law. In Section 4, we rigorously prove the optimal error estimates for the proposed scheme. In Section 5, we perform some numerical simulations to show the accuracy and efficiency of the developed scheme. Section 6 provides some concluding remarks.

2 Preliminaries

2.1 The model system

We use $\mathcal{E}$ to denote the sum of the kinetic and Helmholtz free energy, which is described by

$$\mathcal{E} = E_{kin} + E, \tag{2.1}$$

where E_{kin} is the kinetic energy and E is the free energy, respectively, given by

$$E_{kin} = \int_{\Omega} \frac{1}{2}|\boldsymbol{u}|^2 d\boldsymbol{x}, \;\; E = \int_{\Omega} \boldsymbol{f}_{\text{elast}}(\boldsymbol{d}) d\boldsymbol{x}, \tag{2.2}$$

where $\boldsymbol{u} : \Omega_T \to \mathbb{R}^2$ is the incompressible velocity field and $\boldsymbol{d} : \Omega_T \to \mathbb{R}^2$ is the orientation vector of liquid crystal molecules, where $\Omega_T = \Omega \times (0, T)$, Ω is a bounded open subset of $\mathbb{R}^2$ with boundary $\partial\Omega$ and $T > 0$ is the final time. The energy density $\boldsymbol{f}_{\text{elast}}(\boldsymbol{d})$ is given by

$$\boldsymbol{f}_{\text{elast}}(\boldsymbol{d}) = \frac{\lambda_1}{2}(\nabla \cdot \boldsymbol{d})^2 + \frac{\lambda_2}{2}[\boldsymbol{d} \cdot (\nabla \times \boldsymbol{d})]^2 + \frac{\lambda_3}{2}[\boldsymbol{d} \times (\nabla \times \boldsymbol{d})]^2, \tag{2.3}$$

where λ_1, λ_2 and λ_3 are the Frank elastic constants describing splay, twist and bend deformation, respectively. For simplicity, under the assumption that the Frank elastic constants $\lambda_1 = \lambda_2 = \lambda_3 = \lambda$, and the bulk liquid crystal energy has the form of the Ginzburg-Landau energy for $\boldsymbol{d}$, the potential term in the energy penalizes for deviations of $|\boldsymbol{d}|$ from some constant value and replaces the hard length constraint of the Oseen-Frank theory [43]. Then, the "regularized" bulk energy density of the liquid crystal can be written as

$$\boldsymbol{f}_{\text{elast}}(\boldsymbol{d}) = \frac{\lambda}{2}|\nabla \boldsymbol{d}|^2 + \frac{1}{\varepsilon^2}\boldsymbol{F}(\boldsymbol{d}), \tag{2.4}$$

in which $\lambda > 0$ is the elastic constant, and $\frac{1}{\varepsilon^2}\boldsymbol{F}(\boldsymbol{d})$ is a penalty term of the Ginzburg-Landau energy, where ε is a penalization parameter, $\boldsymbol{f}(\boldsymbol{d}) = \nabla_{\boldsymbol{d}} \boldsymbol{F}(\boldsymbol{d})$ for $\boldsymbol{F}(\boldsymbol{d}) = \frac{1}{4}(|\boldsymbol{d}|^2 - 1)^2$ (see [15, 26, 27]).

By using the L^2-gradient flow approach for the director field $\boldsymbol{d}$, and the incompressible Navier–Stokes equation for the fluid momentum, the hydrodynamics system of the nematic liquid crystal flows is governed by:

$$\boldsymbol{d}_t + \boldsymbol{u} \cdot \nabla \boldsymbol{d} + \gamma \boldsymbol{\omega} = \boldsymbol{0}, \quad \text{in } \Omega_T, \tag{2.5a}$$

$$\boldsymbol{\omega} = -\lambda \Delta \boldsymbol{d} + \tfrac{1}{\varepsilon^2}\boldsymbol{f}(\boldsymbol{d}), \quad \text{in } \Omega_T, \tag{2.5b}$$

$$\boldsymbol{u}_t + (\boldsymbol{u} \cdot \nabla)\boldsymbol{u} - \nu \Delta \boldsymbol{u} + \nabla p - (\nabla \boldsymbol{d})^T \boldsymbol{\omega} = \boldsymbol{0}, \quad \text{in } \Omega_T, \tag{2.5c}$$

$$\nabla \cdot \boldsymbol{u} = 0, \quad \text{in } \Omega_T, \tag{2.5d}$$

where $p : \Omega_T \to \mathbb{R}$ is the pressure, $\boldsymbol{\omega}$ is the chemical potential derived by the variational derivative of the total free energy, $\gamma > 0$ is the mobility constant and $\nu > 0$ is the fluid viscosity.

The above system (2.5a) should be completed by an appropriate initial and boundary condition. For the sake of simplicity, we consider the following initial and boundary conditions:

$$\boldsymbol{d}(\boldsymbol{x}, 0) = \boldsymbol{d}_0(\boldsymbol{x}), \;\; \boldsymbol{u}(\boldsymbol{x}, 0) = \boldsymbol{u}_0(\boldsymbol{x}), \;\; \boldsymbol{x} \in \Omega, \tag{2.6}$$

$$\boldsymbol{d}(\boldsymbol{x},t)=\boldsymbol{0},\ \boldsymbol{u}(\boldsymbol{x},t)=\boldsymbol{0} \text{ on } (\boldsymbol{x},t)\in\partial\Omega\times(0,T), \tag{2.7}$$

where $\boldsymbol{d}_0:\Omega\to\mathbb{R}^2$ and $\boldsymbol{u}_0:\Omega\to\mathbb{R}^2$ are given functions.

2.2 Weak formulation

For $0\le s\le\infty$, $1\le p\le\infty$, we denote by $W^{s,p}(\mathcal{D})$ and $L^p(\mathcal{D})$ the usual Sobolev spaces and Lebesgue spaces on a bound domain $\mathcal{D}$, equipped with the norms $\|\cdot\|_{W^{s,p}(\mathcal{D})}$ and $\|\cdot\|_{L^p(\mathcal{D})}$, respectively. Let $H^s(\mathcal{D})$ represent $W^{s,2}(\mathcal{D})$ (where $H^0(\mathcal{D})$ represents $L^2(\mathcal{D})$), and we define the inner $(\cdot,\cdot)_{s,\mathcal{D}}$ equipped with the norm $\|\cdot\|_{s,\mathcal{D}}$ and seminorm $|\cdot|_{s,\mathcal{D}}$. Especially, if $\mathcal{D}=\Omega$, we denote the L^2 inner product $(\cdot,\cdot)_{0,\Omega}$ by $(\cdot,\cdot)$, while the norm $\|\cdot\|_{s,\Omega}$ and the seminorm $|\cdot|_{s,\Omega}$ are denoted by $\|\cdot\|_s$ and $|\cdot|_s$, respectively. Boldfaced letters will be related to vector spaces, for instance, $\boldsymbol{L}^p$ denotes a vectorial L^p space.

Now, we will introduce the function spaces

$$\begin{aligned}\boldsymbol{X}&:=\boldsymbol{H}_0^1(\Omega),\ \boldsymbol{Y}:=\boldsymbol{L}^2(\Omega),\ \boldsymbol{V}:=\{\boldsymbol{v}\in\boldsymbol{H}_0^1(\Omega):\nabla\cdot\boldsymbol{v}=0\},\\ Q&:=L_0^2(\Omega)=\left\{q\in L^2(\Omega):\int_\Omega q dx=0\right\}.\end{aligned}$$

And we consider the linear forms:

$$\begin{aligned}\mathcal{M}_1(\boldsymbol{\varphi},\boldsymbol{\psi})&:=\sum_{K\in\mathcal{I}_h}\mathcal{M}_1^K(\boldsymbol{\varphi},\boldsymbol{\psi}),\ \forall\boldsymbol{\varphi},\boldsymbol{\psi}\in\boldsymbol{X};\\ \mathcal{M}_2(\boldsymbol{u},\boldsymbol{v})&:=\sum_{K\in\mathcal{I}_h}\mathcal{M}_2^K(\boldsymbol{u},\boldsymbol{v}),\ \forall\boldsymbol{u},\boldsymbol{v}\in\boldsymbol{V};\\ \mathcal{A}_1(\boldsymbol{\varphi},\boldsymbol{\psi})&:=\sum_{K\in\mathcal{I}_h}\mathcal{A}_1^K(\boldsymbol{\varphi},\boldsymbol{\psi}),\ \forall\boldsymbol{\varphi},\boldsymbol{\psi}\in\boldsymbol{X};\\ \mathcal{A}_2(\boldsymbol{u},\boldsymbol{v})&:=\sum_{K\in\mathcal{I}_h}\mathcal{A}_2^K(\boldsymbol{u},\boldsymbol{v}),\ \forall\boldsymbol{u},\boldsymbol{v}\in\boldsymbol{V};\\ \mathcal{B}(\boldsymbol{v},q)&:=\sum_{K\in\mathcal{I}_h}\mathcal{B}^K(\boldsymbol{v},q),\forall\boldsymbol{v}\in\boldsymbol{V},q\in Q;\\ \mathcal{D}(\boldsymbol{v};\boldsymbol{\varphi},\boldsymbol{\psi})&:=\sum_{K\in\mathcal{I}_h}\mathcal{D}^K(\boldsymbol{v};\boldsymbol{\varphi},\boldsymbol{\psi}),\forall\boldsymbol{v}\in\boldsymbol{V},\boldsymbol{\varphi}\in\boldsymbol{X},\boldsymbol{\psi}\in\boldsymbol{Y};\\ \mathcal{C}(\boldsymbol{u};\boldsymbol{v},\boldsymbol{z})&:=\sum_{K\in\mathcal{I}_h}\mathcal{C}^K(\boldsymbol{u};\boldsymbol{v},\boldsymbol{z}),\ \forall\boldsymbol{u},\boldsymbol{v},\boldsymbol{z}\in\boldsymbol{V}.\end{aligned}$$

where the local contributions are given as

$$\begin{aligned}
&\mathcal{M}_1^K(\boldsymbol{\varphi}, \boldsymbol{\psi}) := (\boldsymbol{\varphi}, \boldsymbol{\psi})_{0,K}; \quad \mathcal{M}_2^K(\boldsymbol{u}, \boldsymbol{v}) := (\boldsymbol{u}, \boldsymbol{v})_{0,K};\\
&\mathcal{A}_1^K(\boldsymbol{\varphi}, \boldsymbol{\psi}) := (\nabla\boldsymbol{\varphi}, \nabla\boldsymbol{\psi})_{0,K}; \quad \mathcal{A}_2^K(\boldsymbol{u}, \boldsymbol{v}) := (\nabla\boldsymbol{u}, \nabla\boldsymbol{v})_{0,K};\\
&\mathcal{B}^K(\boldsymbol{v}, q) := (\nabla\cdot\boldsymbol{v}, q)_{0,K}; \quad \mathcal{D}^K(\boldsymbol{v}; \boldsymbol{\varphi}, \boldsymbol{\psi}) := (\boldsymbol{v}\cdot\nabla\boldsymbol{\varphi}, \boldsymbol{\psi})_{0,K};\\
&\mathcal{C}^K(\boldsymbol{u}; \boldsymbol{v}, \boldsymbol{z}) := \frac{1}{2}((\boldsymbol{u}\cdot\nabla)\boldsymbol{v}, \boldsymbol{z})_{0,K} - \frac{1}{2}((\boldsymbol{u}\cdot\nabla)\boldsymbol{z}, \boldsymbol{v})_{0,K}.
\end{aligned}$$

The variational formulation of problem (2.5a) reads as follows: Find $(\boldsymbol{d}, \boldsymbol{\omega}, \boldsymbol{u}, p) \in \boldsymbol{X}\times\boldsymbol{Y}\times\boldsymbol{V}\times Q$, for all $(\boldsymbol{\xi}, \boldsymbol{\theta}, \boldsymbol{v}, q) \in \boldsymbol{X}\times\boldsymbol{Y}\times\boldsymbol{V}\times Q$, for almost all $t \in (0, T)$, there holds

$$\mathcal{M}_1(\boldsymbol{d}_t, \boldsymbol{\theta}) + \mathcal{D}(\boldsymbol{u}; \boldsymbol{d}, \boldsymbol{\theta}) + \gamma\mathcal{M}_1(\boldsymbol{\omega}, \boldsymbol{\theta}) = 0, \tag{2.8a}$$

$$\mathcal{M}_1(\boldsymbol{\omega}, \boldsymbol{\xi}) = \lambda\mathcal{A}_1(\boldsymbol{d}, \boldsymbol{\xi}) + \frac{1}{\varepsilon^2}(\boldsymbol{f}(\boldsymbol{d}), \boldsymbol{\xi}), \tag{2.8b}$$

$$\mathcal{M}_2(\boldsymbol{u}_t, \boldsymbol{v}) + \mathcal{C}(\boldsymbol{u}; \boldsymbol{u}, \boldsymbol{v}) + \nu\mathcal{A}_2(\boldsymbol{u}, \boldsymbol{v}) - \mathcal{B}(\boldsymbol{v}, p) - \mathcal{D}(\boldsymbol{v}; \boldsymbol{d}, \boldsymbol{\omega}) = 0, \tag{2.8c}$$

$$\mathcal{B}(\boldsymbol{u}, q) = 0, \tag{2.8d}$$

where we use the fact $(\boldsymbol{v}\cdot\nabla\boldsymbol{d}, \boldsymbol{\omega})_{0,K} = ((\nabla\boldsymbol{d})^T\boldsymbol{\omega}, \boldsymbol{v})_{0,K}$ (see [21]). We endow (2.9) with initial conditions $\boldsymbol{d}(\cdot, 0) = \boldsymbol{d}_0$ and $\boldsymbol{u}(\cdot, 0) = \boldsymbol{u}_0$. It is straightforward to show that the system (2.8a) admits the law of energy, we state the result as a lemma here.

Lemma 2.1 *Let $(\boldsymbol{d}, \boldsymbol{\omega}, \boldsymbol{u}, p)$ solve (2.8a). Then, the energy law is satisfying*

$$\mathcal{E}(\boldsymbol{u}, \boldsymbol{d}) + \int_0^t (\nu|\boldsymbol{u}|_1^2 + \gamma\|\boldsymbol{\omega}\|_0^2)ds = \mathcal{E}(\boldsymbol{u}_0, \boldsymbol{d}_0),$$

where the energy is defined by

$$\mathcal{E}(\boldsymbol{u}, \boldsymbol{d}) = \frac{1}{2}\|\boldsymbol{u}\|_0^2 + \frac{\lambda}{2}|\boldsymbol{d}|_1^2 + \frac{1}{\varepsilon^2}(\boldsymbol{F}(\boldsymbol{d}), 1).$$

Proof By setting $(\boldsymbol{\theta}, \boldsymbol{\xi}, \boldsymbol{v}, q) = (\boldsymbol{\omega}, \boldsymbol{d}_t, \boldsymbol{u}, p)$ and taking the summation of the four equations in (2.8a), we can easily get

$$\frac{1}{2}\frac{d}{dt}\|\boldsymbol{u}\|_0^2 + \frac{\lambda}{2}\frac{d}{dt}|\boldsymbol{d}|_1^2 + \frac{1}{\varepsilon^2}\frac{d}{dt}(\boldsymbol{F}(\boldsymbol{d}), 1) + \nu|\boldsymbol{u}|_1^2 + \gamma\|\boldsymbol{\omega}\|_0^2 = 0. \tag{2.9}$$

After taking the integration of the above equation (2.9) from 0 to t, the desired result can be obtained. The proof is finished.

3 Fully discrete virtual element scheme

3.1 Virtual element

The purpose of this section is to present the virtual element spaces and discrete bilinear (and trilinear) forms.

3.1.1 Mesh notation and mesh regularity

Let $\{\mathcal{I}_h\}$ be a sequence of decompositions of Ω into polygonal elements K. Furthermore, h_K is the diameter of K, and $h := \max_{K \in \mathcal{I}_h} h_K$. For a given edge $e \in \mathcal{I}_h$, we write h_e for its length. Then, we make the following assumptions on $\mathcal{I}_h$: there exists constants $\rho_0, \rho_1 > 0$ such that for all $K \in \mathcal{I}_h$,

(**S1**) K is star-shaped with respect to a ball of radius $\rho \geq \rho_0 h_K$;

(**S2**) $h_e \geq \rho_1 h_K$ for all $e \in \mathcal{I}_h$.

3.1.2 The construction of virtual element space $\boldsymbol{X}_h$

Using the standard VEM notations, for $k \in \mathbb{N}$, let us define the spaces

- $\mathbb{P}_k(K)$, the set of polynomials of degree at most k on K (especially, $\mathbb{P}_{-1}(K) := \{0\}$).
- $\mathbb{P}_k(e)$, the set of polynomials of degree at most k on e (especially, $\mathbb{P}_{-1}(e) := \{0\}$).
- $\mathbb{B}(\partial K) := \{v \in C^0(\partial K) : v|_e \in \mathbb{P}_k(e) \text{ for all edges } e \in \partial K\}$.
- $\widetilde{\boldsymbol{X}}_{h|K} := \{\boldsymbol{\varphi} \in \boldsymbol{C}^0(K) \cap \boldsymbol{H}^1(K) : \boldsymbol{\varphi}|_{\partial K} \in [\mathbb{B}(\partial K)]^2,\ \Delta\boldsymbol{\varphi} \in [\mathbb{P}_k(K)]^2\}$.

Next, we will introduce the helpful polynomial projections $\boldsymbol{\Pi}_k^{0,K}$ and $\boldsymbol{\Pi}_k^{\nabla,K}$ associated with $K \in \mathcal{I}_h$ as follows:

- The $\boldsymbol{L}^2$-projection $\boldsymbol{\Pi}_k^{0,K} : \boldsymbol{L}^2(K) \to [\mathbb{P}_k(K)]^2$, defined by

$$(\boldsymbol{\Pi}_k^{0,K}\boldsymbol{\varphi}, \boldsymbol{p}_k)_{0,K} = (\boldsymbol{\varphi}, \boldsymbol{p}_k)_{0,K}, \quad \forall \boldsymbol{\varphi} \in \boldsymbol{L}^2(K) \text{ and } \forall \boldsymbol{p}_k \in [\mathbb{P}_k(K)]^2.$$

- The $\boldsymbol{H}^1$-projection $\boldsymbol{\Pi}_k^{\nabla,K} : \boldsymbol{H}^1(K) \to [\mathbb{P}_k(K)]^2$, given by

$$\begin{cases} (\nabla \boldsymbol{\Pi}_k^{\nabla,K}\boldsymbol{\varphi}, \nabla \boldsymbol{p}_k)_{0,K} = (\nabla\boldsymbol{\varphi}, \nabla\boldsymbol{p}_k)_{0,K}, & \forall \boldsymbol{\varphi} \in \boldsymbol{H}^1(K) \text{ and } \forall \boldsymbol{p}_k \in [\mathbb{P}_k(K)]^2, \\ \displaystyle\int_{\partial K} \boldsymbol{\Pi}_k^{\nabla,K}\boldsymbol{\varphi}\, d\boldsymbol{s} = \int_{\partial K} \boldsymbol{\varphi}\, d\boldsymbol{s}. \end{cases}$$

Then, let k be a fixed positive integer and consider the following local virtual element space on each $K \in \mathcal{T}_h$ (see [6])

$$\begin{aligned} \boldsymbol{X}_{h|K} := \{ &\boldsymbol{\varphi} \in \widetilde{\boldsymbol{X}}_{h|K} : (\boldsymbol{\Pi}_k^{\nabla,K}\boldsymbol{\varphi}, \boldsymbol{p}_k)_{0,K} \\ &= (\boldsymbol{\varphi}, \boldsymbol{p}_k)_{0,K}, \ \boldsymbol{p}_k \in [\mathbb{P}_k(K)]^2/[\mathbb{P}_{k-2}(K)]^2 \}, \end{aligned} \tag{3.1}$$

where the symbol $[\mathbb{P}_k(K)]^2/[\mathbb{P}_{k-2}(K)]^2$ denotes the polynomials in $[\mathbb{P}_k(K)]^2$ that are L^2-orthogonal to all polynomials of $[\mathbb{P}_{k-2}(K)]^2$ (observing that $[\mathbb{P}_{k-2}(K)]^2 \subset [\mathbb{P}_k(K)]^2$). And its degrees of freedom are given as follows:

$$\begin{aligned} &\text{I. the values of } \boldsymbol{\varphi} \text{ at the vertices of } K; \\ &\text{II. the values of } \boldsymbol{\varphi} \text{ at } k-1 \text{ uniformly spaced points on each edge } e; \\ &\text{III. the moments } \int_K \boldsymbol{\varphi} \cdot \boldsymbol{p}_{k-2}\, d\boldsymbol{x}, \ \forall \boldsymbol{p}_{k-2} \in [\mathbb{P}_{k-2}(K)]^2. \end{aligned} \tag{3.2}$$

It is noteworthy that $\boldsymbol{\Pi}_k^{0,K}$ and $\boldsymbol{\Pi}_k^{\nabla,K}$ are computable from (3.2) (see [6, 8]). Finally, the global discrete virtual element space can be shown as

$$\boldsymbol{X}_h := \{ \boldsymbol{\varphi} \in \boldsymbol{X} : \boldsymbol{\varphi}|_K \in \boldsymbol{X}_{h|K}, \ \forall K \in \mathcal{T}_h \}. \tag{3.3}$$

Under the assumption (**S1**)-(**S2**), the following estimates can be obtained for the projection and interpolation operators [2, 44].

- For $\forall K \in \mathcal{T}_h$ and $\forall \boldsymbol{\varphi} \in \boldsymbol{H}^{s+1}(K)$ with $s \in \mathbb{N}$, $1 \leq s \leq k$, there holds

$$\|\boldsymbol{\varphi} - \boldsymbol{\Pi}_k^{0,K}\boldsymbol{\varphi}\|_{0,K} + h_K|\boldsymbol{\varphi} - \boldsymbol{\Pi}_k^{0,K}\boldsymbol{\varphi}|_{1,K} \leq C h_K^{s+1}|\boldsymbol{\varphi}|_{s+1,K}. \tag{3.4}$$

- There exists an interpolation $\boldsymbol{\varphi}_I \in \boldsymbol{X}_{h|K}$ such that for $\boldsymbol{\varphi} \in \boldsymbol{H}^{s+1}(K)$ with $1 \leq s \leq k$, there holds

$$\|\boldsymbol{\varphi} - \boldsymbol{\varphi}_I\|_{0,K} + h_K|\boldsymbol{\varphi} - \boldsymbol{\varphi}_I|_{1,K} \leq C h_K^{s+1}|\boldsymbol{\varphi}|_{s+1,K}. \tag{3.5}$$

3.1.3 The construction of virtual element spaces V_h and Q_h

Follow with [12], for $k \geq 2$, let us introduce the spaces

$$\begin{aligned} \mathcal{G}_k(K) &:= \nabla(\mathbb{P}_{k+1}(K)) \subseteq [\mathbb{P}_k(K)]^2, \\ \mathcal{G}_k(K)^{\perp} &:= \boldsymbol{x}^{\perp}[\mathbb{P}_{k-1}(K)] \subseteq [\mathbb{P}_k(K)]^2 \text{ with } \boldsymbol{x}^{\perp} := (x_2, -x_1), \\ \widetilde{\boldsymbol{V}}_{h|K} &:= \Big\{ \boldsymbol{v} \in \boldsymbol{H}^1(K), \ \text{s.t. } \boldsymbol{v}\Big|_{\partial K} \in [\mathbb{B}_k(\partial K)]^2, \\ &\qquad \begin{cases} -\Delta \boldsymbol{v} - \nabla s \in \mathcal{G}_k(K)^{\perp}, \ \text{for some } s \in L^2(K) \\ \operatorname{div}\boldsymbol{v} \in \mathbb{P}_{k-1}(K), \end{cases} \Big\}. \end{aligned}$$

Now we define the virtual element space $\boldsymbol{V}_{h|K}$ as the restriction of $\widetilde{\boldsymbol{V}}_{h|K}$ given by

$$\boldsymbol{V}_{h|K} := \{\boldsymbol{v} \in \widetilde{\boldsymbol{V}}_{h|K} : (\boldsymbol{\Pi}_k^{\nabla,K}\boldsymbol{v}, \boldsymbol{g}_k^{\perp})_{0,K} = (\boldsymbol{v}, \boldsymbol{g}_k^{\perp})_{0,K},\ \boldsymbol{g}_k^{\perp} \in \mathcal{G}_k^{\perp}(K)/\mathcal{G}_{k-2}^{\perp}(K)\}. \tag{3.6}$$

Also, the corresponding unisolvent degrees of freedom in $\boldsymbol{V}_{h|K}$ can be divided into the following four types

$$\begin{aligned}
&\text{(D1). the values of } \boldsymbol{v} \text{ at the vertexes of the polygon } K;\\
&\text{(D2). the values of } \boldsymbol{v} \text{ at } k-1 \text{ distinct points of every edge } e \in \partial K;\\
&\text{(D3). the moments } \int_K \boldsymbol{v}\cdot\boldsymbol{g}_{k-2}^{\perp}\,d\boldsymbol{x},\ \forall \boldsymbol{g}_{k-2}^{\perp} \in \mathcal{G}_{k-2}^{\perp}(K);\\
&\text{(D4). the moments } \int_K (\mathrm{div}\boldsymbol{v})p_{k-1}\,dx,\ \forall p_{k-1} \in \mathbb{P}_{k-1}(K)/\mathbb{R}.
\end{aligned} \tag{3.7}$$

Then, the global virtual element space can be denoted as:

$$\boldsymbol{V}_h := \{\boldsymbol{v} \in \boldsymbol{V} : \boldsymbol{v}|_K \in \boldsymbol{V}_{h|K},\ \forall K \in \mathcal{I}_h\}. \tag{3.8}$$

The following estimates can be obtained by using the assumption (**S1**)-(**S2**) (see [12, 13]):

- For $\forall K \in \mathcal{I}_h$ and $\forall \boldsymbol{v} \in \boldsymbol{H}^{s+1}(K)$ with $s \in \mathbb{N}$, $1 \le s \le k$, we have

$$\|\boldsymbol{v} - \boldsymbol{\Pi}_k^{0,K}\boldsymbol{v}\|_{0,K} + h_K|\boldsymbol{v} - \boldsymbol{\Pi}_k^{0,K}\boldsymbol{v}|_{1,K} \le Ch_K^{s+1}|\boldsymbol{v}|_{s+1,K}. \tag{3.9}$$

- There exists an interpolation $\boldsymbol{v}_I \in \boldsymbol{V}_{h|K}$ such that for $\boldsymbol{v} \in \boldsymbol{H}^{s+1}(K)$ with $1 \le s \le k$, we have

$$\|\boldsymbol{v} - \boldsymbol{v}_I\|_{0,K} + h_K|\boldsymbol{v} - \boldsymbol{v}_I|_{1,K} \le Ch_K^{s+1}|\boldsymbol{v}|_{s+1,K}. \tag{3.10}$$

For the chemical potential and the pressure, we take the standard finite-dimensional spaces

$$\boldsymbol{Y}_{h|K} := [\mathbb{P}_k(K)]^2, \quad Q_{h|K} := \mathbb{P}_{k-1}(K), \tag{3.11}$$

with the corresponding global virtual element spaces

$$\boldsymbol{Y}_h := \{\boldsymbol{\mu} \in \boldsymbol{Y} : \boldsymbol{\mu}|_K \in \boldsymbol{Y}_{h|K},\ \forall K \in \mathcal{I}_h\}, \tag{3.12}$$

$$Q_h := \{q \in Q : q|_K \in Q_{h|K},\ \forall K \in \mathcal{I}_h\}, \tag{3.13}$$

and we also remark that

$$\operatorname{div} \boldsymbol{V}_h \subseteq Q_h. \tag{3.14}$$

3.1.4 The discrete forms and their properties

Next, our aim is to define a discrete version of the linear forms in (2.8a).

- Given $\mathcal{M}_{h1}(\cdot,\cdot) : \boldsymbol{X}_{h|K} \times \boldsymbol{X}_{h|K} \to \mathbb{R}$ and $\mathcal{M}_{h2}(\cdot,\cdot) : \boldsymbol{V}_{h|K} \times \boldsymbol{V}_{h|K} \to \mathbb{R}$, we define

$$\mathcal{M}_{h1}(\boldsymbol{\varphi}_h, \boldsymbol{\psi}_h) := \sum_{K\in\mathcal{I}_h} \mathcal{M}_{h1}^K(\boldsymbol{\varphi}_h, \boldsymbol{\psi}_h),\ \mathcal{M}_{h2}(\boldsymbol{u}_h, \boldsymbol{v}_h) := \sum_{K\in\mathcal{I}_h} \mathcal{M}_{h2}^K(\boldsymbol{u}_h, \boldsymbol{v}_h),$$

where the local contributions are given as

$$\begin{aligned}
\mathcal{M}_{h1}^K(\boldsymbol{\varphi}_h, \boldsymbol{\psi}_h) &:= (\boldsymbol{\Pi}_k^{0,K}\boldsymbol{\varphi}_h, \boldsymbol{\Pi}_k^{0,K}\boldsymbol{\psi}_h)_{0,K} \\
&\quad +|K|S_{\mathcal{M}}^K(\boldsymbol{\varphi}_h - \boldsymbol{\Pi}_k^{0,K}\boldsymbol{\varphi}_h, \boldsymbol{\psi}_h - \boldsymbol{\Pi}_k^{0,K}\boldsymbol{\psi}_h), \\
\mathcal{M}_{h2}^K(\boldsymbol{u}_h, \boldsymbol{v}_h) &:= (\boldsymbol{\Pi}_k^{0,K}\boldsymbol{u}_h, \boldsymbol{\Pi}_k^{0,K}\boldsymbol{v}_h)_{0,K} \\
&\quad +|K|S_{\mathcal{M}}^K(\boldsymbol{u}_h - \boldsymbol{\Pi}_k^{0,K}\boldsymbol{u}_h, \boldsymbol{v}_h - \boldsymbol{\Pi}_k^{0,K}\boldsymbol{v}_h),
\end{aligned}$$

within $S_{\mathcal{M}}^K$ denotes a stabilization term. As a matter of fact, under the mesh assumptions (**S1**)-(**S2**), we can take the following scaled stabilization corresponding to the degrees of freedom

$$\begin{aligned}
S_{\mathcal{M}}^K(\boldsymbol{\varphi}_h - \boldsymbol{\Pi}_k^{0,K}\boldsymbol{\varphi}_h, \boldsymbol{\psi}_h - \boldsymbol{\Pi}_k^{0,K}\boldsymbol{\psi}_h) &= \sum_{j=1}^{\dim \boldsymbol{X}_{h|K}} dof_j^{\boldsymbol{X}_{h|K}}(\boldsymbol{\varphi}_h - \boldsymbol{\Pi}_k^{0,K}\boldsymbol{\varphi}_h) \\
&\quad \cdot dof_j^{\boldsymbol{X}_{h|K}}(\boldsymbol{\psi}_h - \boldsymbol{\Pi}_k^{0,K}\boldsymbol{\psi}_h), \\
S_{\mathcal{M}}^K(\boldsymbol{u}_h - \boldsymbol{\Pi}_k^{0,K}\boldsymbol{u}_h, \boldsymbol{v}_h - \boldsymbol{\Pi}_k^{0,K}\boldsymbol{v}_h) &= \sum_{j=1}^{\dim \boldsymbol{V}_{h|K}} dof_j^{\boldsymbol{V}_{h|K}}(\boldsymbol{u}_h - \boldsymbol{\Pi}_k^{0,K}\boldsymbol{u}_h) \\
&\quad \cdot dof_j^{\boldsymbol{V}_{h|K}}(\boldsymbol{v}_h - \boldsymbol{\Pi}_k^{0,K}\boldsymbol{v}_h).
\end{aligned}$$

- Also, we define $\mathcal{A}_{h1}(\cdot,\cdot) : \boldsymbol{X}_{h|K} \times \boldsymbol{X}_{h|K} \to \mathbb{R}$ and $\mathcal{A}_{h2}(\cdot,\cdot) : \boldsymbol{V}_{h|K} \times \boldsymbol{V}_{h|K} \to \mathbb{R}$, given by

$$\mathcal{A}_{h1}(\boldsymbol{\varphi}_h, \boldsymbol{\psi}_h) := \sum_{K\in\mathcal{I}_h} \mathcal{A}_{h1}^K(\boldsymbol{\varphi}_h, \boldsymbol{\psi}_h), \quad \mathcal{A}_{h2}(\boldsymbol{u}_h, \boldsymbol{v}_h) := \sum_{K\in\mathcal{I}_h} \mathcal{A}_{h2}^K(\boldsymbol{u}_h, \boldsymbol{v}_h),$$

where the local contributions are given as

$$\begin{aligned}\mathcal{A}_{h1}^K(\boldsymbol{\varphi}_h, \boldsymbol{\psi}_h) &:= (\boldsymbol{\Pi}_{k-1}^{0,K}\nabla\boldsymbol{\varphi}_h, \boldsymbol{\Pi}_{k-1}^{0,K}\nabla\boldsymbol{\psi}_h)_{0,K}\\ &\quad + S_{\mathcal{A}}^K(\boldsymbol{\varphi}_h - \boldsymbol{\Pi}_k^{\nabla,K}\boldsymbol{\varphi}_h, \boldsymbol{\psi}_h - \boldsymbol{\Pi}_k^{\nabla,K}\boldsymbol{\psi}_h),\\ \mathcal{A}_{h2}^K(\boldsymbol{u}_h, \boldsymbol{v}_h) &:= (\boldsymbol{\Pi}_{k-1}^{0,K}\nabla\boldsymbol{u}_h, \boldsymbol{\Pi}_{k-1}^{0,K}\nabla\boldsymbol{v}_h)_{0,K}\\ &\quad + S_{\mathcal{A}}^K(\boldsymbol{u}_h - \boldsymbol{\Pi}_k^{\nabla,K}\boldsymbol{u}_h, \boldsymbol{v}_h - \boldsymbol{\Pi}_k^{\nabla,K}\boldsymbol{v}_h),\end{aligned}$$

in which $S_{\mathcal{A}}^K$ is a stabilization term, denoted by

$$\begin{aligned}S_{\mathcal{A}}^K(\boldsymbol{\varphi}_h - \boldsymbol{\Pi}_k^{\nabla,K}\boldsymbol{\varphi}_h, \boldsymbol{\psi}_h - \boldsymbol{\Pi}_k^{\nabla,K}\boldsymbol{\psi}_h) &= \sum_{j=1}^{\dim \boldsymbol{X}_{h|K}} dof_j^{\boldsymbol{X}_{h|K}}(\boldsymbol{\varphi}_h - \boldsymbol{\Pi}_k^{\nabla,K}\boldsymbol{\varphi}_h)\\ &\quad \cdot dof_j^{\boldsymbol{X}_{h|K}}(\boldsymbol{\psi}_h - \boldsymbol{\Pi}_k^{\nabla,K}\boldsymbol{\psi}_h),\\ S_{\mathcal{A}}^K(\boldsymbol{u}_h - \boldsymbol{\Pi}_k^{\nabla,K}\boldsymbol{u}_h, \boldsymbol{v}_h - \boldsymbol{\Pi}_k^{\nabla,K}\boldsymbol{v}_h) &= \sum_{j=1}^{\dim \boldsymbol{V}_{h|K}} dof_j^{\boldsymbol{V}_{h|K}}(\boldsymbol{u}_h - \boldsymbol{\Pi}_k^{\nabla,K}\boldsymbol{u}_h)\\ &\quad \cdot dof_j^{\boldsymbol{V}_{h|K}}(\boldsymbol{v}_h - \boldsymbol{\Pi}_k^{\nabla,K}\boldsymbol{v}_h).\end{aligned}$$

- Regarding $\mathcal{B}(\cdot,\cdot) : \boldsymbol{V}_{h|K} \times Q_{h|K} \to \mathbb{R}$, we simply set

$$\mathcal{B}(\boldsymbol{v}_h, q_h) := \sum_{K\in\mathcal{I}_h} \mathcal{B}^K(\boldsymbol{v}_h, q_h) = \sum_{K\in\mathcal{I}_h} (\nabla\cdot\boldsymbol{v}_h, q_h)_{0,K},$$

  i.e., as stated in [12, 13], we do not introduce any approximation of the bilinear form. We notice that $\mathcal{B}(\boldsymbol{v}_h, q_h)$ is computable from (3.7), since q_h is polynomial in each element $K \in \mathcal{I}_h$.
- Next, given $\mathcal{D}_h(\cdot;\cdot,\cdot) : \boldsymbol{V}_{h|K} \times \boldsymbol{X}_{h|K} \times \boldsymbol{Y}_{h|K} \to \mathbb{R}$, we define

$$\mathcal{D}_h(\boldsymbol{v}_h; \boldsymbol{\varphi}_h, \boldsymbol{\psi}_h) := \sum_{K\in\mathcal{I}_h} \mathcal{D}_h^K(\boldsymbol{v}_h; \boldsymbol{\varphi}_h, \boldsymbol{\psi}_h),$$

  with local contributions

$$\mathcal{D}_h^K(\boldsymbol{v}_h; \boldsymbol{\varphi}_h, \boldsymbol{\psi}_h) := (\boldsymbol{\Pi}_k^{0,K}\boldsymbol{v}_h \cdot \boldsymbol{\Pi}_{k-1}^{0,K}\nabla\boldsymbol{\varphi}_h, \boldsymbol{\Pi}_k^{0,K}\boldsymbol{\psi}_h)_{0,K}.$$

- Moreover, we define $\mathcal{C}_h(\cdot;\cdot,\cdot) : \boldsymbol{V}_{h|K} \times \boldsymbol{V}_{h|K} \times \boldsymbol{V}_{h|K} \to \mathbb{R}$ as

$$\mathcal{C}_h(\boldsymbol{u}_h; \boldsymbol{v}_h, \boldsymbol{z}_h) := \sum_{K\in\mathcal{I}_h} \mathcal{C}_h^K(\boldsymbol{u}_h; \boldsymbol{v}_h, \boldsymbol{z}_h),$$

where

$$\mathcal{C}_h^K(\boldsymbol{u}_h;\boldsymbol{v}_h,\boldsymbol{z}_h) := \frac{1}{2}(\boldsymbol{\Pi}_k^{0,K}\boldsymbol{u}_h\cdot\boldsymbol{\Pi}_{k-1}^{0,K}\nabla\boldsymbol{v}_h,\boldsymbol{\Pi}_k^{0,K}\boldsymbol{z}_h)_{0,K} \\ -\frac{1}{2}(\boldsymbol{\Pi}_k^{0,K}\boldsymbol{u}_h\cdot\boldsymbol{\Pi}_{k-1}^{0,K}\nabla\boldsymbol{z}_h,\boldsymbol{\Pi}_k^{0,K}\boldsymbol{v}_h)_{0,K}.$$

Due to $\mathcal{M}_{h1}(\boldsymbol{\varphi}_h,\boldsymbol{\varphi}_h)\geq 0$, $\mathcal{M}_{h2}(\boldsymbol{v}_h,\boldsymbol{v}_h)\geq 0$, $\mathcal{A}_{h1}(\boldsymbol{\varphi}_h,\boldsymbol{\varphi}_h)\geq 0$ and $\mathcal{A}_{h2}(\boldsymbol{v}_h,\boldsymbol{v}_h)\geq 0$ (see Lemma 3.3), we also define some energy norms, for all $\boldsymbol{\varphi}_h\in\boldsymbol{X}_h$ and $\boldsymbol{v}_h\in\boldsymbol{V}_h$,

$$|||\boldsymbol{\varphi}_h|||_{\mathcal{M}_1}^2 := \mathcal{M}_{h1}(\boldsymbol{\varphi}_h,\boldsymbol{\varphi}_h) = \sum_{K\in\mathcal{I}_h}\mathcal{M}_{h1}^K(\boldsymbol{\varphi}_h,\boldsymbol{\varphi}_h), \tag{3.15}$$

$$|||\boldsymbol{v}_h|||_{\mathcal{M}_2}^2 := \mathcal{M}_{h2}(\boldsymbol{v}_h,\boldsymbol{v}_h) = \sum_{K\in\mathcal{I}_h}\mathcal{M}_{h2}^K(\boldsymbol{v}_h,\boldsymbol{v}_h), \tag{3.16}$$

$$|||\boldsymbol{\varphi}_h|||_{\mathcal{A}_1}^2 := \mathcal{A}_{h1}(\boldsymbol{\varphi}_h,\boldsymbol{\varphi}_h) = \sum_{K\in\mathcal{I}_h}\mathcal{A}_{h1}^K(\boldsymbol{\varphi}_h,\boldsymbol{\varphi}_h), \tag{3.17}$$

$$|||\boldsymbol{v}_h|||_{\mathcal{A}_2}^2 := \mathcal{A}_{h2}(\boldsymbol{v}_h,\boldsymbol{v}_h) = \sum_{K\in\mathcal{I}_h}\mathcal{A}_{h2}^K(\boldsymbol{v}_h,\boldsymbol{v}_h). \tag{3.18}$$

Next, we will collect and prove some crucial properties of the discrete local linear forms as follows.

Lemma 3.1 (see [6, 11]) *The local bilinear forms $\mathcal{M}_{h1}^K$, $\mathcal{M}_{h2}^K$, $\mathcal{A}_{h1}^K$, $\mathcal{A}_{h2}^K$ on each element K satisfy*

(i) Consistency: for all $\boldsymbol{p}_k\in[\mathbb{P}_k(K)]^2$ and $\boldsymbol{\varphi}_h\in\boldsymbol{X}_{h|K}$, $\boldsymbol{v}_h\in\boldsymbol{V}_{h|K}$, there hold

$$\mathcal{M}_{h1}^K(\boldsymbol{p}_k,\boldsymbol{\varphi}_h)=\mathcal{M}_1^K(\boldsymbol{p}_k,\boldsymbol{\varphi}_h),\quad \mathcal{M}_{h2}^K(\boldsymbol{p}_k,\boldsymbol{v}_h)=\mathcal{M}_2^K(\boldsymbol{p}_k,\boldsymbol{v}_h),$$
$$\mathcal{A}_{h1}^K(\boldsymbol{p}_k,\boldsymbol{\varphi}_h)=\mathcal{A}_1^K(\boldsymbol{p}_k,\boldsymbol{\varphi}_h),\quad \mathcal{A}_{h2}^K(\boldsymbol{p}_k,\boldsymbol{v}_h)=\mathcal{A}_2^K(\boldsymbol{p}_k,\boldsymbol{v}_h).$$

(ii) Stability: there exist positive constants $\alpha_i^\star,\alpha_i^*$, $i=1,2,3,4$, independent of h and K, such that for all $\boldsymbol{\varphi}_h\in\boldsymbol{X}_{h|K}$ and $\boldsymbol{v}_h\in\boldsymbol{V}_{h|K}$,

$$\alpha_1^\star\mathcal{M}_1^K(\boldsymbol{\varphi}_h,\boldsymbol{\varphi}_h)\leq\mathcal{M}_{h1}^K(\boldsymbol{\varphi}_h,\boldsymbol{\varphi}_h)\leq\alpha_1^*\mathcal{M}_1^K(\boldsymbol{\varphi}_h,\boldsymbol{\varphi}_h),$$
$$\alpha_2^\star\mathcal{M}_2^K(\boldsymbol{v}_h,\boldsymbol{v}_h)\leq\mathcal{M}_{h2}^K(\boldsymbol{v}_h,\boldsymbol{v}_h)\leq\alpha_2^*\mathcal{M}_2^K(\boldsymbol{v}_h,\boldsymbol{v}_h),$$
$$\alpha_3^\star\mathcal{A}_1^K(\boldsymbol{\varphi}_h,\boldsymbol{\varphi}_h)\leq\mathcal{A}_{h1}^K(\boldsymbol{\varphi}_h,\boldsymbol{\varphi}_h)\leq\alpha_3^*\mathcal{A}_1^K(\boldsymbol{\varphi}_h,\boldsymbol{\varphi}_h),$$
$$\alpha_4^\star\mathcal{A}_2^K(\boldsymbol{v}_h,\boldsymbol{v}_h)\leq\mathcal{A}_{h2}^K(\boldsymbol{v}_h,\boldsymbol{v}_h)\leq\alpha_4^*\mathcal{A}_2^K(\boldsymbol{v}_h,\boldsymbol{v}_h).$$

Since the symmetry of $\mathcal{M}_{h1}^K(\cdot,\cdot)$, $\mathcal{M}_{h2}^K(\cdot,\cdot)$, $\mathcal{A}_{h1}^K(\cdot,\cdot)$, $\mathcal{A}_{h2}^K(\cdot,\cdot)$, we obtain the following continuity results.

Lemma 3.2 (see [6, 12]) *There exist the constants $\tilde{C}_1, \tilde{C}_2, \tilde{C}_3, \tilde{C}_4 > 0$, independent of h, for all $\boldsymbol{\varphi}_h, \boldsymbol{\psi}_h \in \boldsymbol{X}_h$ and $\boldsymbol{u}_h, \boldsymbol{v}_h \in \boldsymbol{V}_h$, such that*

$$\mathcal{M}_{h1}(\boldsymbol{\varphi}_h, \boldsymbol{\psi}_h) \leq \tilde{C}_1\|\boldsymbol{\varphi}_h\|_0\|\boldsymbol{\psi}_h\|_0, \quad \mathcal{M}_{h2}(\boldsymbol{u}_h, \boldsymbol{v}_h) \leq \tilde{C}_2\|\boldsymbol{u}_h\|_0\|\boldsymbol{v}_h\|_0,$$
$$\mathcal{A}_{h1}(\boldsymbol{\varphi}_h, \boldsymbol{\psi}_h) \leq \tilde{C}_3|\boldsymbol{\varphi}_h|_1|\boldsymbol{\psi}_h|_1, \quad \mathcal{A}_{h2}(\boldsymbol{u}_h, \boldsymbol{v}_h) \leq \tilde{C}_4|\boldsymbol{u}_h|_1|\boldsymbol{v}_h|_1.$$

From the stability result in Lemma 3.1, we can get the coercivity of $\mathcal{M}_{h1}^K$, $\mathcal{M}_{h2}^K$, $\mathcal{A}_{h1}^K$, $\mathcal{A}_{h2}^K$.

Lemma 3.3 (see [11, 13]) *There exist the constants $\alpha_1, \alpha_2, \alpha_3, \alpha_4 > 0$, independent of h, for all $\boldsymbol{\varphi}_h \in \boldsymbol{X}_h$ and $\boldsymbol{v}_h \in \boldsymbol{V}_h$, such that*

$$\mathcal{M}_{h1}(\boldsymbol{\varphi}_h, \boldsymbol{\varphi}_h) \geq \alpha_1\|\boldsymbol{\varphi}_h\|_0^2, \quad \mathcal{M}_{h2}(\boldsymbol{v}_h, \boldsymbol{v}_h) \geq \alpha_2\|\boldsymbol{v}_h\|_0^2,$$
$$\mathcal{A}_{h1}(\boldsymbol{\varphi}_h, \boldsymbol{\varphi}_h) \geq \alpha_3|\boldsymbol{\varphi}_h|_1^2, \quad \mathcal{A}_{h2}(\boldsymbol{v}_h, \boldsymbol{v}_h) \geq \alpha_4|\boldsymbol{v}_h|_1^2.$$

The bilinear form $\mathcal{B}(\cdot, \cdot)$ satisfy the discrete inf-sup condition.

Lemma 3.4 (see [12, 13]) *Under the mesh regularity assumption (**S1**)-(**S2**), there exists a positive constant β independent of h such that*

$$\sup_{\boldsymbol{v}_h \in \boldsymbol{V}_h, \boldsymbol{v}_h \neq \boldsymbol{0}} \frac{\mathcal{B}(\boldsymbol{v}_h, q_h)}{|\boldsymbol{v}_h|_1} \geq \beta\|q_h\|_0, \ \forall q_h \in Q_h.$$

Similarly, we have the following continuity properties for $\mathcal{D}_h(\cdot;\cdot,\cdot)$ and $\mathcal{C}_h(\cdot;\cdot,\cdot)$, respectively.

Lemma 3.5 *There exist the constants $\hat{C}_1, \hat{C}_2, \hat{C}_3, \hat{C}_4 > 0$, independent of h, such that for all $\boldsymbol{\varphi}_h \in \boldsymbol{X}_h$, $\boldsymbol{\psi}_h \in \boldsymbol{Y}_h$, $\boldsymbol{u}_h, \boldsymbol{v}_h, \boldsymbol{z}_h \in \boldsymbol{V}_h$,*

$$|\mathcal{D}_h(\boldsymbol{v}_h; \boldsymbol{\varphi}_h, \boldsymbol{\psi}_h)| \leq \hat{C}_1\|\boldsymbol{\varphi}_h\|_{\boldsymbol{W}^{1,\infty}(\Omega)}\|\boldsymbol{v}_h\|_0\|\boldsymbol{\psi}_h\|_0,$$
$$|\mathcal{D}_h(\boldsymbol{v}_h; \boldsymbol{\varphi}_h, \boldsymbol{\psi}_h)| \leq \hat{C}_2\|\boldsymbol{v}_h\|_{\boldsymbol{L}^{\infty}(\Omega)}|\boldsymbol{\varphi}_h|_1\|\boldsymbol{\psi}_h\|_0,$$
$$|\mathcal{C}_h(\boldsymbol{u}_h; \boldsymbol{v}_h, \boldsymbol{z}_h)| \leq \hat{C}_3\|\boldsymbol{u}_h\|_{\boldsymbol{L}^{\infty}(\Omega)}|\boldsymbol{v}_h|_1\|\boldsymbol{z}_h\|_0,$$
$$|\mathcal{C}_h(\boldsymbol{u}_h; \boldsymbol{v}_h, \boldsymbol{z}_h)| \leq \hat{C}_4|\boldsymbol{u}_h|_1|\boldsymbol{v}_h|_1|\boldsymbol{z}_h|_1.$$

Proof The first three inequalities can be obtained by the Hölder inequality, the continuity of the projection $\boldsymbol{\Pi}_k^{0,K}$ with respect to the $\boldsymbol{L}^{\infty}$-norm, and the proof of last inequality can be found in [13]. □

Lemma 3.6 *Under the assumption (**S1**)-(**S2**), consider $\boldsymbol{v} \in \boldsymbol{H}^k(\Omega) \cap \boldsymbol{L}^{\infty}(\Omega)$, $\boldsymbol{\varphi} \in \boldsymbol{H}^{k+1}(\Omega) \cap \boldsymbol{W}^{1,\infty}(\Omega)$ with $k \geq 1$, for $\forall \boldsymbol{\psi}_h \in \boldsymbol{Y}_h$, we can obtain*

$$|\mathcal{D}(\boldsymbol{v}; \boldsymbol{\varphi}, \boldsymbol{\psi}_h) - \mathcal{D}_h(\boldsymbol{v}; \boldsymbol{\varphi}, \boldsymbol{\psi}_h)| \leq Ch^k(\|\boldsymbol{v}\|_{\boldsymbol{L}^{\infty}(\Omega)}\|\boldsymbol{\varphi}\|_{k+1} + \|\boldsymbol{\varphi}\|_{\boldsymbol{W}^{1,\infty}(\Omega)}\|\boldsymbol{v}\|_k)\|\boldsymbol{\psi}_h\|_0.$$

Proof According to the definitions of $\mathcal{D}(\cdot;\cdot,\cdot)$ and $\mathcal{D}_h(\cdot;\cdot,\cdot)$, using the Hölder inequality, the continuity of $\boldsymbol{\Pi}_k^{0,K}$ and $\boldsymbol{\Pi}_{k-1}^{0,K}$, we have

$$\begin{aligned}
&\mathcal{D}(\boldsymbol{v};\boldsymbol{\varphi},\boldsymbol{\psi}_h)-\mathcal{D}_h(\boldsymbol{v};\boldsymbol{\varphi},\boldsymbol{\psi}_h)\\
&=\sum_{K\in\mathcal{I}_h}\{(\boldsymbol{v}\cdot\nabla\boldsymbol{\varphi},\boldsymbol{\psi}_h)_{0,K}-(\boldsymbol{\Pi}_k^{0,K}\boldsymbol{v}\cdot\boldsymbol{\Pi}_{k-1}^{0,K}\nabla\boldsymbol{\varphi},\boldsymbol{\Pi}_k^{0,K}\boldsymbol{\psi}_h)_{0,K}\}\\
&=\sum_{K\in\mathcal{I}_h}\{[(\boldsymbol{v}\cdot\nabla\boldsymbol{\varphi},\boldsymbol{\psi}_h)_{0,K}-(\boldsymbol{\Pi}_{k-1}^{0,K}(\boldsymbol{v}\cdot\nabla\boldsymbol{\varphi}),\boldsymbol{\Pi}_k^{0,K}\boldsymbol{\psi}_h)_{0,K}]\\
&\quad+[(\boldsymbol{\Pi}_{k-1}^{0,K}(\boldsymbol{v}\cdot\nabla\boldsymbol{\varphi}),\boldsymbol{\Pi}_k^{0,K}\boldsymbol{\psi}_h)_{0,K}-(\boldsymbol{\Pi}_{k-1}^{0,K}(\boldsymbol{v}\cdot\boldsymbol{\Pi}_{k-1}^{0,K}\nabla\boldsymbol{\varphi}),\boldsymbol{\Pi}_k^{0,K}\boldsymbol{\psi}_h)_{0,K}]\\
&\quad+[(\boldsymbol{\Pi}_{k-1}^{0,K}(\boldsymbol{v}\cdot\boldsymbol{\Pi}_{k-1}^{0,K}\nabla\boldsymbol{\varphi}),\boldsymbol{\Pi}_k^{0,K}\boldsymbol{\psi}_h)_{0,K}-(\boldsymbol{\Pi}_k^{0,K}\boldsymbol{v}\cdot\boldsymbol{\Pi}_{k-1}^{0,K}\nabla\boldsymbol{\varphi},\boldsymbol{\Pi}_k^{0,K}\boldsymbol{\psi}_h)_{0,K}]\}\\
&=\sum_{K\in\mathcal{I}_h}\{J_1+J_2+J_3\}.
\end{aligned}\tag{3.19}$$

By the definition of $\boldsymbol{\Pi}_k^{0,K}$ and the Hölder inequality, we obtain

$$\begin{aligned}
\sum_{K\in\mathcal{I}_h}J_1&=\sum_{K\in\mathcal{I}_h}(I-\boldsymbol{\Pi}_{k-1}^{0,K})(\boldsymbol{v}\cdot\nabla\boldsymbol{\varphi}),\boldsymbol{\psi}_h)_{0,K}\\
&\le Ch_K^k\sum_{K\in\mathcal{I}_h}\|\boldsymbol{v}\|_{\boldsymbol{L}^\infty(K)}\|\nabla\boldsymbol{\varphi}\|_{k,K}\|\boldsymbol{\psi}_h\|_{0,K}\\
&\le Ch^k\|\boldsymbol{v}\|_{\boldsymbol{L}^\infty(\Omega)}\|\boldsymbol{\varphi}\|_{k+1}\|\boldsymbol{\psi}_h\|_0.
\end{aligned}\tag{3.20}$$

Using the continuity of $\boldsymbol{\Pi}_k^{0,K}$ and $\boldsymbol{\Pi}_{k-1}^{0,K}$, the Hölder inequality and from (3.4), we get

$$\begin{aligned}
\sum_{K\in\mathcal{I}_h}J_2&\le\sum_{K\in\mathcal{I}_h}\|\boldsymbol{v}\|_{\boldsymbol{L}^\infty(K)}\|(I-\boldsymbol{\Pi}_{k-1}^{0,K})\nabla\boldsymbol{\varphi}\|_{0,K}\|\boldsymbol{\psi}_h\|_{0,K}\\
&\le Ch_K^k\sum_{K\in\mathcal{I}_h}\|\boldsymbol{v}\|_{\boldsymbol{L}^\infty(K)}\|\nabla\boldsymbol{\varphi}\|_{k,K}\|\boldsymbol{\psi}_h\|_{0,K}\\
&\le Ch^k\|\boldsymbol{v}\|_{\boldsymbol{L}^\infty(\Omega)}\|\boldsymbol{\varphi}\|_{k+1}\|\boldsymbol{\psi}_h\|_0.
\end{aligned}\tag{3.21}$$

For the term J_3 in (3.19), using the Hölder inequality, we have

$$\begin{aligned}
\sum_{K\in\mathcal{I}_h}J_3&\le\sum_{K\in\mathcal{I}_h}\|\boldsymbol{\Pi}_{k-1}^{0,K}\nabla\boldsymbol{\varphi}\|_{\boldsymbol{L}^\infty(K)}\|(I-\boldsymbol{\Pi}_{k-1}^{0,K})\boldsymbol{v}\|_{0,K}\|\boldsymbol{\psi}_h\|_{0,K}\\
&\le Ch_K^k\sum_{K\in\mathcal{I}_h}\|\boldsymbol{\Pi}_{k-1}^{0,K}\nabla\boldsymbol{\varphi}\|_{\boldsymbol{L}^\infty(K)}\|\boldsymbol{v}\|_{k,K}\|\boldsymbol{\psi}_h\|_{0,K},
\end{aligned}$$

note that, the term $\|\boldsymbol{\Pi}_{k-1}^{0,K}\nabla\boldsymbol{\varphi}\|_{\boldsymbol{L}^\infty(K)}$ can be estimated as

$$\|\boldsymbol{\Pi}_{k-1}^{0,K}\nabla\boldsymbol{\varphi}\|_{\boldsymbol{L}^\infty(K)}\le h_K^{-1}\|\boldsymbol{\Pi}_{k-1}^{0,K}\nabla\boldsymbol{\varphi}\|_{\boldsymbol{L}^\infty(K)}\le h_K^{-1}\|\nabla\boldsymbol{\varphi}\|_{\boldsymbol{L}^\infty(K)}\le\|\boldsymbol{\varphi}\|_{\boldsymbol{W}^{1,\infty}(K)},$$

and thus,

$$\sum_{K\in\mathcal{T}_h} J_3 \le Ch^k\|\boldsymbol{\varphi}\|_{\boldsymbol{W}^{1,\infty}(\Omega)}\|\boldsymbol{v}\|_k\|\boldsymbol{\psi}_h\|_0. \tag{3.22}$$

Consequently, combining (3.20)–(3.22) with (3.19) together, the proof of the desired result is finished.

Lemma 3.7 *Under the assumption (S1)-(S2), consider $\boldsymbol{u},\boldsymbol{v}\in\boldsymbol{X}\cap\boldsymbol{H}^{k+1}$ with $k\ge 1$, for $\forall \boldsymbol{z}_h\in\boldsymbol{V}_h$, we can obtain*

$$|\mathcal{C}(\boldsymbol{u};\boldsymbol{v},\boldsymbol{z}_h)-\mathcal{C}_h(\boldsymbol{u};\boldsymbol{v},\boldsymbol{z}_h)|\le Ch^k(\|\boldsymbol{u}\|_{k+1}(\|\boldsymbol{v}\|_{k+1}+\|\boldsymbol{v}\|_1)\\ +\|\boldsymbol{v}\|_{k+1}(\|\boldsymbol{u}\|_k+\|\boldsymbol{v}\|_1))|\boldsymbol{z}_h|_1.$$

Proof By definition of $\mathcal{C}(\cdot;\cdot,\cdot)$ and $\mathcal{C}_h(\cdot;\cdot,\cdot)$, one can obtain

$$\begin{aligned}\mathcal{C}(\boldsymbol{u};\boldsymbol{v},\boldsymbol{z}_h)-\mathcal{C}_h(\boldsymbol{u};\boldsymbol{v},\boldsymbol{z}_h)&=\frac{1}{2}\sum_{K\in\mathcal{T}_h}[(\boldsymbol{u}\cdot\nabla\boldsymbol{v},\boldsymbol{z}_h)_{0,K}-(\boldsymbol{\Pi}_k^{0,K}\boldsymbol{u}\cdot\boldsymbol{\Pi}_{k-1}^{0,K}\nabla\boldsymbol{v},\boldsymbol{\Pi}_k^{0,K}\boldsymbol{z}_h)_{0,K}]\\&\quad-\frac{1}{2}\sum_{K\in\mathcal{T}_h}[(\boldsymbol{u}\cdot\nabla\boldsymbol{z}_h,\boldsymbol{v})_{0,K}-(\boldsymbol{\Pi}_k^{0,K}\boldsymbol{u}\cdot\boldsymbol{\Pi}_{k-1}^{0,K}\nabla\boldsymbol{z}_h,\boldsymbol{\Pi}_k^{0,K}\boldsymbol{v})_{0,K}]\\&:=\frac{1}{2}T_1-\frac{1}{2}T_2.\end{aligned}\tag{3.23}$$

For the term T_1, by simple calculation, we have

$$\begin{aligned}T_1&=\sum_{K\in\mathcal{T}_h}\{(\boldsymbol{u}\cdot\nabla\boldsymbol{v},(I-\boldsymbol{\Pi}_k^{0,K})\boldsymbol{z}_h)_{0,K}+((I-\boldsymbol{\Pi}_k^{0,K})\boldsymbol{u}\cdot\nabla\boldsymbol{v},\boldsymbol{\Pi}_k^{0,K}\boldsymbol{z}_h)_{0,K}\\&\quad+((\boldsymbol{\Pi}_k^{0,K}\boldsymbol{u})\cdot(I-\boldsymbol{\Pi}_{k-1}^{0,K})\nabla\boldsymbol{v},\boldsymbol{\Pi}_k^{0,K}\boldsymbol{z}_h)_{0,K}\}\\&:=\sum_{K\in\mathcal{T}_h}\{T_{11}+T_{12}+T_{13}\}.\end{aligned}\tag{3.24}$$

Using the definition of $\boldsymbol{\Pi}_k^{0,K}$ and the Hölder inequality, we have

$$\begin{aligned}\sum_{K\in\mathcal{T}_h}T_{11}&=\sum_{K\in\mathcal{T}_h}(\boldsymbol{u}\cdot\nabla\boldsymbol{v},(I-\boldsymbol{\Pi}_k^{0,K})\boldsymbol{z}_h)_{0,K}\\&=\sum_{K\in\mathcal{T}_h}((I-\boldsymbol{\Pi}_{k-2}^{0,K})(\boldsymbol{u}\cdot\nabla\boldsymbol{v}),(I-\boldsymbol{\Pi}_k^{0,K})\boldsymbol{z}_h)_{0,K}\\&\le Ch^k|\boldsymbol{u}\cdot\nabla\boldsymbol{v}|_{k-1}|\boldsymbol{z}_h|_1.\end{aligned}\tag{3.25}$$

and by the Hölder inequality and Sobolev embedding $\boldsymbol{H}^k(\Omega)\subset\boldsymbol{W}^{k-1,4}(\Omega)$, we infer

$$|\boldsymbol{u}\cdot\nabla\boldsymbol{v}|_{k-1}\le\|\boldsymbol{u}\|_{\boldsymbol{W}^{k-1,4}}\|\nabla\boldsymbol{v}\|_{\boldsymbol{W}^{k-1,4}}\le C\|\boldsymbol{u}\|_k\|\nabla\boldsymbol{v}\|_k. \tag{3.26}$$

By (3.25) and (3.26) we finally obtain

$$\sum_{K \in \mathcal{I}_h} T_{11} \leq Ch^k \|\boldsymbol{u}\|_k \|\boldsymbol{v}\|_{k+1} |\boldsymbol{z}_h|_1. \tag{3.27}$$

For the term T_{12} in (3.24), using the Hölder inequality, we have

$$\begin{aligned} T_{12} &= ((I - \boldsymbol{\Pi}_k^{0,K})\boldsymbol{u} \cdot \nabla \boldsymbol{v}, \boldsymbol{\Pi}_k^{0,K} \boldsymbol{z}_h)_{0,K} \\ &\leq \|\nabla \boldsymbol{v}\|_{0,K} \|(I - \boldsymbol{\Pi}_k^{0,K})\boldsymbol{u}\|_{\boldsymbol{L}^4(K)} \|\boldsymbol{\Pi}_k^{0,K} \boldsymbol{z}_h\|_{\boldsymbol{L}^4(K)}. \end{aligned} \tag{3.28}$$

From (3.10), we know that, there exists a polynomial $\boldsymbol{u}_\pi \in \mathbb{P}_k(K)$ such that

$$\|\boldsymbol{u} - \boldsymbol{u}_\pi\|_{\boldsymbol{L}^4(K)} \leq Ch_K^k |\boldsymbol{u}|_{\boldsymbol{W}^{k,4}(K)},$$

and thus, by the continuity of $\boldsymbol{\Pi}_K^{0,k}$ with respect to the $\boldsymbol{L}^2$-norm

$$\begin{aligned} \|(I - \boldsymbol{\Pi}_k^{0,K})\boldsymbol{u}\|_{\boldsymbol{L}^4(K)} &\leq \|\boldsymbol{u} - \boldsymbol{u}_\pi\|_{\boldsymbol{L}^4(K)} + \|\boldsymbol{\Pi}_k^{0,K}(\boldsymbol{u} - \boldsymbol{u}_\pi)\|_{\boldsymbol{L}^4(K)} \\ &\leq C\|\boldsymbol{u} - \boldsymbol{u}_\pi\|_{\boldsymbol{L}^4(K)} \leq Ch_K^k |\boldsymbol{u}|_{\boldsymbol{W}^{k,4}(K)}. \end{aligned} \tag{3.29}$$

Applying the Hölder inequality and Sobolev embeddings $\boldsymbol{H}^1(\Omega) \subset \boldsymbol{L}^4(\Omega)$ and $\boldsymbol{H}^{k+1}(\Omega) \subset \boldsymbol{W}^{k,4}(\Omega)$, by (3.28) and (3.29), we obtain

$$\begin{aligned} \sum_{K \in \mathcal{I}_h} T_{12} &\leq Ch_K^k \sum_{K \in \mathcal{I}_h} \|\nabla \boldsymbol{v}\|_{0,K} |\boldsymbol{u}|_{\boldsymbol{W}^{k,4}(K)} \|\boldsymbol{z}_h\|_{\boldsymbol{L}^4(K)} \\ &\leq Ch^k \|\boldsymbol{v}\|_1 \|\boldsymbol{u}\|_{k+1} |\boldsymbol{z}_h|_1. \end{aligned} \tag{3.30}$$

For the term T_{13} in (3.24), it holds that

$$\begin{aligned} \sum_{K \in \mathcal{I}_h} T_{13} &= \sum_{K \in \mathcal{I}_h} ((\boldsymbol{\Pi}_k^{0,K} \boldsymbol{u}) \cdot (I - \boldsymbol{\Pi}_{k-1}^{0,K}) \nabla \boldsymbol{v}, \boldsymbol{\Pi}_k^{0,K} \boldsymbol{z}_h)_{0,K} \\ &\leq Ch^k |\nabla \boldsymbol{v}|_{k,K} \|\boldsymbol{u}\|_{\boldsymbol{L}^4(K)} \|\boldsymbol{z}_h\|_{\boldsymbol{L}^4(K)} \\ &\leq Ch^k \|\boldsymbol{v}\|_{k+1} \|\boldsymbol{u}\|_1 |\boldsymbol{z}_h|_1. \end{aligned} \tag{3.31}$$

By combining (3.27), (3.30) and (3.31), we get

$$|T_1| \leq Ch^k (\|\boldsymbol{u}\|_k \|\boldsymbol{v}\|_{k+1} + \|\boldsymbol{v}\|_1 \|\boldsymbol{u}\|_{k+1} + \|\boldsymbol{v}\|_{k+1} \|\boldsymbol{u}\|_1) |\boldsymbol{z}_h|_1. \tag{3.32}$$

For the second term T_2, applying the Hölder inequality and the Sobolev embedding, we obtain

$$\begin{aligned} T_2 = \sum_{K\in\mathcal{I}_h} \{&(\boldsymbol{u}\cdot\nabla z_h, (I-\boldsymbol{\Pi}_k^{0,K})\boldsymbol{v})_{0,K} + ((I-\boldsymbol{\Pi}_k^{0,K})\boldsymbol{u}\cdot\nabla z_h, \boldsymbol{\Pi}_k^{0,K}\boldsymbol{v})_{0,K} \\ &+ ((\boldsymbol{\Pi}_k^{0,K}\boldsymbol{u})\cdot(I-\boldsymbol{\Pi}_{k-1}^{0,K})\nabla z_h, \boldsymbol{\Pi}_k^{0,K}\boldsymbol{v})_{0,K}\} \\ \le\, & Ch^k(\|\boldsymbol{u}\|_{k+1}\|\boldsymbol{v}\|_{k+1} + \|\boldsymbol{v}\|_1\|\boldsymbol{u}\|_{k+1} + \|\boldsymbol{v}\|_{k+1}\|\boldsymbol{u}\|_1)|z_h|_1. \end{aligned} \tag{3.33}$$

We finish the proof by combining (3.32)–(3.33) with (3.23).

3.2 Fully discrete scheme

We choose the time step size $\tau = T/N$, where N represents the number of the time sequence, and we give $t^n = n\tau, n = 0,\dots,N$. Moreover, for any sufficiently regular time function $\boldsymbol{\varphi}(\cdot,t)$, we denote $\boldsymbol{\varphi}^n = \boldsymbol{\varphi}(\cdot,t^n)$, and also introduce the backward differential operator δ_t satisfying

$$\delta_t\boldsymbol{\varphi}^n = \frac{\boldsymbol{\varphi}^n - \boldsymbol{\varphi}^{n-1}}{\tau}.$$

For convenience, the following notations will be used throughout this paper

$$\begin{aligned} \boldsymbol{d}^{n+\frac{1}{2}} &= \frac{\boldsymbol{d}^{n+1}+\boldsymbol{d}^n}{2}, \quad \widetilde{\boldsymbol{d}}^{n+\frac{1}{2}} = \frac{3\boldsymbol{d}^n - \boldsymbol{d}^{n-1}}{2}, \\ \boldsymbol{u}^{n+\frac{1}{2}} &= \frac{\boldsymbol{u}^{n+1}+\boldsymbol{u}^n}{2}, \quad \widetilde{\boldsymbol{u}}^{n+\frac{1}{2}} = \frac{3\boldsymbol{u}^n - \boldsymbol{u}^{n-1}}{2}. \end{aligned}$$

Due to the strong nonlinearity of the penalty function, a challenging issue to solve the system (2.5a) numerically is how to design efficient schemes that preserve the energy stability of the discrete system. In this study, we will regularize the penalty function through the idea of convex splitting. More precisely, we rewrite $\boldsymbol{F}(\boldsymbol{d})$ as the sum of a convex function and a concave function

$$\boldsymbol{F}(\boldsymbol{d}) = \boldsymbol{F}_v(\boldsymbol{d}) + \boldsymbol{F}_c(\boldsymbol{d}) := \frac{1}{4}\boldsymbol{d}^4 + (-\frac{1}{2}\boldsymbol{d}^2 + \frac{1}{4}),$$

and accordingly $\boldsymbol{f}(\boldsymbol{d}) = \boldsymbol{f}_v(\boldsymbol{d}) + \boldsymbol{f}_c(\boldsymbol{d}) := \boldsymbol{d}^3 - \boldsymbol{d}$.

The idea of convex splitting is to use explicit discretization for the concave part (i.e., $\boldsymbol{f}_c(\widetilde{\boldsymbol{d}}^{n+\frac{1}{2}})$) and implicit discretization for the convex part. Thus, we approximate $\boldsymbol{f}_v(\boldsymbol{d}^{n+\frac{1}{2}})$ by the Crank-Nicolson scheme

$$\boldsymbol{f}_v(\boldsymbol{d}^{n+\frac{1}{2}}) \approx \frac{\boldsymbol{F}_v(\boldsymbol{d}^{n+1}) - \boldsymbol{F}_v(\boldsymbol{d}^n)}{\boldsymbol{d}^{n+1} - \boldsymbol{d}^n} = \frac{1}{2}((\boldsymbol{d}^{n+1})^2 + (\boldsymbol{d}^n)^2)\boldsymbol{d}^{n+\frac{1}{2}}.$$

Now, we will propose a fully discrete virtual element scheme with second-order temporal accuracy as follows.

Find $(\boldsymbol{d}_h^{n+1}, \boldsymbol{\omega}_h^{n+1}, \boldsymbol{u}_h^{n+1}, p_h^{n+1}) \in \boldsymbol{X}_h \times \boldsymbol{Y}_h \times \boldsymbol{V}_h \times Q_h$ such that for $n = 0, \cdots, N-1$ and $(\boldsymbol{\xi}_h, \boldsymbol{\theta}_h, \boldsymbol{v}_h, q_h) \in \boldsymbol{X}_h \times \boldsymbol{Y}_h \times \boldsymbol{V}_h \times Q_h$, there hold

$$\mathcal{M}_{h1}(\delta_t \boldsymbol{d}_h^{n+1}, \boldsymbol{\theta}_h) + \mathcal{D}_h(\boldsymbol{u}_h^{n+\frac{1}{2}}; \widetilde{\boldsymbol{d}}_h^{n+\frac{1}{2}}, \boldsymbol{\theta}_h) + \gamma \mathcal{M}_{h1}(\boldsymbol{\omega}_h^{n+\frac{1}{2}}, \boldsymbol{\theta}_h) = 0, \tag{3.34a}$$

$$\mathcal{M}_{h1}(\boldsymbol{\omega}_h^{n+\frac{1}{2}}, \boldsymbol{\xi}_h) = \frac{1}{2\varepsilon^2}(((\boldsymbol{\Pi}_k^0 \boldsymbol{d}_h^{n+1})^2 + (\boldsymbol{\Pi}_k^0 \boldsymbol{d}_h^n)^2)\boldsymbol{\Pi}_k^0 \boldsymbol{d}_h^{n+\frac{1}{2}}, \boldsymbol{\Pi}_k^0 \boldsymbol{\xi}_h) \tag{3.34b}$$
$$-\frac{1}{\varepsilon^2}(\boldsymbol{\Pi}_k^0 \widetilde{\boldsymbol{d}}_h^{n+\frac{1}{2}}, \boldsymbol{\Pi}_k^0 \boldsymbol{\xi}_h) + \lambda \mathcal{A}_{h1}(\boldsymbol{d}_h^{n+\frac{1}{2}}, \boldsymbol{\xi}_h),$$

$$\mathcal{M}_{h2}(\delta_t \boldsymbol{u}_h^{n+1}, \boldsymbol{v}_h) + \mathcal{C}_h(\widetilde{\boldsymbol{u}}_h^{n+\frac{1}{2}}; \boldsymbol{u}_h^{n+\frac{1}{2}}, \boldsymbol{v}_h) + \nu \mathcal{A}_{h2}(\boldsymbol{u}_h^{n+\frac{1}{2}}, \boldsymbol{v}_h) \tag{3.34c}$$
$$-\mathcal{B}(\boldsymbol{v}_h, p_h^{n+\frac{1}{2}}) - \mathcal{D}_h(\boldsymbol{v}_h; \widetilde{\boldsymbol{d}}_h^{n+\frac{1}{2}}, \boldsymbol{\omega}_h^{n+\frac{1}{2}}) = 0,$$

$$\mathcal{B}(\boldsymbol{u}_h^{n+\frac{1}{2}}, q_h) = 0, \tag{3.34d}$$

where we set $\boldsymbol{d}_h^0 = \boldsymbol{d}_I^0$, $\boldsymbol{\omega}_h^0 = \boldsymbol{\omega}_I^0$, $\boldsymbol{u}_h^0 = \boldsymbol{u}_I^0$, and $\boldsymbol{d}_I^0$, $\boldsymbol{\omega}_I^0$, $\boldsymbol{u}_I^0$ denote the suitable interpolations of $\boldsymbol{d}_0$, $\boldsymbol{\omega}_0$, $\boldsymbol{u}_0$ (see (3.5) and (3.10)), respectively. Let $\boldsymbol{\Pi}_k^0$ be the projection onto the piecewise (with respect to $\mathcal{I}_h$) polynomials up to degree k satisfying $\boldsymbol{\Pi}_k^0 \boldsymbol{\xi}_h|_K = \boldsymbol{\Pi}_k^{0,K} \boldsymbol{\xi}_h$ for all $\boldsymbol{\xi}_h \in \boldsymbol{X}_h$.

Remark 3.1 *Since the extrapolated C-N scheme (3.34a) is a two-step scheme, it needs two initial values to achieve second-order accuracy. For simplicity, as in [3], we define $\boldsymbol{d}_h^{-1} = \boldsymbol{d}_h^0$ and $\boldsymbol{u}_h^{-1} = \boldsymbol{u}_h^0$ to be interpolant of $\boldsymbol{d}^0$ and $\boldsymbol{u}^0$. In addition, we also take $\boldsymbol{d}(\boldsymbol{x}, t) = \boldsymbol{d}_0$ and $\boldsymbol{u}(\boldsymbol{x}, t) = \boldsymbol{u}_0$ for $t \leq 0$, which can be seen as a contraction from the internal to the negative time direction.*

The equation (3.34d) along with the property (3.14), implies that the discrete velocity $\boldsymbol{u}_h^{n+\frac{1}{2}} \in \boldsymbol{V}_h$ is exactly divergence-free. More generally, introducing the continuous and discrete kernels:

$$\boldsymbol{W} = \{\boldsymbol{v} \in \boldsymbol{V} : \mathcal{B}(\boldsymbol{v}, q) = 0, \ \forall q \in Q\}, \ \boldsymbol{W}_h = \{\boldsymbol{v} \in \boldsymbol{V}_h : \mathcal{B}(\boldsymbol{v}, q) = 0, \ \forall q \in Q_h\},$$

we can readily check that $\boldsymbol{W}_h \subseteq \boldsymbol{V}_h$. Therefore, we consider the following reduced problem, which is equivalent to the scheme (3.34a).

Find $(\boldsymbol{d}_h^{n+1}, \boldsymbol{\omega}_h^{n+1}, \boldsymbol{u}_h^{n+1}) \in \boldsymbol{X}_h \times \boldsymbol{Y}_h \times \boldsymbol{W}_h$ such that for $n = 0, \cdots, N-1$ and $(\boldsymbol{\xi}_h, \boldsymbol{\theta}_h, \boldsymbol{v}_h) \in \boldsymbol{X}_h \times \boldsymbol{Y}_h \times \boldsymbol{W}_h$, there hold

$$\mathcal{M}_{h1}(\delta_t \boldsymbol{d}_h^{n+1}, \boldsymbol{\theta}_h) + \mathcal{D}_h(\boldsymbol{u}_h^{n+\frac{1}{2}}; \widetilde{\boldsymbol{d}}_h^{n+\frac{1}{2}}, \boldsymbol{\theta}_h) + \gamma \mathcal{M}_{h1}(\boldsymbol{\omega}_h^{n+\frac{1}{2}}, \boldsymbol{\theta}_h) = 0, \tag{3.35a}$$

$$\mathcal{M}_{h1}(\boldsymbol{\omega}_h^{n+\frac{1}{2}}, \boldsymbol{\xi}_h) = \frac{1}{2\varepsilon^2}(((\boldsymbol{\Pi}_k^0 \boldsymbol{d}_h^{n+1})^2 + (\boldsymbol{\Pi}_k^0 \boldsymbol{d}_h^n)^2)\boldsymbol{\Pi}_k^0 \boldsymbol{d}_h^{n+\frac{1}{2}}, \boldsymbol{\Pi}_k^0 \boldsymbol{\xi}_h) \tag{3.35b}$$

$$
\begin{aligned}
&-\frac{1}{\varepsilon^2}(\boldsymbol{\Pi}_k^0\widetilde{\boldsymbol{d}}_h^{n+\frac{1}{2}}, \boldsymbol{\Pi}_k^0\boldsymbol{\xi}_h) + \lambda\mathcal{A}_{h1}(\boldsymbol{d}_h^{n+\frac{1}{2}}, \boldsymbol{\xi}_h),\\
&\mathcal{M}_{h2}(\delta_t\boldsymbol{u}_h^{n+1}, \boldsymbol{v}_h) + \mathcal{C}_h(\widetilde{\boldsymbol{u}}_h^{n+\frac{1}{2}}; \boldsymbol{u}_h^{n+\frac{1}{2}}, \boldsymbol{v}_h) + \nu\mathcal{A}_{h2}(\boldsymbol{u}_h^{n+\frac{1}{2}}, \boldsymbol{v}_h)\\
&-\mathcal{D}_h(\boldsymbol{v}_h; \widetilde{\boldsymbol{d}}_h^{n+\frac{1}{2}}, \boldsymbol{\omega}_h^{n+\frac{1}{2}}) = 0. \qquad (3.35c)
\end{aligned}
$$

The design of convex splitting approach enables us to prove the unconditional stability of the proposed scheme. We now establish a discrete energy law of the fully discrete virtual element scheme, which show that the total discrete energy is non-increasing and is therefore unconditionally stable.

Theorem 3.1 *The scheme (3.35a) admits the following discrete energy dissipation law*

$$
\begin{aligned}
\mathcal{E}_h(\boldsymbol{u}_h^{m+1}, \boldsymbol{d}_h^{m+1}) &+ \sum_{n=0}^{m}\{\nu\tau|||\boldsymbol{u}_h^{n+\frac{1}{2}}|||_{\mathcal{A}_2}^2 + \gamma\tau|||\boldsymbol{\omega}_h^{n+\frac{1}{2}}|||_{\mathcal{M}_1}^2\\
&+ \frac{1}{4\varepsilon^2}\|\boldsymbol{\Pi}_k^0\boldsymbol{d}_h^{n+1} - 2\boldsymbol{\Pi}_k^0\boldsymbol{d}_h^{n} + \boldsymbol{\Pi}_k^0\boldsymbol{d}_h^{n-1}\|_0^2\} = \mathcal{E}_h(\boldsymbol{u}_h^0, \boldsymbol{d}_h^0),
\end{aligned}
$$

where the discrete energy $\mathcal{E}_h$ is defined by

$$
\begin{aligned}
\mathcal{E}_h(\boldsymbol{u}_h^{m+1}, \boldsymbol{d}_h^{m+1}) &= \frac{1}{2}|||\boldsymbol{u}_h^{m+1}|||_{\mathcal{M}_2}^2 + \frac{\lambda}{2}|||\boldsymbol{d}_h^{m+1}|||_{\mathcal{A}_1}^2 + \frac{1}{\varepsilon^2}(\boldsymbol{F}(\boldsymbol{\Pi}_k^0\boldsymbol{d}_h^{m+1}), 1)\\
&+\frac{1}{4\varepsilon^2}\|\boldsymbol{\Pi}_k^0\boldsymbol{d}_h^{m+1} - \boldsymbol{\Pi}_k^0\boldsymbol{d}_h^{m}\|_0^2.
\end{aligned}
$$

Proof By taking $\boldsymbol{\theta}_h = \tau\boldsymbol{\omega}_h^{n+\frac{1}{2}}$ in (3.35a), we obtain

$$
\mathcal{M}_{h1}(\boldsymbol{d}_h^{n+1} - \boldsymbol{d}_h^{n}, \boldsymbol{\omega}_h^{n+\frac{1}{2}}) + \tau\mathcal{D}_h(\boldsymbol{u}_h^{n+\frac{1}{2}}; \widetilde{\boldsymbol{d}}_h^{n+\frac{1}{2}}, \boldsymbol{\omega}_h^{n+\frac{1}{2}}) + \gamma\tau|||\boldsymbol{\omega}_h^{n+\frac{1}{2}}|||_{\mathcal{M}_1}^2 = 0. \qquad (3.36)
$$

Taking $\boldsymbol{\xi}_h = \boldsymbol{d}_h^{n+1} - \boldsymbol{d}_h^{n}$ in (3.35b), it is easy to check that

$$
\begin{aligned}
&\frac{1}{2}(((\boldsymbol{\Pi}_k^0\boldsymbol{d}_h^{n+1})^2 + (\boldsymbol{\Pi}_k^0\boldsymbol{d}_h^{n})^2)\boldsymbol{\Pi}_k^0\boldsymbol{d}_h^{n+\frac{1}{2}}, \boldsymbol{\Pi}_k^0\boldsymbol{d}_h^{n+1} - \boldsymbol{\Pi}_k^0\boldsymbol{d}_h^{n})\\
&\quad = \frac{1}{4}\int_\Omega |\boldsymbol{\Pi}_k^0\boldsymbol{d}_h^{n+1}|^4 - |\boldsymbol{\Pi}_k^0\boldsymbol{d}_h^{n}|^4 d\boldsymbol{x},
\end{aligned}
$$

and

$$
\begin{aligned}
&(\mathbf{\Pi}_k^0\widetilde{\boldsymbol{d}}_h^{n+\frac{1}{2}}, \mathbf{\Pi}_k^0\boldsymbol{d}_h^{n+1} - \mathbf{\Pi}_k^0\boldsymbol{d}_h^n)\\
&= \frac{1}{2}(3\mathbf{\Pi}_k^0\boldsymbol{d}_h^n - \mathbf{\Pi}_k^0\boldsymbol{d}_h^{n-1}, \mathbf{\Pi}_k^0\boldsymbol{d}_h^{n+1} - \mathbf{\Pi}_k^0\boldsymbol{d}_h^n)\\
&= \frac{1}{2}(\mathbf{\Pi}_k^0\boldsymbol{d}_h^{n+1} + \mathbf{\Pi}_k^0\boldsymbol{d}_h^n, \mathbf{\Pi}_k^0\boldsymbol{d}_h^{n+1} - \mathbf{\Pi}_k^0\boldsymbol{d}_h^n)\\
&\quad -\frac{1}{2}(\mathbf{\Pi}_k^0\boldsymbol{d}_h^{n+1} - 2\mathbf{\Pi}_k^0\boldsymbol{d}_h^n + \mathbf{\Pi}_k^0\boldsymbol{d}_h^{n-1}, \mathbf{\Pi}_k^0\boldsymbol{d}_h^{n+1} - \mathbf{\Pi}_k^0\boldsymbol{d}_h^n)\\
&= \frac{1}{2}(\|\mathbf{\Pi}_k^0\boldsymbol{d}_h^{n+1}\|_0^2 - \|\mathbf{\Pi}_k^0\boldsymbol{d}_h^n\|_0^2) - \frac{1}{4}(\|\mathbf{\Pi}_k^0\boldsymbol{d}_h^{n+1} - \mathbf{\Pi}_k^0\boldsymbol{d}_h^n\|_0^2 - \|\mathbf{\Pi}_k^0\boldsymbol{d}_h^n - \mathbf{\Pi}_k^0\boldsymbol{d}_h^{n-1}\|_0^2\\
&\quad +||\mathbf{\Pi}_k^0\boldsymbol{d}_h^{n+1} - 2\mathbf{\Pi}_k^0\boldsymbol{d}_h^n + \mathbf{\Pi}_k^0\boldsymbol{d}_h^{n-1}||_0^2).
\end{aligned}
$$

From the definition of $\boldsymbol{F}(\boldsymbol{d})$, we deduce

$$
\begin{aligned}
\mathcal{M}_{h1}(\boldsymbol{\omega}_h^{n+\frac{1}{2}}, \boldsymbol{d}_h^{n+1} - \boldsymbol{d}_h^n) = &\frac{\lambda}{2}|||\boldsymbol{d}_h^{n+1}|||_{\mathcal{A}_1}^2 - \frac{\lambda}{2}|||\boldsymbol{d}_h^n|||_{\mathcal{A}_1}^2\\
&+\frac{1}{\varepsilon^2}(\boldsymbol{F}(\mathbf{\Pi}_k^0\boldsymbol{d}_h^{n+1}) - \boldsymbol{F}(\mathbf{\Pi}_k^0\boldsymbol{d}_h^n), 1)\\
&+\frac{1}{4\varepsilon^2}(\|\mathbf{\Pi}_k^0\boldsymbol{d}_h^{n+1} - \mathbf{\Pi}_k^0\boldsymbol{d}_h^n\|_0^2 - \|\mathbf{\Pi}_k^0\boldsymbol{d}_h^n - \mathbf{\Pi}_k^0\boldsymbol{d}_h^{n-1}\|_0^2\\
&+\|\mathbf{\Pi}_k^0\boldsymbol{d}_h^{n+1} - 2\mathbf{\Pi}_k^0\boldsymbol{d}_h^n + \mathbf{\Pi}_k^0\boldsymbol{d}_h^{n-1}\|_0^2).
\end{aligned}
\tag{3.37}
$$

Setting $\boldsymbol{v}_h = \tau\boldsymbol{u}_h^{n+\frac{1}{2}}$ in (3.35c), we have

$$
\begin{aligned}
\frac{1}{2}|||\boldsymbol{u}_h^{n+1}|||_{\mathcal{M}_2}^2 - \frac{1}{2}|||\boldsymbol{u}_h^n|||_{\mathcal{M}_2}^2 + \nu\tau|||\boldsymbol{u}_h^{n+\frac{1}{2}}|||_{\mathcal{A}_2}^2&\\
- \tau\mathcal{D}_h(\boldsymbol{u}^{n+\frac{1}{2}}; \widetilde{\boldsymbol{d}}_h^{n+\frac{1}{2}}, \boldsymbol{\omega}_h^{n+\frac{1}{2}}) = 0.&
\end{aligned}
\tag{3.38}
$$

Summing up (3.36)- (3.38), we obtain

$$
\begin{aligned}
&\frac{1}{2}|||\boldsymbol{u}_h^{n+1}|||_{\mathcal{M}_2}^2 + \frac{\lambda}{2}|||\boldsymbol{d}_h^{n+1}|||_{\mathcal{A}_1}^2 + \frac{1}{\varepsilon^2}(\boldsymbol{F}(\mathbf{\Pi}_k^0\boldsymbol{d}_h^{n+1}), 1) + \frac{1}{4\varepsilon^2}\|\mathbf{\Pi}_k^0\boldsymbol{d}_h^{n+1} - \mathbf{\Pi}_k^0\boldsymbol{d}_h^n\|_0^2\\
&+ \nu\tau|||\boldsymbol{u}_h^{n+\frac{1}{2}}|||_{\mathcal{A}_2}^2 + \gamma\tau|||\boldsymbol{\omega}_h^{n+\frac{1}{2}}|||_{\mathcal{M}_1}^2 + \frac{1}{4\varepsilon^2}\|\mathbf{\Pi}_k^0\boldsymbol{d}_h^{n+1} - 2\mathbf{\Pi}_k^0\boldsymbol{d}_h^n + \mathbf{\Pi}_k^0\boldsymbol{d}_h^{n-1}\|_0^2\\
&= \frac{1}{2}|||\boldsymbol{u}_h^n|||_{\mathcal{M}_2}^2 + \frac{\lambda}{2}|||\boldsymbol{d}_h^n|||_{\mathcal{A}_1}^2 + \frac{1}{\varepsilon^2}(\boldsymbol{F}(\mathbf{\Pi}_k^0\boldsymbol{d}_h^n), 1) + \frac{1}{4\varepsilon^2}\|\mathbf{\Pi}_k^0\boldsymbol{d}_h^n - \mathbf{\Pi}_k^0\boldsymbol{d}_h^{n-1}\|_0^2.
\end{aligned}
\tag{3.39}
$$

Finally, the desired result follows from the application of the operator $\sum_{n=0}^m$ to (3.39). Next, we prove the existence and uniqueness of the numerical solution in (3.35a) by using the Brouwer's fixed point theorem.

Theorem 3.2 *The fully discrete scheme* (3.35a) *admits a unique solution* $(\boldsymbol{d}_h^{n+1}, \boldsymbol{\omega}_h^{n+1}, \boldsymbol{u}_h^{n+1}) \in \boldsymbol{X}_h \times \boldsymbol{Y}_h \times \boldsymbol{W}_h$.

Proof To begin with, for any $(\boldsymbol{\xi}_h, \boldsymbol{\theta}_h, \boldsymbol{v}_h) \in \boldsymbol{X}_h \times \boldsymbol{Y}_h \times \boldsymbol{W}_h$, we can rewrite (3.35a) as

$$
\begin{aligned}
&2\mathcal{M}_{h1}(\boldsymbol{d}_h^{n+\frac{1}{2}}, \boldsymbol{\theta}_h) - 2\mathcal{M}_{h1}(\boldsymbol{d}_h^n, \boldsymbol{\theta}_h) + \tau\mathcal{D}_h(\boldsymbol{u}_h^{n+\frac{1}{2}}; \widetilde{\boldsymbol{d}}_h^{n+\frac{1}{2}}, \boldsymbol{\theta}_h) + \gamma\tau\mathcal{M}_{h1}(\boldsymbol{\omega}_h^{n+\frac{1}{2}}, \boldsymbol{\theta}_h) \\
&- 2\mathcal{M}_{h1}(\boldsymbol{\omega}_h^{n+\frac{1}{2}}, \boldsymbol{\xi}_h) + 2\lambda\mathcal{A}_{h1}(\boldsymbol{d}_h^{n+\frac{1}{2}}, \boldsymbol{\xi}_h) \\
&+ \frac{1}{\varepsilon^2}(((2\boldsymbol{\Pi}_k^0\boldsymbol{d}_h^{n+\frac{1}{2}} - \boldsymbol{\Pi}_k^0\boldsymbol{d}_h^n)^2 + (\boldsymbol{\Pi}_k^0\boldsymbol{d}_h^n)^2)\boldsymbol{\Pi}_k^0\boldsymbol{d}_h^{n+\frac{1}{2}}, \boldsymbol{\Pi}_k^0\boldsymbol{\xi}_h) \\
&- \frac{2}{\varepsilon^2}(\boldsymbol{\Pi}_k^0\widetilde{\boldsymbol{d}}_h^{n+\frac{1}{2}}, \boldsymbol{\Pi}_k^0\boldsymbol{\xi}_h) + 2\mathcal{M}_{h2}(\boldsymbol{u}_h^{n+\frac{1}{2}}, \boldsymbol{v}_h) - 2\mathcal{M}_{h2}(\boldsymbol{u}_h^n, \boldsymbol{v}_h) \\
&+ \tau\mathcal{C}_h(\widetilde{\boldsymbol{u}}_h^{n+\frac{1}{2}}; \boldsymbol{u}_h^{n+\frac{1}{2}}, \boldsymbol{v}_h) + \nu\tau\mathcal{A}_{h2}(\boldsymbol{u}_h^{n+\frac{1}{2}}, \boldsymbol{v}_h) - \tau\mathcal{D}_h(\boldsymbol{v}_h; \widetilde{\boldsymbol{d}}_h^{n+\frac{1}{2}}, \boldsymbol{\omega}_h^{n+\frac{1}{2}}) = 0.
\end{aligned}
\tag{3.40}
$$

Then, we define a mapping $\Psi : \boldsymbol{X}_h \times \boldsymbol{Y}_h \times \boldsymbol{W}_h \to \boldsymbol{X}_h \times \boldsymbol{Y}_h \times \boldsymbol{W}_h$. Given $(\boldsymbol{d}_h^{n-1}, \boldsymbol{u}_h^{n-1}) \in \boldsymbol{X}_h \times \boldsymbol{W}_h$ and $(\boldsymbol{d}_h^n, \boldsymbol{\omega}_h^n, \boldsymbol{u}_h^n) \in \boldsymbol{X}_h \times \boldsymbol{Y}_h \times \boldsymbol{W}_h$, find $(z_1, z_2, z_3) \in \boldsymbol{X}_h \times \boldsymbol{Y}_h \times \boldsymbol{W}_h$ such that

$$
\begin{aligned}
&(\Psi(z_1, z_2, z_3), (\boldsymbol{\xi}_h, \boldsymbol{\theta}_h, \boldsymbol{v}_h)) \\
&= 2\mathcal{M}_{h1}(z_1, \boldsymbol{\theta}_h) - 2\mathcal{M}_{h1}(\boldsymbol{d}_h^n, \boldsymbol{\theta}_h) + \tau\mathcal{D}_h(z_3; \widetilde{\boldsymbol{d}}_h^{n+\frac{1}{2}}, \boldsymbol{\theta}_h) \\
&\quad + \gamma\tau\mathcal{M}_{h1}(z_2, \boldsymbol{\theta}_h) - 2\mathcal{M}_{h1}(z_2, \boldsymbol{\xi}_h) + 2\lambda\mathcal{A}_{h1}(z_1, \boldsymbol{\xi}_h) \\
&\quad + \frac{1}{\varepsilon^2}(((2\boldsymbol{\Pi}_k^0 z_1 - \boldsymbol{\Pi}_k^0\boldsymbol{d}_h^n)^2 + (\boldsymbol{\Pi}_k^0\boldsymbol{d}_h^n)^2)\boldsymbol{\Pi}_k^0 z_1, \boldsymbol{\Pi}_k^0\boldsymbol{\xi}_h) \\
&\quad - \frac{2}{\varepsilon^2}(\boldsymbol{\Pi}_k^0\widetilde{\boldsymbol{d}}_h^{n+\frac{1}{2}}, \boldsymbol{\Pi}_k^0\boldsymbol{\xi}_h) + 2\mathcal{M}_{h2}(z_3, \boldsymbol{v}_h) - 2\mathcal{M}_{h2}(\boldsymbol{u}_h^n, \boldsymbol{v}_h) \\
&\quad + \tau\mathcal{C}_h(\widetilde{\boldsymbol{u}}_h^{n+\frac{1}{2}}; z_3, \boldsymbol{v}_h) + \nu\tau\mathcal{A}_{h2}(z_3, \boldsymbol{v}_h) - \tau\mathcal{D}_h(\boldsymbol{v}_h; \widetilde{\boldsymbol{d}}_h^{n+\frac{1}{2}}, z_2),
\end{aligned}
\tag{3.41}
$$

for any $(\boldsymbol{\xi}_h, \boldsymbol{\theta}_h, \boldsymbol{v}_h) \in \boldsymbol{X}_h \times \boldsymbol{Y}_h \times \boldsymbol{W}_h$. By applying the Lemma 3.3, Lemma 3.5, the Cauchy-Schwarz inequality and inverse inequality, we have

$$
\begin{aligned}
&(\Psi(z_1, z_2, z_3), (\boldsymbol{\xi}_h, \boldsymbol{\theta}_h, \boldsymbol{v}_h)) \\
&\le \tilde{C}_1\|z_1\|_0\|\boldsymbol{\theta}_h\|_0 + \tilde{C}_1\|\boldsymbol{d}_h^n\|_0\|\boldsymbol{\theta}_h\|_0 + \hat{C}_1\tau h^{-1}|\widetilde{\boldsymbol{d}}_h^{n+\frac{1}{2}}|_1\|z_3\|_0\|\boldsymbol{\theta}_h\|_0 \\
&\quad + \tilde{C}_1\gamma\tau\|z_2\|_0\|\boldsymbol{\theta}_h\|_0 + \tilde{C}_1\|z_2\|_0\|\boldsymbol{\xi}_h\|_0 + \tilde{C}_3\lambda|z_1|_1|\boldsymbol{\xi}_h|_1 \\
&\quad + \frac{1}{\varepsilon^2}(4\|(\boldsymbol{\Pi}_k^0 z_1)^3\|_0 + 4h^{-1}\|\boldsymbol{\Pi}_k^0\boldsymbol{d}_h^n\|_0\|(\boldsymbol{\Pi}_k^0 z_1)^2\|_0 \\
&\quad + 2h^{-1}\|(\boldsymbol{\Pi}_k^0\boldsymbol{d}_h^n)^2\|_0\|\boldsymbol{\Pi}_k^0 z_1\|_0)\|\boldsymbol{\Pi}_k^0\boldsymbol{\xi}_h\|_0 \\
&\quad + \frac{2}{\varepsilon^2}\|\boldsymbol{\Pi}_k^0\widetilde{\boldsymbol{d}}_h^{n+\frac{1}{2}}\|_0\|\boldsymbol{\Pi}_k^0\boldsymbol{\xi}_h\|_0 + \tilde{C}_2\|z_3\|_0\|\boldsymbol{v}_h\|_0 + \tilde{C}_2\|\boldsymbol{u}_h^n\|_0\|\boldsymbol{v}_h\|_0 \\
&\quad + \hat{C}_4\tau|\widetilde{\boldsymbol{u}}_h^{n+\frac{1}{2}}|_1|z_3|_1|\boldsymbol{v}_h|_1 + \tilde{C}_4\nu\tau|z_3|_1|\boldsymbol{v}_h|_1 + \hat{C}_1\tau h^{-1}|\widetilde{\boldsymbol{d}}_h^{n+\frac{1}{2}}|_1\|\boldsymbol{v}_h\|_0\|z_2\|_0 \\
&\le C^*\{(\|z_1\|_0 + \|z_2\|_0 + \|z_3\|_0)\|\boldsymbol{\theta}_h\|_0 + (\|z_1\|_1 + \|z_2\|_0)\|\boldsymbol{\xi}_h\|_1 \\
&\quad + (\|z_2\|_0 + \|z_3\|_1)\|\boldsymbol{v}_h\|_1\}.
\end{aligned}
\tag{3.42}
$$

where C^* depends on $\tau, h, \gamma, \lambda, \varepsilon, \nu, \|\boldsymbol{d}_h^n\|_0, \|\boldsymbol{u}_h^n\|_0, |\widetilde{\boldsymbol{d}}_h^{n+\frac{1}{2}}|_1, |\widetilde{\boldsymbol{u}}_h^{n+\frac{1}{2}}|_1$. Therefore, we can get that the mapping Ψ is continuous.

Setting $(\boldsymbol{\xi}_h, \boldsymbol{\theta}_h, \boldsymbol{v}_h) = (z_1, z_2, z_3)$ in (3.41), from Lemma 3.2 and Lemma 3.3, the Cauchy-Schwarz inequality and inverse inequality, we obtain

$$
\begin{aligned}
&(\Psi(z_1, z_2, z_3), (z_1, z_2, z_3)) \\
&= 2\lambda|||z_1|||^2_{\mathcal{A}_1} + \frac{1}{\varepsilon^2}(((2\boldsymbol{\Pi}_k^0 z_1 - \boldsymbol{\Pi}_k^0 \boldsymbol{d}_h^n)^2 + (\boldsymbol{\Pi}_k^0 \boldsymbol{d}_h^n)^2)\boldsymbol{\Pi}_k^0 z_1, \boldsymbol{\Pi}_k^0 z_1) \\
&\quad - \frac{2}{\varepsilon^2}(\boldsymbol{\Pi}_k^0 \widetilde{\boldsymbol{d}}_h^{n+\frac{1}{2}}, \boldsymbol{\Pi}_k^0 z_1) \\
&\quad - 2\mathcal{M}_{h1}(\boldsymbol{d}_h^n, z_2) + \gamma\tau|||z_2|||^2_{\mathcal{M}_1} + 2|||z_3|||^2_{\mathcal{M}_2} - 2\mathcal{M}_{h2}(\boldsymbol{u}_h^n, z_3) \\
&\quad + \nu\tau|||z_3|||^2_{\mathcal{A}_2} \\
&\geq 2(\frac{\alpha_3\lambda}{h^2}\|z_1\|_0 - \frac{1}{\varepsilon^2}\|\widetilde{\boldsymbol{d}}_h^{n+\frac{1}{2}}\|_0)\|z_1\|_0 + (\alpha_1\gamma\tau\|z_2\|_0 - 2\tilde{C}_1\|\boldsymbol{d}_h^n\|_0)\|z_2\|_0 \\
&\quad + 2(\alpha_2\|z_3\|_0 - \tilde{C}_2\|\boldsymbol{u}_h^n\|_0)\|z_3\|_0 + \alpha_4\nu\tau|z_3|_1^2 \\
&\quad + \frac{1}{\varepsilon^2}\int_\Omega |2\boldsymbol{\Pi}_k^0 z_1 - \boldsymbol{\Pi}_k^0 \boldsymbol{d}_h^n|^2 |\boldsymbol{\Pi}_k^0 z_1|^2 d\boldsymbol{x} + \frac{1}{\varepsilon^2}\int_\Omega |\boldsymbol{\Pi}_k^0 \boldsymbol{d}_h^n|^2 |\boldsymbol{\Pi}_k^0 z_1|^2 d\boldsymbol{x}.
\end{aligned}
\tag{3.43}
$$

Hence, from (3.43) we infer that the mapping Ψ satisfies the following properties: there exists $\|\widetilde{\boldsymbol{d}}_h^{n+\frac{1}{2}}\|_0, \|\boldsymbol{d}_h^n\|_0, \|\boldsymbol{u}_h^n\|_0$ such that for $\forall(z_1, z_2, z_3) \in \boldsymbol{X}_h \times \boldsymbol{Y}_h \times \boldsymbol{W}_h$,

$$(\Psi(z_1, z_2, z_3), (z_1, z_2, z_3)) \geq 0,$$

with

$$\|z_1\|_0 = \frac{h^2}{\alpha_3\lambda\varepsilon^2}\|\widetilde{\boldsymbol{d}}_h^{n+\frac{1}{2}}\|_0, \;\; \|z_2\|_0 = \frac{2\tilde{C}_1}{\alpha_1\gamma\tau}\|\boldsymbol{d}_h^n\|_0, \;\; \|z_3\|_0 = \frac{\tilde{C}_2}{\alpha_2}\|\boldsymbol{u}_h^n\|_0.$$

It follows from the Brouwer's fixed point theorem (see [38]) that there exists $(\boldsymbol{d}_h^{n+\frac{1}{2}}, \boldsymbol{\omega}_h^{n+\frac{1}{2}}, \boldsymbol{u}_h^{n+\frac{1}{2}}) \in \boldsymbol{X}_h \times \boldsymbol{Y}_h \times \boldsymbol{W}_h$ such that

$$\Psi(\boldsymbol{d}_h^{n+\frac{1}{2}}, \boldsymbol{\omega}_h^{n+\frac{1}{2}}, \boldsymbol{u}_h^{n+\frac{1}{2}}) = 0,$$

which also implies the existence of the solution to (3.35a). Next, it suffices to establish the uniqueness of the solution to (3.35a).

Assume $(\boldsymbol{d}_{h1}^{n+1}, \boldsymbol{\omega}_{h1}^{n+1}, \boldsymbol{u}_{h1}^{n+1})$ and $(\boldsymbol{d}_{h2}^{n+1}, \boldsymbol{\omega}_{h2}^{n+1}, \boldsymbol{u}_{h2}^{n+1})$ are two solutions to (3.35a). Let $\boldsymbol{d}_h^{n+\frac{1}{2}} = \boldsymbol{d}_{h1}^{n+\frac{1}{2}} - \boldsymbol{d}_{h2}^{n+\frac{1}{2}}$, $\boldsymbol{\omega}_h^{n+\frac{1}{2}} = \boldsymbol{\omega}_{h1}^{n+\frac{1}{2}} - \boldsymbol{\omega}_{h2}^{n+\frac{1}{2}}$ and $\boldsymbol{u}_h^{n+\frac{1}{2}} = \boldsymbol{u}_{h1}^{n+\frac{1}{2}} - \boldsymbol{u}_{h2}^{n+\frac{1}{2}}$, for any $(\boldsymbol{\xi}_h, \boldsymbol{\theta}_h, \boldsymbol{v}_h) \in \boldsymbol{X}_h \times \boldsymbol{Y}_h \times \boldsymbol{W}_h$, we can get

$$\begin{aligned}
&2\mathcal{M}_{h1}(\boldsymbol{d}_h^{n+\frac{1}{2}}, \boldsymbol{\theta}_h) + \tau\mathcal{D}_h(\boldsymbol{u}_h^{n+\frac{1}{2}}; \widetilde{\boldsymbol{d}}_h^{n+\frac{1}{2}}, \boldsymbol{\theta}_h) + \gamma\tau\mathcal{M}_{h1}(\boldsymbol{\omega}_h^{n+\frac{1}{2}}, \boldsymbol{\theta}_h) \\
&- 2\mathcal{M}_{h1}(\boldsymbol{\omega}_h^{n+\frac{1}{2}}, \boldsymbol{\xi}_h) \\
&+ 2\lambda\mathcal{A}_{h1}(\boldsymbol{d}_h^{n+\frac{1}{2}}, \boldsymbol{\xi}_h) + \frac{1}{\varepsilon^2}(((2\boldsymbol{\Pi}_k^0\boldsymbol{d}_{h1}^{n+\frac{1}{2}} - \boldsymbol{\Pi}_k^0\boldsymbol{d}_h^n)^2 \\
&+ (\boldsymbol{\Pi}_k^0\boldsymbol{d}_h^n)^2)\boldsymbol{\Pi}_k^0\boldsymbol{d}_{h1}^{n+\frac{1}{2}}, \boldsymbol{\Pi}_k^0\boldsymbol{\xi}_h) \\
&- \frac{1}{\varepsilon^2}(((2\boldsymbol{\Pi}_k^0\boldsymbol{d}_{h2}^{n+\frac{1}{2}} - \boldsymbol{\Pi}_k^0\boldsymbol{d}_h^n)^2 + (\boldsymbol{\Pi}_k^0\boldsymbol{d}_h^n)^2)\boldsymbol{\Pi}_k^0\boldsymbol{d}_{h2}^{n+\frac{1}{2}}, \boldsymbol{\Pi}_k^0\boldsymbol{\xi}_h) + 2\mathcal{M}_{h2}(\boldsymbol{u}_h^{n+\frac{1}{2}}, \boldsymbol{v}_h) \\
&+ \tau\mathcal{C}_h(\widetilde{\boldsymbol{u}}_h^{n+\frac{1}{2}}; \boldsymbol{u}_h^{n+\frac{1}{2}}, \boldsymbol{v}_h) + \nu\tau\mathcal{A}_{h2}(\boldsymbol{u}_h^{n+\frac{1}{2}}, \boldsymbol{v}_h) - \tau\mathcal{D}_h(\boldsymbol{v}_h; \widetilde{\boldsymbol{d}}_h^{n+\frac{1}{2}}, \boldsymbol{\omega}_h^{n+\frac{1}{2}}) = 0.
\end{aligned} \tag{3.44}$$

By taking $\boldsymbol{\theta}_h = \boldsymbol{\omega}_h^{n+\frac{1}{2}}$, $\boldsymbol{\xi}_h = \boldsymbol{d}_h^{n+\frac{1}{2}}$ and $\boldsymbol{v}_h = \boldsymbol{u}_h^{n+\frac{1}{2}}$ in (3.44), we can obtain

$$\begin{aligned}
&\gamma\tau|||\boldsymbol{\omega}_h^{n+\frac{1}{2}}|||_{\mathcal{M}_1}^2 + 2\lambda|||\boldsymbol{d}_h^{n+\frac{1}{2}}|||_{\mathcal{A}_1}^2 + 2|||\boldsymbol{u}_h^{n+\frac{1}{2}}|||_{\mathcal{M}_2}^2 + \nu\tau|||\boldsymbol{u}_h^{n+\frac{1}{2}}|||_{\mathcal{A}_2}^2 \\
&+ \frac{1}{\varepsilon^2}|\boldsymbol{\Pi}_k^0\boldsymbol{d}_h^n|^2\|\boldsymbol{\Pi}_k^0\boldsymbol{d}_h^{n+\frac{1}{2}}\|_0^2 + \frac{1}{\varepsilon^2}((2\boldsymbol{\Pi}_k^0\boldsymbol{d}_{h1}^{n+\frac{1}{2}} - \boldsymbol{\Pi}_k^0\boldsymbol{d}_h^n)^2\boldsymbol{\Pi}_k^0\boldsymbol{d}_{h1}^{n+\frac{1}{2}}, \boldsymbol{\Pi}_k^0\boldsymbol{d}_h^{n+\frac{1}{2}}) \\
&- \frac{1}{\varepsilon^2}((2\boldsymbol{\Pi}_k^0\boldsymbol{d}_{h2}^{n+\frac{1}{2}} - \boldsymbol{\Pi}_k^0\boldsymbol{d}_h^n)^2\boldsymbol{\Pi}_k^0\boldsymbol{d}_{h2}^{n+\frac{1}{2}}, \boldsymbol{\Pi}_k^0\boldsymbol{d}_h^{n+\frac{1}{2}}) = 0.
\end{aligned} \tag{3.45}$$

Using the inequality $\big||2\boldsymbol{a}_1 - \boldsymbol{a}|^2\boldsymbol{a}_1 - |2\boldsymbol{a}_2 - \boldsymbol{a}|^2\boldsymbol{a}_2\big| \le 4(|\boldsymbol{a}_1| + |\boldsymbol{a}_2| + \frac{1}{2}|\boldsymbol{a}|)^2|\boldsymbol{a}_1 - \boldsymbol{a}_2|$ (see [4, 25]), from Theorem 3.1 we have

$$\begin{aligned}
&\frac{1}{\varepsilon^2}((2\boldsymbol{\Pi}_k^0\boldsymbol{d}_{h1}^{n+\frac{1}{2}} - \boldsymbol{\Pi}_k^0\boldsymbol{d}_h^n)^2\boldsymbol{\Pi}_k^0\boldsymbol{d}_{h1}^{n+\frac{1}{2}}, \boldsymbol{\Pi}_k^0\boldsymbol{d}_h^{n+\frac{1}{2}}) \\
&- \frac{1}{\varepsilon^2}((2\boldsymbol{\Pi}_k^0\boldsymbol{d}_{h2}^{n+\frac{1}{2}} - \boldsymbol{\Pi}_k^0\boldsymbol{d}_h^n)^2\boldsymbol{\Pi}_k^0\boldsymbol{d}_{h2}^{n+\frac{1}{2}}, \boldsymbol{\Pi}_k^0\boldsymbol{d}_h^{n+\frac{1}{2}}) \\
&\le \frac{1}{\varepsilon^2}(\max\{|\boldsymbol{\Pi}_k^0\boldsymbol{d}_{h1}^{n+\frac{1}{2}}|, |\boldsymbol{\Pi}_k^0\boldsymbol{d}_{h2}^{n+\frac{1}{2}}|, |\boldsymbol{\Pi}_k^0\boldsymbol{d}_h^n|\})^2\|\boldsymbol{\Pi}_k^0\boldsymbol{d}_h^{n+\frac{1}{2}}\|_0^2 \le C(\varepsilon, \boldsymbol{d}_h^0)\|\boldsymbol{\Pi}_k^0\boldsymbol{d}_h^{n+\frac{1}{2}}\|_0^2.
\end{aligned} \tag{3.46}$$

Choosing the proper parameters ε such that $\frac{1}{\varepsilon^2}|\boldsymbol{\Pi}_k^0\boldsymbol{d}_h^n|^2 - C(\varepsilon, \boldsymbol{d}_h^0) \ge 0$, combining (3.45)–(3.46), we can arrive at

$$\gamma\tau|||\boldsymbol{\omega}_h^{n+\frac{1}{2}}|||_{\mathcal{M}_1}^2 + 2\lambda|||\boldsymbol{d}_h^{n+\frac{1}{2}}|||_{\mathcal{A}_1}^2 + 2|||\boldsymbol{u}_h^{n+\frac{1}{2}}|||_{\mathcal{M}_2}^2 + \nu\tau|||\boldsymbol{u}_h^{n+\frac{1}{2}}|||_{\mathcal{A}_2}^2 \le 0. \tag{3.47}$$

Therefore, we conclude that

$$\boldsymbol{d}_h^{n+\frac{1}{2}} = 0,\ \boldsymbol{\omega}_h^{n+\frac{1}{2}} = 0,\ \boldsymbol{u}_h^{n+\frac{1}{2}} = 0.$$

The proof is finished.

4 Error estimates

This section is devoted to the error estimates of the scheme (3.35a). We henceforth denote by C a generic constant that is independent of the mesh size h and the time step τ but possibly depends on the data and the solution. Whenever no confusion is possible we use the expression $a \lesssim b$ to say that there exists a generic constant C such that $a \leq Cb$.

In order to derive the error estimates for the numerical scheme in terms of time and space discretization, we shall assume that the weak solution to the system (2.5a) are regular enough. More precisely, we assume

$$(\mathbf{A}): \begin{cases} \boldsymbol{d}, \boldsymbol{d}_t, \boldsymbol{d}_{tt} \in L^\infty(0,T;\boldsymbol{H}^{k+1}(\Omega)\cap \boldsymbol{W}^{1,\infty}(\Omega)),\ \boldsymbol{d}_{ttt} \in L^\infty(0,T;\boldsymbol{X}); \\ \boldsymbol{\omega}, \boldsymbol{\omega}_t \in L^\infty(0,T;\boldsymbol{H}^{k+1}(\Omega)\cap \boldsymbol{L}^{\infty}(\Omega)),\ \boldsymbol{\omega}_{tt} \in L^\infty(0,T;\boldsymbol{Y}); \\ \boldsymbol{u}, \boldsymbol{u}_t, \boldsymbol{u}_{tt} \in L^\infty(0,T;\boldsymbol{H}^{k+1}(\Omega)\cap \boldsymbol{L}^{\infty}(\Omega)),\ \boldsymbol{u}_{ttt} \in L^\infty(0,T;\boldsymbol{V}). \end{cases}$$

The weak formulation of problem (2.5a) satisfies the following truncation forms:

$$\mathcal{M}_1(\delta_t\boldsymbol{d}^{n+1},\boldsymbol{\theta}_h)+\frac{1}{2}\mathcal{D}(\boldsymbol{u}^{n+1};\boldsymbol{d}^{n+1},\boldsymbol{\theta}_h)+\frac{1}{2}\mathcal{D}(\boldsymbol{u}^{n};\boldsymbol{d}^{n},\boldsymbol{\theta}_h) \tag{4.1a}$$
$$+\gamma\mathcal{M}_1(\boldsymbol{\omega}^{n+\frac{1}{2}},\boldsymbol{\theta}_h)=\mathcal{M}_1(R_{\boldsymbol{d}}^{n+\frac{1}{2}},\boldsymbol{\theta}_h),$$
$$\mathcal{M}_1(\boldsymbol{\omega}^{n+\frac{1}{2}},\boldsymbol{\xi}_h)=\lambda\mathcal{A}_1(\boldsymbol{d}^{n+\frac{1}{2}},\boldsymbol{\xi}_h)$$
$$+\frac{1}{2\varepsilon^2}((\boldsymbol{d}^{n+1})^3-\boldsymbol{d}^{n+1}+(\boldsymbol{d}^{n})^3-\boldsymbol{d}^{n},\boldsymbol{\xi}_h), \tag{4.1b}$$
$$\mathcal{M}_2(\delta_t\boldsymbol{u}^{n+1},\boldsymbol{v}_h)+\frac{1}{2}\mathcal{C}(\boldsymbol{u}^{n+1};\boldsymbol{u}^{n+1},\boldsymbol{v}_h)+\frac{1}{2}\mathcal{C}(\boldsymbol{u}^{n};\boldsymbol{u}^{n},\boldsymbol{v}_h)$$
$$+\nu\mathcal{A}_2(\boldsymbol{u}^{n+\frac{1}{2}},\boldsymbol{v}_h) \tag{4.1c}$$
$$-\frac{1}{2}\mathcal{D}(\boldsymbol{v}_h;\boldsymbol{d}^{n+1},\boldsymbol{\omega}^{n+1})-\frac{1}{2}\mathcal{D}(\boldsymbol{v}_h;\boldsymbol{d}^{n+1},\boldsymbol{\omega}^{n+1})=\mathcal{M}_2(R_{\boldsymbol{u}}^{n+\frac{1}{2}},\boldsymbol{v}_h),$$

where $R_{\boldsymbol{d}}^{n+\frac{1}{2}} := \delta_t\boldsymbol{d}^{n+1}-\boldsymbol{d}_t^{n+\frac{1}{2}}$, $R_{\boldsymbol{u}}^{n+\frac{1}{2}} := \delta_t\boldsymbol{u}^{n+1}-\boldsymbol{u}_t^{n+\frac{1}{2}}$ denote the truncation errors. Thus, we can easily establish the following estimate, provided that the exact solutions are sufficiently smooth or in the assumption (**A**).

Lemma 4.1 *Under the assumption (**A**), it holds*

$$\|R_{\boldsymbol{d}}^{n+\frac{1}{2}}\|_0+\|R_{\boldsymbol{u}}^{n+\frac{1}{2}}\|_0 \lesssim \tau^2,\ n=0,1,\cdots,N-1.$$

Proof Using the Taylor expansions, we have

$$
\begin{aligned}
\|R_{\boldsymbol{d}}^{n+\frac{1}{2}}\|_0^2 s &= \|\frac{1}{2\tau}\int_{t^n}^{t^{n+1}}(t^{n+1}-t)^2\boldsymbol{d}_{ttt}ds - \frac{1}{2}\int_{t^n}^{t^{n+1}}(t^{n+1}-t)\boldsymbol{d}_{ttt}ds\|_0^2 \\
&\lesssim \frac{1}{\tau^2}\int_{t^n}^{t^{n+1}}(t^{n+1}-t)^4 ds\cdot\int_{t^n}^{t^{n+1}}\|\boldsymbol{d}_{ttt}\|_0^2 ds + \int_{t^n}^{t^{n+1}}(t^{n+1}-t)^2 ds \\
&\quad \cdot\int_{t^n}^{t^{n+1}}\|\boldsymbol{d}_{ttt}\|_0^2 ds \\
&\lesssim \tau^3\int_{t^n}^{t^{n+1}}\|\boldsymbol{d}_{ttt}\|_0^2 ds \lesssim \tau^4.
\end{aligned}
$$

Similarly, we can prove that

$$
\|R_{\boldsymbol{u}}^{n+\frac{1}{2}}\|_0^2 \lesssim \tau^4.
$$

This completes the proof.

Let $(\boldsymbol{d},\boldsymbol{\omega},\boldsymbol{u},p)$ be the solution of (2.8a) and $(\boldsymbol{d}_h^n,\boldsymbol{\omega}_h^n,\boldsymbol{u}_h^n)$ be the solution of (3.35a), we introduce the following error decompositions:

$$
\begin{aligned}
e_{\boldsymbol{d}}^n &:= \boldsymbol{d}_h^n - \boldsymbol{d}^n = \eta_{\boldsymbol{d}}^n + \chi_{\boldsymbol{d}}^n, \quad \eta_{\boldsymbol{d}}^n := \boldsymbol{d}_h^n - \boldsymbol{d}_I^n, \quad \chi_{\boldsymbol{d}}^n := \boldsymbol{d}_I^n - \boldsymbol{d}^n; \\
e_{\boldsymbol{\omega}}^n &:= \boldsymbol{\omega}_h^n - \boldsymbol{\omega}^n = \eta_{\boldsymbol{\omega}}^n + \chi_{\boldsymbol{\omega}}^n, \quad \eta_{\boldsymbol{\omega}}^n := \boldsymbol{\omega}_h^n - \boldsymbol{\omega}_I^n, \quad \chi_{\boldsymbol{\omega}}^n := \boldsymbol{\omega}_I^n - \boldsymbol{\omega}^n; \\
e_{\boldsymbol{u}}^n &:= \boldsymbol{u}_h^n - \boldsymbol{u}^n = \eta_{\boldsymbol{u}}^n + \chi_{\boldsymbol{u}}^n, \quad \eta_{\boldsymbol{u}}^n := \boldsymbol{u}_h^n - \boldsymbol{u}_I^n, \quad \chi_{\boldsymbol{u}}^n := \boldsymbol{u}_I^n - \boldsymbol{u}^n,
\end{aligned}
$$

there exist $\boldsymbol{d}_I \in \boldsymbol{X}_h$, $\boldsymbol{\omega}_I \in \boldsymbol{Y}_h$, $\boldsymbol{u}_I \in \boldsymbol{W}_h$ as the interpolations of the exact solution $\boldsymbol{d}$, $\boldsymbol{\omega}$, $\boldsymbol{u}$ of the problem (2.8a), which satisfy (3.35a), (3.10), respectively.

By subtracting the corresponding fully discrete scheme (3.35a) from the equations (4.1a), we derive the error equations as follows

$$
\begin{aligned}
&\mathcal{M}_{h1}(\delta_t\eta_{\boldsymbol{d}}^{n+1},\boldsymbol{\theta}_h) = \mathcal{M}_1(\delta_t\boldsymbol{d}^{n+1},\boldsymbol{\theta}_h) - \mathcal{M}_{h1}(\delta_t\boldsymbol{d}_I^{n+1},\boldsymbol{\theta}_h) \\
&\quad + \frac{1}{2}\mathcal{D}(\boldsymbol{u}^{n+1};\boldsymbol{d}^{n+1},\boldsymbol{\theta}_h) + \frac{1}{2}\mathcal{D}(\boldsymbol{u}^n;\boldsymbol{d}^n,\boldsymbol{\theta}_h) - \mathcal{D}_h(\boldsymbol{u}_h^{n+\frac{1}{2}};\widetilde{\boldsymbol{d}}_h^{n+\frac{1}{2}},\boldsymbol{\theta}_h) \\
&\quad + \gamma\mathcal{M}_1(\boldsymbol{\omega}^{n+\frac{1}{2}},\boldsymbol{\theta}_h) - \gamma\mathcal{M}_{h1}(\boldsymbol{\omega}_h^{n+\frac{1}{2}},\boldsymbol{\theta}_h) - \mathcal{M}_1(R_{\boldsymbol{d}}^{n+\frac{1}{2}},\boldsymbol{\theta}_h),
\end{aligned}
\tag{4.2}
$$

$$
\begin{aligned}
&\lambda\mathcal{A}_{h1}(\eta_{\boldsymbol{d}}^{n+\frac{1}{2}},\boldsymbol{\xi}_h) = \lambda\mathcal{A}_1(\boldsymbol{d}^{n+\frac{1}{2}},\boldsymbol{\xi}_h) - \lambda\mathcal{A}_{h1}(\boldsymbol{d}_I^{n+\frac{1}{2}},\boldsymbol{\xi}_h) \\
&\quad - \mathcal{M}_1(\boldsymbol{\omega}^{n+\frac{1}{2}},\boldsymbol{\xi}_h) + \mathcal{M}_{h1}(\boldsymbol{\omega}_h^{n+\frac{1}{2}},\boldsymbol{\xi}_h) - \frac{1}{\varepsilon^2}(\boldsymbol{d}^{n+\frac{1}{2}},\boldsymbol{\xi}_h) + \frac{1}{\varepsilon^2}(\boldsymbol{\Pi}_k^0\widetilde{\boldsymbol{d}}_h^{n+\frac{1}{2}},\boldsymbol{\Pi}_k^0\boldsymbol{\xi}_h) \\
&\quad + \frac{1}{2\varepsilon^2}((\boldsymbol{d}^{n+1})^3 + (\boldsymbol{d}^n)^3,\boldsymbol{\xi}_h) - \frac{1}{2\varepsilon^2}(((\boldsymbol{\Pi}_k^0\boldsymbol{d}_h^{n+1})^2 + (\boldsymbol{\Pi}_k^0\boldsymbol{d}_h^n)^2)\boldsymbol{\Pi}_k^0\boldsymbol{d}_h^{n+\frac{1}{2}},\boldsymbol{\Pi}_k^0\boldsymbol{\xi}_h),
\end{aligned}
\tag{4.3}
$$

$$\begin{aligned}&\mathcal{M}_{h2}(\delta_t\eta_{\boldsymbol{u}}^{n+1},\boldsymbol{v}_h)+\nu\mathcal{A}_{h2}(\eta_{\boldsymbol{u}}^{n+\frac{1}{2}},\boldsymbol{v}_h)=\mathcal{M}_2(\delta_t\boldsymbol{u}^{n+1},\boldsymbol{v}_h)-\mathcal{M}_{h2}(\delta_t\boldsymbol{u}_I^{n+1},\boldsymbol{v}_h)\\&+\nu\mathcal{A}_2(\boldsymbol{u}^{n+\frac{1}{2}},\boldsymbol{v}_h)-\nu\mathcal{A}_{h2}(\boldsymbol{u}_I^{n+\frac{1}{2}},\boldsymbol{v}_h)+\frac{1}{2}\mathcal{C}(\boldsymbol{u}^{n+1};\boldsymbol{u}^{n+1},\boldsymbol{v}_h)+\frac{1}{2}\mathcal{C}(\boldsymbol{u}^n;\boldsymbol{u}^n,\boldsymbol{v}_h)\\&-\mathcal{C}_h(\widetilde{\boldsymbol{u}}_h^{n+\frac{1}{2}};\boldsymbol{u}_h^{n+\frac{1}{2}},\boldsymbol{v}_h)-\frac{1}{2}\mathcal{D}(\boldsymbol{v}_h;\boldsymbol{d}^{n+1},\boldsymbol{\omega}^{n+1})-\frac{1}{2}\mathcal{D}(\boldsymbol{v}_h;\boldsymbol{d}^n,\boldsymbol{\omega}^n)\\&+\mathcal{D}_h(\boldsymbol{v}_h;\widetilde{\boldsymbol{d}}_h^{n+\frac{1}{2}},\boldsymbol{\omega}_h^{n+\frac{1}{2}})-\mathcal{M}_2(R_{\boldsymbol{u}}^{n+\frac{1}{2}},\boldsymbol{v}_h).\end{aligned} \tag{4.4}$$

Theorem 4.1 *Under the assumption (**A**), the following inequality holds*

$$\|e_{\boldsymbol{u}}^{m+1}\|_0^2+|e_{\boldsymbol{d}}^{m+1}|_1^2+\tau\sum_{n=0}^{m}(|e_{\boldsymbol{u}}^{n+\frac{1}{2}}|_1^2+\|\delta_te_{\boldsymbol{d}}^{n+1}\|_0^2+\|e_{\boldsymbol{\omega}}^{n+\frac{1}{2}}\|_0^2)\lesssim\tau^4+h^{2k}.$$

Proof First of all, we make the following induction assumption for the error functions at the previous time steps:

$$\|\eta_{\boldsymbol{u}}^m\|_0^2+|\eta_{\boldsymbol{d}}^m|_1^2\le C_0^\dagger(\tau^4+h^{2k}), \tag{4.5}$$

for $n\le m\le N-1$. Such an induction assumption will be recovered by the error estimate at the next time step t^{m+1}.

The application of the induction assumption (4.5) (for $n\le m\le N-1$) and the assumption (**A**) yields (see [40, 42, 48, 49])

$$\begin{aligned}\|\boldsymbol{d}_h^m\|_{\boldsymbol{W}^{1,\infty}(\Omega)}^2&\le C\|\boldsymbol{d}^m\|_{\boldsymbol{W}^{1,\infty}(\Omega)}^2+C\|\boldsymbol{d}_I^m-\boldsymbol{d}^m\|_{\boldsymbol{W}^{1,\infty}(\Omega)}^2+C\|\eta_{\boldsymbol{d}}^m\|_{\boldsymbol{W}^{1,\infty}(\Omega)}^2\\&\le C\|\boldsymbol{d}^m\|_{\boldsymbol{W}^{1,\infty}(\Omega)}^2+Ch^{k-2}|\boldsymbol{d}^m|_k^2+CC_0^\dagger h^{-2}(\tau^4+h^{2k})\le C,\end{aligned} \tag{4.6}$$

$$\begin{aligned}\|\boldsymbol{u}_h^m\|_{\boldsymbol{L}^\infty(\Omega)}^2&\le C\|\boldsymbol{u}^m\|_{\boldsymbol{L}^\infty(\Omega)}^2+C\|\boldsymbol{u}_I^m-\boldsymbol{u}^m\|_{\boldsymbol{L}^\infty(\Omega)}^2+C\|\eta_{\boldsymbol{u}}^m\|_{\boldsymbol{L}^\infty(\Omega)}^2\\&\le C\|\boldsymbol{u}^m\|_{\boldsymbol{L}^\infty(\Omega)}^2+Ch^k|\boldsymbol{u}^m|_{k+1}^2+CC_0^\dagger h^{-2}(\tau^4+h^{2k})\le C,\end{aligned} \tag{4.7}$$

for $\tau\le\frac{h^2}{\sqrt{CC_0^\dagger}}$ and $h<h_0$, where h_0 is a small positive constant. Subsequently, we will establish the error estimate at t^{m+1} and recover (4.5). By taking $\boldsymbol{\theta}_h=\tau\delta_t\eta_{\boldsymbol{d}}^{n+1}$ and $\tau\eta_{\boldsymbol{\omega}}^{n+\frac{1}{2}}$ in (4.2), we obtain

$$\begin{aligned}&\tau|||\delta_t\eta_{\boldsymbol{d}}^{n+1}|||_{\mathcal{M}_1}^2=\tau\mathcal{M}_1(\delta_t\boldsymbol{d}^{n+1},\delta_t\eta_{\boldsymbol{d}}^{n+1})-\tau\mathcal{M}_{h1}(\delta_t\boldsymbol{d}_I^{n+1},\delta_t\eta_{\boldsymbol{d}}^{n+1})\\&+\frac{\tau}{2}\mathcal{D}(\boldsymbol{u}^{n+1};\boldsymbol{d}^{n+1},\delta_t\eta_{\boldsymbol{d}}^{n+1})+\frac{\tau}{2}\mathcal{D}(\boldsymbol{u}^n;\boldsymbol{d}^n,\delta_t\eta_{\boldsymbol{d}}^{n+1})\\&-\tau\mathcal{D}_h(\boldsymbol{u}_h^{n+\frac{1}{2}};\widetilde{\boldsymbol{d}}_h^{n+\frac{1}{2}},\delta_t\eta_{\boldsymbol{d}}^{n+1})\\&+\gamma\tau\mathcal{M}_1(\boldsymbol{\omega}^{n+\frac{1}{2}},\delta_t\eta_{\boldsymbol{d}}^{n+1})-\gamma\tau\mathcal{M}_{h1}(\boldsymbol{\omega}_h^{n+\frac{1}{2}},\delta_t\eta_{\boldsymbol{d}}^{n+1})-\tau\mathcal{M}_1(R_{\boldsymbol{d}}^{n+\frac{1}{2}},\delta_t\eta_{\boldsymbol{d}}^{n+1}),\end{aligned} \tag{4.8}$$

and

$$
\begin{aligned}
\gamma\tau|||\eta_{\boldsymbol{\omega}}^{n+\frac{1}{2}}|||_{\mathcal{M}_1}^2 &= \tau\mathcal{M}_1(\delta_t \boldsymbol{d}^{n+1}, \eta_{\boldsymbol{\omega}}^{n+\frac{1}{2}}) - \tau\mathcal{M}_{h1}(\delta_t \boldsymbol{d}_I^{n+1}, \eta_{\boldsymbol{\omega}}^{n+\frac{1}{2}}) \\
&- \tau\mathcal{M}_{h1}(\delta_t \eta_{\boldsymbol{d}}^{n+1}, \eta_{\boldsymbol{\omega}}^{n+\frac{1}{2}}) \\
&+ \frac{\tau}{2}\mathcal{D}(\boldsymbol{u}^{n+1}; \boldsymbol{d}^{n+1}, \eta_{\boldsymbol{\omega}}^{n+\frac{1}{2}}) + \frac{\tau}{2}\mathcal{D}(\boldsymbol{u}^{n}; \boldsymbol{d}^{n}, \eta_{\boldsymbol{\omega}}^{n+\frac{1}{2}}) - \tau\mathcal{D}_h(\boldsymbol{u}_h^{n+\frac{1}{2}}; \widetilde{\boldsymbol{d}}_h^{n+\frac{1}{2}}, \eta_{\boldsymbol{\omega}}^{n+\frac{1}{2}}) \\
&+ \gamma\tau\mathcal{M}_1(\boldsymbol{\omega}^{n+\frac{1}{2}}, \eta_{\boldsymbol{\omega}}^{n+\frac{1}{2}}) - \gamma\tau\mathcal{M}_{h1}(\boldsymbol{\omega}_I^{n+\frac{1}{2}}, \eta_{\boldsymbol{\omega}}^{n+\frac{1}{2}}) - \tau\mathcal{M}_1(R_{\boldsymbol{d}}^{n+\frac{1}{2}}, \eta_{\boldsymbol{\omega}}^{n+\frac{1}{2}}).
\end{aligned} \tag{4.9}
$$

Taking $\boldsymbol{\xi}_h = \gamma\tau\delta_t\eta_{\boldsymbol{d}}^{n+1}$ and $\tau\delta_t\eta_{\boldsymbol{d}}^{n+1}$ in (4.3), we derive

$$
\begin{aligned}
\frac{\lambda\gamma}{2}|||\eta_{\boldsymbol{d}}^{n+1}|||_{\mathcal{A}_1}^2 - \frac{\lambda\gamma}{2}|||\eta_{\boldsymbol{d}}^{n}|||_{\mathcal{A}_1}^2 &= \lambda\gamma\tau\mathcal{A}_1(\boldsymbol{d}^{n+\frac{1}{2}}, \delta_t\eta_{\boldsymbol{d}}^{n+1}) \\
&- \lambda\gamma\tau\mathcal{A}_{h1}(\boldsymbol{d}_I^{n+\frac{1}{2}}, \delta_t\eta_{\boldsymbol{d}}^{n+1}) \\
&- \gamma\tau\mathcal{M}_1(\boldsymbol{\omega}^{n+\frac{1}{2}}, \delta_t\eta_{\boldsymbol{d}}^{n+1}) + \gamma\tau\mathcal{M}_{h1}(\boldsymbol{\omega}_h^{n+\frac{1}{2}}, \delta_t\eta_{\boldsymbol{d}}^{n+1}) - \frac{\gamma\tau}{\varepsilon^2}(\boldsymbol{d}^{n+\frac{1}{2}}, \delta_t\eta_{\boldsymbol{d}}^{n+1}) \\
&+ \frac{\gamma\tau}{\varepsilon^2}(\boldsymbol{\Pi}_k^0\widetilde{\boldsymbol{d}}_h^{n+\frac{1}{2}}, \boldsymbol{\Pi}_k^0\delta_t\eta_{\boldsymbol{d}}^{n+1}) + \frac{\gamma\tau}{2\varepsilon^2}((\boldsymbol{d}^{n+1})^3 + (\boldsymbol{d}^n)^3, \delta_t\eta_{\boldsymbol{d}}^{n+1}) \\
&- \frac{\gamma\tau}{2\varepsilon^2}(((\boldsymbol{\Pi}_k^0\boldsymbol{d}_h^{n+1})^2 + (\boldsymbol{\Pi}_k^0\boldsymbol{d}_h^{n})^2)\boldsymbol{\Pi}_k^0\boldsymbol{d}_h^{n+\frac{1}{2}}, \boldsymbol{\Pi}_k^0\delta_t\eta_{\boldsymbol{d}}^{n+1}),
\end{aligned} \tag{4.10}
$$

and

$$
\begin{aligned}
\frac{\lambda}{2}|||\eta_{\boldsymbol{d}}^{n+1}|||_{\mathcal{A}_1}^2 - \frac{\lambda}{2}|||\eta_{\boldsymbol{d}}^{n}|||_{\mathcal{A}_1}^2 &= \lambda\tau\mathcal{A}_1(\boldsymbol{d}^{n+\frac{1}{2}}, \delta_t\eta_{\boldsymbol{d}}^{n+1}) - \lambda\tau\mathcal{A}_{h1}(\boldsymbol{d}_I^{n+\frac{1}{2}}, \delta_t\eta_{\boldsymbol{d}}^{n+1}) \\
&- \tau\mathcal{M}_1(\boldsymbol{\omega}^{n+\frac{1}{2}}, \delta_t\eta_{\boldsymbol{d}}^{n+1}) + \tau\mathcal{M}_{h1}(\boldsymbol{\omega}_I^{n+\frac{1}{2}}, \delta_t\eta_{\boldsymbol{d}}^{n+1}) + \tau\mathcal{M}_{h1}(\eta_{\boldsymbol{\omega}}^{n+\frac{1}{2}}, \delta_t\eta_{\boldsymbol{d}}^{n+1}) \\
&- \frac{\tau}{\varepsilon^2}(\boldsymbol{d}^{n+\frac{1}{2}}, \delta_t\eta_{\boldsymbol{d}}^{n+1}) + \frac{\tau}{\varepsilon^2}(\boldsymbol{\Pi}_k^0\widetilde{\boldsymbol{d}}_h^{n+\frac{1}{2}}, \boldsymbol{\Pi}_k^0\delta_t\eta_{\boldsymbol{d}}^{n+1}) + \frac{\tau}{2\varepsilon^2}((\boldsymbol{d}^{n+1})^3 + (\boldsymbol{d}^n)^3, \delta_t\eta_{\boldsymbol{d}}^{n+1}) \\
&- \frac{\tau}{2\varepsilon^2}(((\boldsymbol{\Pi}_k^0\boldsymbol{d}_h^{n+1})^2 + (\boldsymbol{\Pi}_k^0\boldsymbol{d}_h^{n})^2)\boldsymbol{\Pi}_k^0\boldsymbol{d}_h^{n+\frac{1}{2}}, \boldsymbol{\Pi}_k^0\delta_t\eta_{\boldsymbol{d}}^{n+1}).
\end{aligned} \tag{4.11}
$$

Setting $\boldsymbol{v}_h = \tau\eta_{\boldsymbol{u}}^{n+\frac{1}{2}}$ in (4.4), we have

$$
\begin{aligned}
\frac{1}{2}|||\eta_{\boldsymbol{u}}^{n+1}|||_{\mathcal{M}_2}^2 - \frac{1}{2}|||\eta_{\boldsymbol{u}}^{n}|||_{\mathcal{M}_2}^2 + \nu\tau|||\eta_{\boldsymbol{u}}^{n+\frac{1}{2}}|||_{\mathcal{A}_2}^2 &= -\tau\mathcal{M}_2(R_{\boldsymbol{u}}^{n+\frac{1}{2}}, \eta_{\boldsymbol{u}}^{n+\frac{1}{2}}) \\
&+ \tau\mathcal{M}_2(\delta_t\boldsymbol{u}^{n+1}, \eta_{\boldsymbol{u}}^{n+\frac{1}{2}}) \\
&- \tau\mathcal{M}_{h2}(\delta_t\boldsymbol{u}_I^{n+1}, \eta_{\boldsymbol{u}}^{n+\frac{1}{2}}) + \nu\tau\mathcal{A}_2(\boldsymbol{u}^{n+\frac{1}{2}}, \eta_{\boldsymbol{u}}^{n+\frac{1}{2}}) - \nu\tau\mathcal{A}_{h2}(\boldsymbol{u}_I^{n+\frac{1}{2}}, \eta_{\boldsymbol{u}}^{n+\frac{1}{2}}) \\
&+ \frac{\tau}{2}\mathcal{C}(\boldsymbol{u}^{n+1}; \boldsymbol{u}^{n+1}, \eta_{\boldsymbol{u}}^{n+\frac{1}{2}}) + \frac{\tau}{2}\mathcal{C}(\boldsymbol{u}^{n}; \boldsymbol{u}^{n}, \eta_{\boldsymbol{u}}^{n+\frac{1}{2}}) - \tau\mathcal{C}_h(\widetilde{\boldsymbol{u}}_h^{n+\frac{1}{2}}; \boldsymbol{u}_h^{n+\frac{1}{2}}, \eta_{\boldsymbol{u}}^{n+\frac{1}{2}}) \\
&- \frac{\tau}{2}\mathcal{D}(\eta_{\boldsymbol{u}}^{n+1}; \boldsymbol{d}^{n+1}, \boldsymbol{\omega}^{n+\frac{1}{2}}) - \frac{\tau}{2}\mathcal{D}(\eta_{\boldsymbol{u}}^{n}; \boldsymbol{d}^{n}, \boldsymbol{\omega}^{n+\frac{1}{2}}) + \tau\mathcal{D}_h(\eta_{\boldsymbol{u}}^{n+\frac{1}{2}}; \widetilde{\boldsymbol{d}}_h^{n+\frac{1}{2}}, \boldsymbol{\omega}_h^{n+\frac{1}{2}}).
\end{aligned} \tag{4.12}
$$

Combining (4.8)–(4.12), we can get

$$
\begin{aligned}
&\frac{1}{2}|||\eta_{\boldsymbol{u}}^{n+1}|||_{\mathcal{M}_2}^2 - \frac{1}{2}|||\eta_{\boldsymbol{u}}^{n}|||_{\mathcal{M}_2}^2 + \frac{\lambda(1+\gamma)}{2}|||\eta_{\boldsymbol{d}}^{n+1}|||_{\mathcal{A}_1}^2 - \frac{\lambda(1+\gamma)}{2}|||\eta_{\boldsymbol{d}}^{n}|||_{\mathcal{A}_1}^2 \\
&+ \nu\tau|||\eta_{\boldsymbol{u}}^{n+\frac{1}{2}}|||_{\mathcal{A}_2}^2 + \tau|||\delta_t\eta_{\boldsymbol{d}}^{n+1}|||_{\mathcal{M}_1}^2 + \gamma\tau|||\eta_{\boldsymbol{\omega}}^{n+\frac{1}{2}}|||_{\mathcal{M}_1}^2 \\
&= -\tau\mathcal{M}_1(R_{\boldsymbol{d}}^{n+\frac{1}{2}}, \delta_t\eta_{\boldsymbol{d}}^{n+1}) - \tau\mathcal{M}_1(R_{\boldsymbol{d}}^{n+\frac{1}{2}}, \eta_{\boldsymbol{\omega}}^{n+\frac{1}{2}}) - \tau\mathcal{M}_2(R_{\boldsymbol{u}}^{n+\frac{1}{2}}, \eta_{\boldsymbol{u}}^{n+\frac{1}{2}}) \\
&+ \tau[\mathcal{M}_1(\delta_t\boldsymbol{d}^{n+1}, \delta_t\eta_{\boldsymbol{d}}^{n+1}) - \mathcal{M}_{h1}(\delta_t\boldsymbol{d}_I^{n+1}, \delta_t\eta_{\boldsymbol{d}}^{n+1})] \\
&+ \tau[\mathcal{M}_1(\delta_t\boldsymbol{d}^{n+1}, \eta_{\boldsymbol{\omega}}^{n+\frac{1}{2}}) - \mathcal{M}_{h1}(\delta_t\boldsymbol{d}_I^{n+1}, \eta_{\boldsymbol{\omega}}^{n+\frac{1}{2}})] \\
&+ \tau[\mathcal{M}_2(\delta_t\boldsymbol{u}^{n+1}, \eta_{\boldsymbol{u}}^{n+\frac{1}{2}}) - \mathcal{M}_{h2}(\delta_t\boldsymbol{u}_I^{n+1}, \eta_{\boldsymbol{u}}^{n+\frac{1}{2}})] \\
&+ \gamma\tau[\mathcal{M}_1(\boldsymbol{\omega}^{n+\frac{1}{2}}, \eta_{\boldsymbol{\omega}}^{n+\frac{1}{2}}) - \mathcal{M}_{h1}(\boldsymbol{\omega}_I^{n+\frac{1}{2}}, \eta_{\boldsymbol{\omega}}^{n+\frac{1}{2}})] \\
&- \tau[\mathcal{M}_1(\boldsymbol{\omega}^{n+\frac{1}{2}}, \delta_t\eta_{\boldsymbol{d}}^{n+1}) - \mathcal{M}_{h1}(\boldsymbol{\omega}_I^{n+\frac{1}{2}}, \delta_t\eta_{\boldsymbol{d}}^{n+1})] \\
&+ \nu\tau[\mathcal{A}_2(\boldsymbol{u}^{n+\frac{1}{2}}, \eta_{\boldsymbol{u}}^{n+\frac{1}{2}}) - \mathcal{A}_{h2}(\boldsymbol{u}_I^{n+\frac{1}{2}}, \eta_{\boldsymbol{u}}^{n+\frac{1}{2}})] \\
&+ \lambda(1+\gamma)\tau[\mathcal{A}_1(\boldsymbol{d}^{n+\frac{1}{2}}, \delta_t\eta_{\boldsymbol{d}}^{n+1}) - \mathcal{A}_{h1}(\boldsymbol{d}_I^{n+\frac{1}{2}}, \delta_t\eta_{\boldsymbol{d}}^{n+1})] \\
&+ \tau[\frac{1}{2}\mathcal{C}(\boldsymbol{u}^{n+1}; \boldsymbol{u}^{n+1}, \eta_{\boldsymbol{u}}^{n+\frac{1}{2}}) + \frac{1}{2}\mathcal{C}(\boldsymbol{u}^{n}; \boldsymbol{u}^{n}, \eta_{\boldsymbol{u}}^{n+\frac{1}{2}}) - \mathcal{C}_h(\widetilde{\boldsymbol{u}}_h^{n+\frac{1}{2}}; \boldsymbol{u}_h^{n+\frac{1}{2}}, \eta_{\boldsymbol{u}}^{n+\frac{1}{2}})] \\
&- \tau[\frac{1}{2}\mathcal{D}(\eta_{\boldsymbol{u}}^{n+\frac{1}{2}}; \boldsymbol{d}^{n+1}, \boldsymbol{\omega}^{n+1}) + \frac{1}{2}\mathcal{D}(\eta_{\boldsymbol{u}}^{n+\frac{1}{2}}; \boldsymbol{d}^{n}, \boldsymbol{\omega}^{n}) - \mathcal{D}_h(\eta_{\boldsymbol{u}}^{n+\frac{1}{2}}; \widetilde{\boldsymbol{d}}_h^{n+\frac{1}{2}}, \boldsymbol{\omega}_h^{n+\frac{1}{2}})] \\
&+ \tau[\frac{1}{2}\mathcal{D}(\boldsymbol{u}^{n+1}; \boldsymbol{d}^{n+1}, \delta_t\eta_{\boldsymbol{d}}^{n+1}) + \frac{1}{2}\mathcal{D}(\boldsymbol{u}^{n}; \boldsymbol{d}^{n}, \delta_t\eta_{\boldsymbol{d}}^{n+1}) - \mathcal{D}_h(\boldsymbol{u}_h^{n+\frac{1}{2}}; \widetilde{\boldsymbol{d}}_h^{n+\frac{1}{2}}, \delta_t\eta_{\boldsymbol{d}}^{n+1})] \\
&+ \tau[\frac{1}{2}\mathcal{D}(\boldsymbol{u}^{n+1}; \boldsymbol{d}^{n+1}, \eta_{\boldsymbol{\omega}}^{n+\frac{1}{2}}) + \frac{1}{2}\mathcal{D}(\boldsymbol{u}^{n}; \boldsymbol{d}^{n}, \eta_{\boldsymbol{\omega}}^{n+\frac{1}{2}}) - \mathcal{D}_h(\boldsymbol{u}_h^{n+\frac{1}{2}}; \widetilde{\boldsymbol{d}}_h^{n+\frac{1}{2}}, \eta_{\boldsymbol{\omega}}^{n+\frac{1}{2}})] \\
&- \frac{(1+\gamma)\tau}{\varepsilon^2}[(\boldsymbol{d}^{n+\frac{1}{2}}, \delta_t\eta_{\boldsymbol{d}}^{n+1}) - (\boldsymbol{\Pi}_k^0\widetilde{\boldsymbol{d}}_h^{n+\frac{1}{2}}, \boldsymbol{\Pi}_k^0\delta_t\eta_{\boldsymbol{d}}^{n+1})] \\
&+ \frac{(1+\gamma)\tau}{2\varepsilon^2}[((\boldsymbol{d}^{n+1})^3 + (\boldsymbol{d}^{n})^3, \delta_t\eta_{\boldsymbol{d}}^{n+1}) \\
&\qquad - (((\boldsymbol{\Pi}_k^0\boldsymbol{d}_h^{n+1})^2 + (\boldsymbol{\Pi}_k^0\boldsymbol{d}_h^{n})^2)\boldsymbol{\Pi}_k^0\boldsymbol{d}_h^{n+\frac{1}{2}}, \boldsymbol{\Pi}_k^0\delta_t\eta_{\boldsymbol{d}}^{n+1})] \\
&:= I_1 + I_2 + \cdots + I_{16}.
\end{aligned}
\tag{4.13}
$$

Applying the Cauchy-Schwarz inequality and Young's inequality, from Lemma 4.1 we have

$$
\begin{aligned}
I_1 + I_2 + I_3 &\lesssim \tau\|R_{\boldsymbol{d}}^{n+\frac{1}{2}}\|_0\|\delta_t\eta_{\boldsymbol{d}}^{n+1}\|_0 + \tau\|R_{\boldsymbol{d}}^{n+\frac{1}{2}}\|_0\|\eta_{\boldsymbol{\omega}}^{n+\frac{1}{2}}\|_0 + \tau\|R_{\boldsymbol{u}}^{n+\frac{1}{2}}\|_0\|\eta_{\boldsymbol{u}}^{n+\frac{1}{2}}\|_0 \\
&\lesssim \tau^5 + \frac{\tau}{14}\|\delta_t\eta_{\boldsymbol{d}}^{n+1}\|_0^2 + \frac{\gamma\tau}{8}\|\eta_{\boldsymbol{\omega}}^{n+\frac{1}{2}}\|_0^2 + \frac{\nu\tau}{10}\|\eta_{\boldsymbol{u}}^{n+\frac{1}{2}}\|_0^2.
\end{aligned}
\tag{4.14}
$$

According to the consistency of $\mathcal{M}_{h1}^K$, using the Cauchy-Schwarz inequality, Young's inequality, Lemma 3.2, (3.4) and (3.5), we obtain

$$\begin{aligned}
I_4 =&\tau\mathcal{M}_1(\delta_t(\boldsymbol{d}^{n+1}-\boldsymbol{\Pi}_k^0\boldsymbol{d}^{n+1}),\delta_t\eta_{\boldsymbol{d}}^{n+1})+\tau\mathcal{M}_{h1}(\delta_t(\boldsymbol{\Pi}_k^0\boldsymbol{d}^{n+1}-\boldsymbol{d}^{n+1}),\delta_t\eta_{\boldsymbol{d}}^{n+1})\\
&+\tau\mathcal{M}_{h1}(\delta_t(\boldsymbol{d}^{n+1}-\boldsymbol{d}_I^{n+1}),\delta_t\eta_{\boldsymbol{d}}^{n+1})\\
\lesssim&\tau(\int_{t^n}^{t^{n+1}}\frac{1}{\tau^2}dt)(\int_{t^n}^{t^{n+1}}\|(\boldsymbol{d}_t-\boldsymbol{\Pi}_k^0\boldsymbol{d}_t)\|_0^2+\|\boldsymbol{d}_t-(\boldsymbol{d}_I)_t\|_0^2dt)\\
&+\frac{\tau}{14}\|\delta_t\eta_{\boldsymbol{d}}^{n+1}\|_0^2\\
\lesssim&h^{2k+2}\int_{t^n}^{t^{n+1}}\|\boldsymbol{d}_t\|_0^2dt+\frac{\tau}{14}\|\delta_t\eta_{\boldsymbol{d}}^{n+1}\|_0^2\lesssim\tau h^{2k+2}+\frac{\tau}{14}\|\delta_t\eta_{\boldsymbol{d}}^{n+1}\|_0^2.
\end{aligned}\tag{4.15}$$

Similarly, we have

$$I_5\lesssim h^{2k+2}\int_{t^n}^{t^{n+1}}\|\boldsymbol{d}_t\|_0^2dt+\frac{\lambda\gamma\tau}{8}\|\eta_{\boldsymbol{\omega}}^{n+\frac{1}{2}}\|_0^2\lesssim\tau h^{2k+2}+\frac{\gamma\tau}{8}\|\eta_{\boldsymbol{\omega}}^{n+\frac{1}{2}}\|_0^2,\tag{4.16}$$

$$I_6\lesssim h^{2k+2}\int_{t^n}^{t^{n+1}}\|\boldsymbol{u}_t\|_0^2dt+\frac{\nu\tau}{10}\|\eta_{\boldsymbol{u}}^{n+\frac{1}{2}}\|_0^2\lesssim\tau h^{2k+2}+\frac{\nu\tau}{10}\|\eta_{\boldsymbol{u}}^{n+\frac{1}{2}}\|_0^2.\tag{4.17}$$

According to the consistency of $\mathcal{M}_{h1}^K$, Lemma 3.2, (3.4) and (3.5), we have

$$\begin{aligned}
I_7 =&\gamma\tau\mathcal{M}_1(\boldsymbol{\omega}^{n+\frac{1}{2}}-\boldsymbol{\Pi}_k^0\boldsymbol{\omega}^{n+\frac{1}{2}},\eta_{\boldsymbol{\omega}}^{n+\frac{1}{2}})+\gamma\tau\mathcal{M}_{h1}(\boldsymbol{\Pi}_k^0\boldsymbol{\omega}^{n+1}-\boldsymbol{\omega}^{n+\frac{1}{2}},\eta_{\boldsymbol{\omega}}^{n+\frac{1}{2}})\\
&+\gamma\tau\mathcal{M}_{h1}(\boldsymbol{\omega}^{n+\frac{1}{2}}-\boldsymbol{\omega}_I^{n+\frac{1}{2}},\eta_{\boldsymbol{\omega}}^{n+\frac{1}{2}})\\
\lesssim&\gamma\tau(\|\boldsymbol{\omega}^{n+\frac{1}{2}}-\boldsymbol{\Pi}_k^0\boldsymbol{\omega}^{n+\frac{1}{2}}\|_0+\|\boldsymbol{\omega}^{n+\frac{1}{2}}-\boldsymbol{\omega}_I^{n+\frac{1}{2}}\|_0)\|\eta_{\boldsymbol{\omega}}^{n+\frac{1}{2}}\|_0\\
\lesssim&\tau h^{2k+2}+\frac{\gamma\tau}{8}\|\eta_{\boldsymbol{\omega}}^{n+\frac{1}{2}}\|_0^2.
\end{aligned}\tag{4.18}$$

Using the same argument as in (4.18), we have

$$\begin{aligned}
I_8&\lesssim\tau(\|\boldsymbol{\omega}^{n+\frac{1}{2}}-\boldsymbol{\Pi}_k^0\boldsymbol{\omega}^{n+\frac{1}{2}}\|_0+\|\boldsymbol{\omega}^{n+\frac{1}{2}}-\boldsymbol{\omega}_I^{n+\frac{1}{2}}\|_0)\|\delta_t\eta_{\boldsymbol{d}}^{n+1}\|_0\\
&\lesssim\tau h^{2k+2}+\frac{\tau}{14}\|\delta_t\eta_{\boldsymbol{d}}^{n+1}\|_0^2,
\end{aligned}\tag{4.19}$$

$$\begin{aligned}
I_9&\lesssim\nu\tau(|\boldsymbol{u}^{n+\frac{1}{2}}-\boldsymbol{\Pi}_k^0\boldsymbol{u}^{n+\frac{1}{2}}|_1+|\boldsymbol{u}^{n+\frac{1}{2}}-\boldsymbol{u}_I^{n+\frac{1}{2}}|_1)|\eta_{\boldsymbol{u}}^{n+\frac{1}{2}}|_1\\
&\lesssim\tau h^{2k}+\frac{\nu\tau}{10}|\eta_{\boldsymbol{u}}^{n+\frac{1}{2}}|_1^2.
\end{aligned}\tag{4.20}$$

According to the consistency of $\mathcal{A}_{h1}^{K}$, Lemma 3.2, (3.4) and (3.5), and the Courant-Friedrichs-Lewy (CFL) condition: $\tau \le Ch^2$, we have

$$
\begin{aligned}
I_{10} \lesssim & \lambda(1+\gamma)\tau(|\boldsymbol{d}^{n+\frac{1}{2}} - \boldsymbol{\Pi}_k^0 \boldsymbol{d}^{n+\frac{1}{2}}|_1 + |\boldsymbol{d}^{n+\frac{1}{2}} - \boldsymbol{d}_I^{n+\frac{1}{2}}|_1)|\delta_t \eta_{\boldsymbol{d}}^{n+1}|_1 \\
\lesssim & \tau h^{-1}(|\boldsymbol{d}^{n+\frac{1}{2}} - \boldsymbol{\Pi}_k^0 \boldsymbol{d}^{n+\frac{1}{2}}|_1 + |\boldsymbol{d}^{n+\frac{1}{2}} - \boldsymbol{d}_I^{n+\frac{1}{2}}|_1)\|\delta_t \eta_{\boldsymbol{d}}^{n+1}\|_0 \\
\lesssim & h^{2k} + \frac{\tau}{14}\|\delta_t \eta_{\boldsymbol{d}}^{n+1}\|_0^2.
\end{aligned} \tag{4.21}
$$

For the trilinear term, we have

$$
\begin{aligned}
I_{11} = & \frac{\tau}{2}\mathcal{C}(\boldsymbol{u}^{n+1} - 2\boldsymbol{u}^n + \boldsymbol{u}^{n-1}; \boldsymbol{u}^{n+\frac{1}{2}}, \eta_{\boldsymbol{u}}^{n+\frac{1}{2}}) + \frac{\tau}{4}\mathcal{C}(\boldsymbol{u}^{n+1} - \boldsymbol{u}^n; \boldsymbol{u}^{n+1} - \boldsymbol{u}^n, \eta_{\boldsymbol{u}}^{n+\frac{1}{2}}) \\
& + \tau[\mathcal{C}(\widetilde{\boldsymbol{u}}^{n+\frac{1}{2}}; \boldsymbol{u}^{n+\frac{1}{2}}, \eta_{\boldsymbol{u}}^{n+\frac{1}{2}}) - \mathcal{C}_h(\widetilde{\boldsymbol{u}}^{n+\frac{1}{2}}; \boldsymbol{u}^{n+\frac{1}{2}}, \eta_{\boldsymbol{u}}^{n+\frac{1}{2}})] \\
& + \tau\mathcal{C}_h(\widetilde{\boldsymbol{u}}^{n+\frac{1}{2}} - \widetilde{\boldsymbol{u}}_h^{n+\frac{1}{2}}; \boldsymbol{u}^{n+\frac{1}{2}}, \eta_{\boldsymbol{u}}^{n+\frac{1}{2}}) + \tau\mathcal{C}_h(\widetilde{\boldsymbol{u}}_h^{n+\frac{1}{2}}; \boldsymbol{u}^{n+\frac{1}{2}} - \boldsymbol{u}_h^{n+\frac{1}{2}}, \eta_{\boldsymbol{u}}^{n+\frac{1}{2}}) \\
\lesssim & \tau|\boldsymbol{u}^{n+1} - 2\boldsymbol{u}^n + \boldsymbol{u}^{n-1}|_1|\boldsymbol{u}^{n+\frac{1}{2}}|_1|\eta_{\boldsymbol{u}}^{n+\frac{1}{2}}|_1 + \tau|\boldsymbol{u}^{n+1} - \boldsymbol{u}^n|_1|\boldsymbol{u}^{n+1} - \boldsymbol{u}^n|_1|\eta_{\boldsymbol{u}}^{n+\frac{1}{2}}|_1 \\
& + \tau h^k(\|\widetilde{\boldsymbol{u}}^{n+\frac{1}{2}}\|_{k+1}(\|\boldsymbol{u}^{n+\frac{1}{2}}\|_{k+1} + \|\boldsymbol{u}^{n+\frac{1}{2}}\|_1) + \|\boldsymbol{u}^{n+\frac{1}{2}}\|_{k+1}(\|\widetilde{\boldsymbol{u}}^{n+\frac{1}{2}}\|_k + \|\widetilde{\boldsymbol{u}}^{n+\frac{1}{2}}\|_1))|\eta_{\boldsymbol{u}}^{n+\frac{1}{2}}|_1 \\
& + \tau\|\boldsymbol{u}^{n+\frac{1}{2}}\|_{\boldsymbol{L}^\infty(\Omega)}(\|e_{\boldsymbol{u}}^n\|_0 + \|e_{\boldsymbol{u}}^{n-1}\|_0)|\eta_{\boldsymbol{u}}^{n+\frac{1}{2}}|_1 + \tau|\widetilde{\boldsymbol{u}}_h^{n+\frac{1}{2}}|_1|\chi_{\boldsymbol{u}}^{n+\frac{1}{2}}|_1|\eta_{\boldsymbol{u}}^{n+\frac{1}{2}}|_1 \\
\lesssim & \tau^5 + \tau h^{2k} + \tau h^{2k+2} + \tau\|\eta_{\boldsymbol{u}}^n\|_0^2 + \tau\|\eta_{\boldsymbol{u}}^{n-1}\|_0^2 + \frac{\nu\tau}{10}|\eta_{\boldsymbol{u}}^{n+\frac{1}{2}}|_1^2,
\end{aligned} \tag{4.22}
$$

Similarly, we obtain

$$
\begin{aligned}
I_{12} = & -\frac{\tau}{2}\mathcal{D}(\eta_{\boldsymbol{u}}^{n+\frac{1}{2}}; \boldsymbol{d}^{n+1} - 2\boldsymbol{d}^n + \boldsymbol{d}^{n-1}, \boldsymbol{\omega}^{n+\frac{1}{2}}) - \frac{\tau}{4}\mathcal{D}(\eta_{\boldsymbol{u}}^{n+\frac{1}{2}}; \boldsymbol{d}^{n+1} - \boldsymbol{d}^n, \boldsymbol{\omega}^{n+1} - \boldsymbol{\omega}^n) \\
& - \tau[\mathcal{D}(\eta_{\boldsymbol{u}}^{n+\frac{1}{2}}; \widetilde{\boldsymbol{d}}^{n+\frac{1}{2}}, \boldsymbol{\omega}^{n+\frac{1}{2}}) - \mathcal{D}_h(\eta_{\boldsymbol{u}}^{n+\frac{1}{2}}; \widetilde{\boldsymbol{d}}^{n+\frac{1}{2}}, \boldsymbol{\omega}^{n+\frac{1}{2}})] \\
& - \tau\mathcal{D}_h(\eta_{\boldsymbol{u}}^{n+\frac{1}{2}}; \widetilde{\boldsymbol{d}}^{n+\frac{1}{2}} - \widetilde{\boldsymbol{d}}_h^{n+\frac{1}{2}}, \boldsymbol{\omega}^{n+\frac{1}{2}}) \\
& - \tau\mathcal{D}_h(\eta_{\boldsymbol{u}}^{n+\frac{1}{2}}; \widetilde{\boldsymbol{d}}_h^{n+\frac{1}{2}}, \chi_{\boldsymbol{\omega}}^{n+\frac{1}{2}}) - \tau\mathcal{D}_h(\eta_{\boldsymbol{u}}^{n+\frac{1}{2}}; \widetilde{\boldsymbol{d}}_h^{n+\frac{1}{2}}, \eta_{\boldsymbol{\omega}}^{n+\frac{1}{2}}) \\
:= & R_1 + R_2 + \cdots + R_6,
\end{aligned} \tag{4.23}
$$

which can be estimated through

$$
\begin{aligned}
& R_1 + R_2 + \cdots + R_5 \\
& \lesssim \tau|\eta_{\boldsymbol{u}}^{n+\frac{1}{2}}|_1|\boldsymbol{d}^{n+1} - 2\boldsymbol{d}^n + \boldsymbol{d}^{n-1}|_1|\boldsymbol{\omega}^{n+\frac{1}{2}}|_1 + \tau|\eta_{\boldsymbol{u}}^{n+\frac{1}{2}}|_1|\boldsymbol{d}^{n+1} - \boldsymbol{d}^n|_1|\boldsymbol{\omega}^{n+1} - \boldsymbol{\omega}^n|_1 \\
& + \tau h^k(\|\boldsymbol{\omega}^{n+\frac{1}{2}} \cdot \nabla\widetilde{\boldsymbol{d}}^{n+\frac{1}{2}}\|_k + \|\boldsymbol{\omega}^{n+\frac{1}{2}}\|_{\boldsymbol{L}^\infty(\Omega)}\|\widetilde{\boldsymbol{d}}^{n+\frac{1}{2}}\|_{k+1} \\
& + \|\widetilde{\boldsymbol{d}}^{n+\frac{1}{2}}\|_{\boldsymbol{W}^{1,\infty}(\Omega)}\|\boldsymbol{\omega}^{n+\frac{1}{2}}\|_k)\|\eta_{\boldsymbol{u}}^{n+\frac{1}{2}}\|_0 \\
& + \tau|\eta_{\boldsymbol{u}}^{n+\frac{1}{2}}|_1|\widetilde{\boldsymbol{d}}_h^{n+\frac{1}{2}} - \widetilde{\boldsymbol{d}}_h^{n+\frac{1}{2}}|_1|\boldsymbol{\omega}^{n+\frac{1}{2}}|_1 + \tau|\eta_{\boldsymbol{u}}^{n+\frac{1}{2}}|_1|\widetilde{\boldsymbol{d}}_h^{n+\frac{1}{2}}|_1|\chi_{\boldsymbol{\omega}}^{n+\frac{1}{2}}|_1 \\
& \lesssim \tau^5 + \tau h^{2k} + \tau|\eta_{\boldsymbol{d}}^n|_1^2 + \tau|\eta_{\boldsymbol{d}}^{n-1}|_1^2 + \frac{\nu\tau}{10}|\eta_{\boldsymbol{u}}^{n+\frac{1}{2}}|_1^2.
\end{aligned} \tag{4.24}
$$

Noting that, the term R_6 in (4.23) and the term S_6 add up to 0. For I_{13}, we obtain

$$
\begin{aligned}
I_{13} &= \frac{\tau}{2}\mathcal{D}(\boldsymbol{u}^{n+\frac{1}{2}}; \boldsymbol{d}^{n+1} - 2\boldsymbol{d}^n + \boldsymbol{d}^{n-1}, \delta_t \eta_{\boldsymbol{d}}^{n+1}) \\
&+ \frac{\tau}{4}\mathcal{D}(\boldsymbol{u}^{n+1} - \boldsymbol{u}^n; \boldsymbol{d}^{n+1} - \boldsymbol{d}^n, \delta_t \eta_{\boldsymbol{d}}^{n+1}) \\
&+ \tau[\mathcal{D}(\boldsymbol{u}^{n+\frac{1}{2}}; \widetilde{\boldsymbol{d}}^{n+\frac{1}{2}}, \delta_t \eta_{\boldsymbol{d}}^{n+1}) - \mathcal{D}_h(\boldsymbol{u}^{n+\frac{1}{2}}; \widetilde{\boldsymbol{d}}^{n+\frac{1}{2}}, \delta_t \eta_{\boldsymbol{d}}^{n+1})] \\
&+ \tau\mathcal{D}_h(\boldsymbol{u}^{n+\frac{1}{2}}; \widetilde{\boldsymbol{d}}^{n+\frac{1}{2}} - \widetilde{\boldsymbol{d}}_h^{n+\frac{1}{2}}, \delta_t \eta_{\boldsymbol{d}}^{n+1}) + \tau\mathcal{D}_h(\boldsymbol{u}^{n+\frac{1}{2}} - \boldsymbol{u}_h^{n+\frac{1}{2}}; \widetilde{\boldsymbol{d}}_h^{n+\frac{1}{2}}, \delta_t \eta_{\boldsymbol{d}}^{n+1}) \\
&\lesssim \tau\|\boldsymbol{u}^{n+\frac{1}{2}}\|_{\boldsymbol{L}^\infty}|\boldsymbol{d}^{n+1} - 2\boldsymbol{d}^n + \boldsymbol{d}^{n-1}|_1\|\delta_t \eta_{\boldsymbol{d}}^{n+1}\|_0 + \tau\|\boldsymbol{u}^{n+1} - \boldsymbol{u}^n\|_{\boldsymbol{L}^\infty}|\boldsymbol{d}^{n+1} \\
&- \boldsymbol{d}^n|_1\|\delta_t \eta_{\boldsymbol{d}}^{n+1}\|_0 \\
&+ \tau h^k(\|\boldsymbol{u}^{n+\frac{1}{2}} \cdot \nabla\widetilde{\boldsymbol{d}}^{n+\frac{1}{2}}\|_k + \|\boldsymbol{u}^{n+\frac{1}{2}}\|_{\boldsymbol{L}^\infty(\Omega)}\|\widetilde{\boldsymbol{d}}^{n+\frac{1}{2}}\|_{k+1} \\
&+ \|\widetilde{\boldsymbol{d}}^{n+\frac{1}{2}}\|_{\boldsymbol{W}^{1,\infty}(\Omega)}\|\boldsymbol{u}^{n+\frac{1}{2}}\|_k)\|\delta_t \eta_{\boldsymbol{d}}^{n+1}\|_0 \\
&+ \tau\|\boldsymbol{u}^{n+\frac{1}{2}}\|_{\boldsymbol{L}^\infty(\Omega)}(|e_{\boldsymbol{d}}^n|_1 + |e_{\boldsymbol{d}}^{n-1}|_1)\|\delta_t \eta_{\boldsymbol{d}}^{n+1}\|_0 + \tau\|\widetilde{\boldsymbol{d}}_h^{n+\frac{1}{2}}\|_{\boldsymbol{W}^{1,\infty}(\Omega)}\|\chi_{\boldsymbol{u}}^{n+\frac{1}{2}} \\
&+ \eta_{\boldsymbol{u}}^{n+\frac{1}{2}}\|_0\|\delta_t \eta_{\boldsymbol{d}}^{n+1}\|_0 \\
&\lesssim \tau^5 + \tau h^{2k} + \tau h^{2k+2} + \tau|\eta_{\boldsymbol{d}}^n|_1^2 + \tau|\eta_{\boldsymbol{d}}^{n-1}|_1^2 + \tau\|\eta_{\boldsymbol{u}}^{n+1}\|_0^2 + \tau\|\eta_{\boldsymbol{u}}^n\|_0^2 \\
&+ \frac{\tau}{14}\|\delta_t \eta_{\boldsymbol{d}}^{n+1}\|_0^2,
\end{aligned}
\tag{4.25}
$$

where we use the result (4.6). For I_{14}, we have

$$
\begin{aligned}
I_{14} &= \frac{\tau}{2}\mathcal{D}(\boldsymbol{u}^{n+\frac{1}{2}}; \boldsymbol{d}^{n+1} - 2\boldsymbol{d}^n + \boldsymbol{d}^{n-1}, \eta_{\boldsymbol{\omega}}^{n+\frac{1}{2}}) + \frac{\tau}{4}\mathcal{D}(\boldsymbol{u}^{n+1} - \boldsymbol{u}^n; \boldsymbol{d}^{n+1} - \boldsymbol{d}^n, \eta_{\boldsymbol{\omega}}^{n+\frac{1}{2}}) \\
&+ \tau[\mathcal{D}(\boldsymbol{u}^{n+\frac{1}{2}}; \widetilde{\boldsymbol{d}}^{n+\frac{1}{2}}, \eta_{\boldsymbol{\omega}}^{n+\frac{1}{2}}) - \mathcal{D}_h(\boldsymbol{u}^{n+\frac{1}{2}}; \widetilde{\boldsymbol{d}}^{n+\frac{1}{2}}, \eta_{\boldsymbol{\omega}}^{n+\frac{1}{2}})] \\
&+ \tau\mathcal{D}_h(\boldsymbol{u}^{n+\frac{1}{2}}; \widetilde{\boldsymbol{d}}^{n+\frac{1}{2}} - \widetilde{\boldsymbol{d}}_h^{n+\frac{1}{2}}, \eta_{\boldsymbol{\omega}}^{n+\frac{1}{2}}) \\
&+ \tau\mathcal{D}_h(\chi_{\boldsymbol{u}}^{n+\frac{1}{2}}; \widetilde{\boldsymbol{d}}_h^{n+\frac{1}{2}}, \eta_{\boldsymbol{\omega}}^{n+\frac{1}{2}}) + \tau\mathcal{D}_h(\eta_{\boldsymbol{u}}^{n+\frac{1}{2}}; \widetilde{\boldsymbol{d}}_h^{n+\frac{1}{2}}, \eta_{\boldsymbol{\omega}}^{n+\frac{1}{2}}) \\
&:= S_1 + S_2 + \cdots + S_6,
\end{aligned}
\tag{4.26}
$$

which can be estimated through

$$
\begin{aligned}
S_1 + S_2 + \cdots + S_5 &\lesssim \tau^5 + \tau h^{2k} + \tau h^{2k+2} + \tau|\eta_{\boldsymbol{d}}^n|_1^2 + \tau|\eta_{\boldsymbol{d}}^{n-1}|_1^2 \\
&+ \frac{\gamma\tau}{8}\|\eta_{\boldsymbol{\omega}}^{n+\frac{1}{2}}\|_0^2,
\end{aligned}
\tag{4.27}
$$

Applying the Cauchy-Schwarz inequality and Young's inequality, we have

$$\begin{aligned} I_{15} =& -\frac{(1+\gamma)\tau}{\varepsilon^2}\{(\boldsymbol{d}^{n+\frac{1}{2}} - \widetilde{\boldsymbol{d}}^{n+\frac{1}{2}}, \delta_t \eta_{\boldsymbol{d}}^{n+1}) \\ &+ [(\widetilde{\boldsymbol{d}}^{n+\frac{1}{2}}, \delta_t \eta_{\boldsymbol{d}}^{n+1}) - (\boldsymbol{\Pi}_k^0 \widetilde{\boldsymbol{d}}^{n+\frac{1}{2}}, \boldsymbol{\Pi}_k^0 \delta_t \eta_{\boldsymbol{d}}^{n+1})] \\ &+ (\boldsymbol{\Pi}_k^0 \widetilde{\boldsymbol{d}}^{n+\frac{1}{2}} - \boldsymbol{\Pi}_k^0 \widetilde{\boldsymbol{d}}_h^{n+\frac{1}{2}}, \boldsymbol{\Pi}_k^0 \delta_t \eta_{\boldsymbol{d}}^{n+1})\} \\ \lesssim& \tau \|\boldsymbol{d}^{n+1} - 2\boldsymbol{d}^n + \boldsymbol{d}^{n-1}\|_0 \|\delta_t \eta_{\boldsymbol{d}}^{n+1}\|_0 + \tau \|\widetilde{\boldsymbol{d}}^{n+\frac{1}{2}} - \boldsymbol{\Pi}_k^0 \widetilde{\boldsymbol{d}}^{n+\frac{1}{2}}\| \delta_t \eta_{\boldsymbol{d}}^{n+1}\|_0 \\ &+ \tau \|\widetilde{\boldsymbol{d}}^{n+\frac{1}{2}} - \widetilde{\boldsymbol{d}}_h^{n+\frac{1}{2}}\|_0 \|\delta_t \eta_{\boldsymbol{d}}^{n+1}\|_0 \\ \lesssim& \tau^5 + \tau h^{2k+2} + \tau \|\eta_{\boldsymbol{d}}^n\|_0^2 + \tau \|\eta_{\boldsymbol{d}}^{n-1}\|_0^2 + \frac{\tau}{14} \|\delta_t \eta_{\boldsymbol{d}}^{n+1}\|_0^2. \end{aligned} \tag{4.28}$$

Using the inequality $\left||\boldsymbol{a}_1|^2|\boldsymbol{b}_1| - |\boldsymbol{a}_2|^2|\boldsymbol{b}_2|\right| \leq (\max\{|\boldsymbol{a}_1|, |\boldsymbol{b}_1|, |\boldsymbol{a}_2|, |\boldsymbol{b}_2|\})^2(2|\boldsymbol{a}_1 - \boldsymbol{a}_2| - |\boldsymbol{b}_1 - \boldsymbol{b}_2|)$ (see [4, 25]), the Cauchy-Schwarz inequality and Young's inequality, we have

$$\begin{aligned} I_{16} =& \frac{(1+\gamma)\tau}{2\varepsilon^2}\{((\boldsymbol{d}^{n+1})^3 + (\boldsymbol{d}^n)^3 - ((\boldsymbol{d}^{n+1})^2 + (\boldsymbol{d}^n)^2)\boldsymbol{d}^{n+\frac{1}{2}}, \delta_t \eta_{\boldsymbol{d}}^{n+1}) \\ &+ [(((\boldsymbol{d}^{n+1})^2 + (\boldsymbol{d}^n)^2)\boldsymbol{d}^{n+\frac{1}{2}}, \delta_t \eta_{\boldsymbol{d}}^{n+1}) - (\boldsymbol{\Pi}_k^0(((\boldsymbol{d}^{n+1})^2 \\ &+ (\boldsymbol{d}^n)^2)\boldsymbol{d}^{n+\frac{1}{2}}), \boldsymbol{\Pi}_k^0 \delta_t \eta_{\boldsymbol{d}}^{n+1})] \\ &+ (\boldsymbol{\Pi}_k^0(((\boldsymbol{d}^{n+1})^2 + (\boldsymbol{d}^n)^2)\boldsymbol{d}^{n+\frac{1}{2}}) - ((\boldsymbol{\Pi}_k^0 \boldsymbol{d}^{n+1})^2 \\ &+ (\boldsymbol{\Pi}_k^0 \boldsymbol{d}^n)^2)\boldsymbol{\Pi}_k^0 \boldsymbol{d}^{n+\frac{1}{2}}, \boldsymbol{\Pi}_k^0 \delta_t \eta_{\boldsymbol{d}}^{n+1}) \\ &+ (((\boldsymbol{\Pi}_k^0 \boldsymbol{d}^{n+1})^2 + (\boldsymbol{\Pi}_k^0 \boldsymbol{d}^n)^2)\boldsymbol{\Pi}_k^0 \boldsymbol{d}^{n+\frac{1}{2}} - ((\boldsymbol{\Pi}_k^0 \boldsymbol{d}_h^{n+1})^2 \\ &+ (\boldsymbol{\Pi}_k^0 \boldsymbol{d}_h^n)^2)\boldsymbol{\Pi}_k^0 \boldsymbol{d}_h^{n+\frac{1}{2}}, \boldsymbol{\Pi}_k^0 \delta_t \eta_{\boldsymbol{d}}^{n+1})\} \\ \lesssim& \tau \|\boldsymbol{d}^{n+\frac{1}{2}}\|_{\boldsymbol{L}^\infty(\Omega)} \|\boldsymbol{d}^{n+1} - \boldsymbol{d}^n\|_0^2 \|\delta_t \eta_{\boldsymbol{d}}^{n+1}\|_0 \\ &+ \tau \|((\boldsymbol{d}^{n+1})^2 + (\boldsymbol{d}^n)^2)\boldsymbol{d}^{n+\frac{1}{2}} - \boldsymbol{\Pi}_k^0(((\boldsymbol{d}^{n+1})^2 + (\boldsymbol{d}^n)^2)\boldsymbol{d}^{n+\frac{1}{2}})\|_0 \|\delta_t \eta_{\boldsymbol{d}}^{n+1}\|_0 \\ &+ \tau(\|\boldsymbol{d}^{n+1} - \boldsymbol{\Pi}_k^0 \boldsymbol{d}^{n+1}\|_0 + \|\boldsymbol{d}^n - \boldsymbol{\Pi}_k^0 \boldsymbol{d}^n\|_0)\|\delta_t \eta_{\boldsymbol{d}}^{n+1}\|_0 \\ &+ \tau(\|\boldsymbol{d}^{n+1} - \boldsymbol{d}_h^{n+1}\|_0 + \|\boldsymbol{d}^n - \boldsymbol{d}_h^n\|_0)\|\delta_t \eta_{\boldsymbol{d}}^{n+1}\|_0 \\ \lesssim& \tau^5 + \tau h^{2k+2} + \tau \|\eta_{\boldsymbol{d}}^{n+1}\|_0^2 + \tau \|\eta_{\boldsymbol{d}}^n\|_0^2 + \frac{\tau}{14}\|\delta_t \eta_{\boldsymbol{d}}^{n+1}\|_0^2. \end{aligned} \tag{4.29}$$

Combining the above estimates (4.14)–(4.29) and using Lemma 3.3, we have

$$\begin{aligned} &\frac{1}{2}|||\eta_{\boldsymbol{u}}^{n+1}|||_{\mathcal{M}_2}^2 - \frac{1}{2}|||\eta_{\boldsymbol{u}}^n|||_{\mathcal{M}_2}^2 + \frac{\lambda(1+\gamma)}{2}|||\eta_{\boldsymbol{d}}^{n+1}|||_{\mathcal{A}_1}^2 - \frac{\lambda(1+\gamma)}{2}|||\eta_{\boldsymbol{d}}^n|||_{\mathcal{A}_1}^2 \\ &+ \frac{\nu\tau}{2}|||\eta_{\boldsymbol{u}}^{n+\frac{1}{2}}|||_{\mathcal{A}_2}^2 + \frac{\tau}{2}|||\delta_t \eta_{\boldsymbol{d}}^{n+1}|||_{\mathcal{M}_1}^2 + \frac{\gamma\tau}{2}|||\eta_{\boldsymbol{\omega}}^{n+\frac{1}{2}}|||_{\mathcal{M}_1}^2 \\ \lesssim& h^{2k} + \tau^5 + \tau h^{2k} + \tau h^{2k+2} + \tau|||\eta_{\boldsymbol{u}}^{n-1}|||_{\mathcal{M}_2}^2 + \tau|||\eta_{\boldsymbol{u}}^n|||_{\mathcal{M}_2}^2 + \tau|||\eta_{\boldsymbol{u}}^{n+1}|||_{\mathcal{M}_2}^2 \\ &+ \tau|||\eta_{\boldsymbol{d}}^{n-1}|||_{\mathcal{A}_1}^2 + \tau|||\eta_{\boldsymbol{d}}^n|||_{\mathcal{A}_1}^2 + \tau|||\eta_{\boldsymbol{d}}^{n+1}|||_{\mathcal{A}_1}^2. \end{aligned} \tag{4.30}$$

Summing (4.30) over n from 0 to m, using the fact that $\eta_{\boldsymbol{u}}^{-1} = \eta_{\boldsymbol{u}}^{0} = 0$ and $\eta_{\boldsymbol{d}}^{-1} = \eta_{\boldsymbol{d}}^{0} = 0$, we have

$$
\begin{aligned}
&|||\eta_{\boldsymbol{u}}^{m+1}|||_{\mathcal{M}_2}^2 + |||\eta_{\boldsymbol{d}}^{m+1}|||_{\mathcal{A}_1}^2 + \tau \sum_{n=0}^{m} (|\eta_{\boldsymbol{u}}^{n+\frac{1}{2}}|_1^2 + \|\delta_t \eta_{\boldsymbol{d}}^{n+1}\|_0^2 + \|\eta_{\boldsymbol{\omega}}^{n+\frac{1}{2}}\|_0^2) \\
&\lesssim \tau^4 + h^{2k} + \tau \sum_{n=0}^{m} (\tau^4 + h^{2k}) + C_0 \tau \sum_{n=0}^{m} (|||\eta_{\boldsymbol{u}}^{n}|||_{\mathcal{M}_2}^2 + |||\eta_{\boldsymbol{u}}^{n+1}|||_{\mathcal{M}_2}^2 \\
&\quad + |||\eta_{\boldsymbol{d}}^{n}|||_{\mathcal{A}_1}^2 + |||\eta_{\boldsymbol{d}}^{n+1}|||_{\mathcal{A}_1}^2).
\end{aligned} \tag{4.31}
$$

When $0 < \tau \leq \tau_0 := \frac{1}{2C_0} < \frac{1}{C_0}$, for any $0 < n \leq M - 1$, since $1 \leq \frac{1}{1 - C_0 \tau} \leq 2$ and from (4.31), it can be readily seen that

$$
\begin{aligned}
&|||\eta_{\boldsymbol{u}}^{m+1}|||_{\mathcal{M}_2}^2 + |||\eta_{\boldsymbol{d}}^{m+1}|||_{\mathcal{A}_1}^2 + \tau \sum_{n=0}^{m} (|\eta_{\boldsymbol{u}}^{n+\frac{1}{2}}|_1^2 + \|\delta_t \eta_{\boldsymbol{d}}^{n+1}\|_0^2 + \|\eta_{\boldsymbol{\omega}}^{n+\frac{1}{2}}\|_0^2) \\
&\lesssim \frac{1 + \sum_{n=0}^{m} \tau}{1 - C_0 \tau} (\tau^4 + h^{2k}) + \frac{C_0 \tau}{1 - C_0 \tau} \sum_{n=0}^{m} (|||\eta_{\boldsymbol{u}}^{n}|||_{\mathcal{M}_2}^2 + |||\eta_{\boldsymbol{d}}^{n}|||_{\mathcal{A}_1}^2).
\end{aligned} \tag{4.32}
$$

By using the Gronwall's inequality and from Lemma 3.3, we have

$$
\|\eta_{\boldsymbol{u}}^{m+1}\|_0^2 + |\eta_{\boldsymbol{d}}^{m+1}|_1^2 + \tau \sum_{n=0}^{m} (|\eta_{\boldsymbol{u}}^{n+\frac{1}{2}}|_1^2 + \|\delta_t \eta_{\boldsymbol{d}}^{n+1}\|_0^2 + \|\eta_{\boldsymbol{\omega}}^{n+\frac{1}{2}}\|_0^2) \lesssim \tau^4 + h^{2k} \tag{4.33}
$$

Finally, by applying the triangle inequality, we can obtain

$$
\|e_{\boldsymbol{u}}^{m+1}\|_0^2 + |e_{\boldsymbol{d}}^{m+1}|_1^2 + \tau \sum_{n=0}^{m} (|e_{\boldsymbol{u}}^{n+\frac{1}{2}}|_1^2 + \|\delta_t e_{\boldsymbol{d}}^{n+1}\|_0^2 + \|e_{\boldsymbol{\omega}}^{n+\frac{1}{2}}\|_0^2) \lesssim \tau^4 + h^{2k}.
$$

The above estimate implies that the induction assumption (4.5) could be recovered at t_{m+1}. Thus the mathematical induction is closed.

Remark 4.1 *Using the Poincaré inequality and Theorem 4.1, we can easily get*

$$
\|e_{\boldsymbol{u}}^{m+1}\|_0^2 + \|e_{\boldsymbol{d}}^{m+1}\|_0^2 \lesssim \tau^4 + h^{2k}.
$$

Theorem 4.2 *Under the assumption (**A**), the following inequality holds*

$$
\tau \sum_{n=0}^{m} \|e_p^{n+\frac{1}{2}}\|_0^2 \lesssim \tau^4 + h^{2k}.
$$

Proof Setting $\boldsymbol{v}_h = \tau\delta_t\eta_{\boldsymbol{u}}^{n+1}$ in (4.4), we obtain

$$
\begin{aligned}
&\frac{\nu}{2}|||\eta_{\boldsymbol{u}}^{n+1}|||_{\mathcal{A}_2} - \frac{\nu}{2}|||\eta_{\boldsymbol{u}}^{n}|||_{\mathcal{A}_2} + \tau|||\delta_t\eta_{\boldsymbol{u}}^{n+1}|||_{\mathcal{M}_2}^2 \\
&= -\tau\mathcal{M}_2(R_{\boldsymbol{u}}^{n+\frac{1}{2}}, \delta_t\eta_{\boldsymbol{u}}^{n+1}) + \tau[\mathcal{M}_2(\delta_t\boldsymbol{u}^{n+1}, \delta_t\eta_{\boldsymbol{u}}^{n+1}) - \tau\mathcal{M}_{h2}(\delta_t\boldsymbol{u}_I^{n+1}, \delta_t\eta_{\boldsymbol{u}}^{n+1})] \\
&\quad + \nu\tau[\mathcal{A}_2(\boldsymbol{u}^{n+\frac{1}{2}}, \delta_t\eta_{\boldsymbol{u}}^{n+1}) - \mathcal{A}_{h2}(\boldsymbol{u}_I^{n+\frac{1}{2}}, \delta_t\eta_{\boldsymbol{u}}^{n+1})] \\
&\quad + \tau[\frac{1}{2}\mathcal{C}(\boldsymbol{u}^{n+1}; \boldsymbol{u}^{n+1}, \delta_t\eta_{\boldsymbol{u}}^{n+1}) + \frac{1}{2}\mathcal{C}(\boldsymbol{u}^{n}; \boldsymbol{u}^{n}, \delta_t\eta_{\boldsymbol{u}}^{n+1}) \\
&\quad - \mathcal{C}_h(\widetilde{\boldsymbol{u}}_h^{n+\frac{1}{2}}; \boldsymbol{u}_h^{n+\frac{1}{2}}, \delta_t\eta_{\boldsymbol{u}}^{n+1})] \\
&\quad - \tau[\frac{1}{2}\mathcal{D}(\delta_t\eta_{\boldsymbol{u}}^{n+1}; \boldsymbol{d}^{n+1}, \boldsymbol{\omega}^{n+1}) + \frac{1}{2}\mathcal{D}(\delta_t\eta_{\boldsymbol{u}}^{n+1}; \boldsymbol{d}^{n}, \boldsymbol{\omega}^{n}) \\
&\quad - \mathcal{D}_h(\delta_t\eta_{\boldsymbol{u}}^{n+1}; \widetilde{\boldsymbol{d}}_h^{n+\frac{1}{2}}, \boldsymbol{\omega}_h^{n+\frac{1}{2}})].
\end{aligned}
\tag{4.34}
$$

By using a similar procedure for the proof of Theorem 4.1, we can get

$$
|e_{\boldsymbol{u}}^{n+1}|_1^2 + \tau\sum_{n=0}^{m}\|\delta_t e_{\boldsymbol{u}}^{n+1}\|_0^2 \lesssim \tau^4 + h^{2k}. \tag{4.35}
$$

By subtracting (3.34c) from the equations (2.8c), according to the consistency of $\mathcal{M}_{h2}^K$ and $\mathcal{A}_{h2}^K$, we have

$$
\begin{aligned}
&\mathcal{B}(\boldsymbol{v}_h, e_p^{n+\frac{1}{2}}) = -\mathcal{M}_2(\delta_t(\boldsymbol{u}^{n+1} - \boldsymbol{\Pi}_k^0\boldsymbol{u}^{n+1}), \boldsymbol{v}_h) - \mathcal{M}_{h2}(\delta_t(\boldsymbol{\Pi}_k^0\boldsymbol{u}^{n+1} - \boldsymbol{u}^{n+1}), \boldsymbol{v}_h) \\
&\quad + \mathcal{M}_{h2}(\delta_t e_{\boldsymbol{u}}^{n+1}, \boldsymbol{v}_h) - \nu\mathcal{A}_2(\boldsymbol{u}^{n+\frac{1}{2}} - \boldsymbol{\Pi}_k^0\boldsymbol{u}^{n+\frac{1}{2}}, \boldsymbol{v}_h) - \nu\mathcal{A}_{h2}(\boldsymbol{\Pi}_k^0\boldsymbol{u}^{n+\frac{1}{2}} - \boldsymbol{u}^{n+\frac{1}{2}}, \boldsymbol{v}_h) \\
&\quad + \nu\mathcal{A}_{h2}(e_{\boldsymbol{u}}^{n+\frac{1}{2}}, \boldsymbol{v}_h) - \frac{1}{2}\mathcal{C}(\boldsymbol{u}^{n+1} - 2\boldsymbol{u}^{n} + \boldsymbol{u}^{n-1}; \boldsymbol{u}^{n+\frac{1}{2}}, \boldsymbol{v}_h) \\
&\quad - \frac{1}{4}\mathcal{C}(\boldsymbol{u}^{n+1} - \boldsymbol{u}^{n}; \boldsymbol{u}^{n+1} - \boldsymbol{u}^{n}, \boldsymbol{v}_h) \\
&\quad - [\mathcal{C}(\widetilde{\boldsymbol{u}}^{n+\frac{1}{2}}; \boldsymbol{u}^{n+\frac{1}{2}}, \boldsymbol{v}_h) - \mathcal{C}_h(\widetilde{\boldsymbol{u}}^{n+\frac{1}{2}}; \boldsymbol{u}^{n+\frac{1}{2}}, \boldsymbol{v}_h)] - \mathcal{C}_h(\widetilde{\boldsymbol{u}}^{n+\frac{1}{2}} - \widetilde{\boldsymbol{u}}_h^{n+\frac{1}{2}}; \boldsymbol{u}^{n+\frac{1}{2}}, \boldsymbol{v}_h) \\
&\quad - \mathcal{C}_h(\widetilde{\boldsymbol{u}}_h^{n+\frac{1}{2}}; \boldsymbol{u}^{n+\frac{1}{2}} - \boldsymbol{u}_h^{n+\frac{1}{2}}, \boldsymbol{v}_h) + \frac{1}{2}\mathcal{D}(\boldsymbol{v}_h; \boldsymbol{d}^{n+1} - 2\boldsymbol{d}^{n} + \boldsymbol{d}^{n-1}, \boldsymbol{\omega}^{n+\frac{1}{2}}) \\
&\quad + \frac{1}{4}\mathcal{D}(\boldsymbol{v}_h; \boldsymbol{d}^{n+1} - \boldsymbol{d}^{n}, \boldsymbol{\omega}^{n+1} - \boldsymbol{\omega}^{n}) \\
&\quad + [\mathcal{D}(\boldsymbol{v}_h; \widetilde{\boldsymbol{d}}^{n+\frac{1}{2}}, \boldsymbol{\omega}^{n+\frac{1}{2}}) - \mathcal{D}_h(\boldsymbol{v}_h; \widetilde{\boldsymbol{d}}^{n+\frac{1}{2}}, \boldsymbol{\omega}^{n+\frac{1}{2}})] \\
&\quad + \mathcal{D}_h(\boldsymbol{v}_h; \widetilde{\boldsymbol{d}}^{n+\frac{1}{2}} - \widetilde{\boldsymbol{d}}_h^{n+\frac{1}{2}}, \boldsymbol{\omega}^{n+\frac{1}{2}}) + \mathcal{D}_h(\boldsymbol{v}_h; \widetilde{\boldsymbol{d}}_h^{n+\frac{1}{2}}, \boldsymbol{\omega}_h^{n+\frac{1}{2}} - \boldsymbol{\omega}^{n+\frac{1}{2}}).
\end{aligned}
\tag{4.36}
$$

Using the Cauchy-Schwarz inequality, Poincaré-Friedrichs inequality, (3.9)–(3.10), Lemma 3.5, Lemma 3.6 and Lemma 3.7, we can get

$$
\begin{aligned}
&\mathcal{B}(\boldsymbol{v}_h, e_p^{n+\frac{1}{2}}) \\
&\lesssim h^{k+1}\|\boldsymbol{v}_h\|_0 + \|\delta_t e_{\boldsymbol{u}}^{n+1}\|_0\|\boldsymbol{v}_h\|_0 + h^k|\boldsymbol{v}_h|_1 + |e_{\boldsymbol{u}}^{n+\frac{1}{2}}|_1|\boldsymbol{v}_h|_1 + \tau^2|\boldsymbol{v}_h|_1 \\
&+ h^k(\|\widetilde{\boldsymbol{u}}^{n+\frac{1}{2}}\|_{k+1}(\|\boldsymbol{u}^{n+\frac{1}{2}}\|_{k+1} + \|\boldsymbol{u}^{n+\frac{1}{2}}\|_1) \\
&+ \|\boldsymbol{u}^{n+\frac{1}{2}}\|_{k+1}(\|\widetilde{\boldsymbol{u}}^{n+\frac{1}{2}}\|_k + \|\widetilde{\boldsymbol{u}}^{n+\frac{1}{2}}\|_1))|\boldsymbol{v}_h|_1 \\
&+ h^k(\|\boldsymbol{\omega}^{n+\frac{1}{2}} \cdot \nabla\widetilde{\boldsymbol{d}}^{n+\frac{1}{2}}\|_k + \|\boldsymbol{\omega}^{n+\frac{1}{2}}\|_{\boldsymbol{L}^\infty(\Omega)}\|\widetilde{\boldsymbol{d}}^{n+\frac{1}{2}}\|_{k+1} \\
&+ \|\widetilde{\boldsymbol{d}}^{n+\frac{1}{2}}\|_{\boldsymbol{W}^{1,\infty}(\Omega)}\|\boldsymbol{\omega}^{n+\frac{1}{2}}\|_k)\|\boldsymbol{v}_h\|_0 \\
&+ (\|e_{\boldsymbol{u}}^{n+1}\|_0 + \|e_{\boldsymbol{u}}^n\|_0 + \|e_{\boldsymbol{u}}^{n-1}\|_0)|\boldsymbol{v}_h|_1 + (|e_{\boldsymbol{d}}^n|_1 + |e_{\boldsymbol{d}}^{n-1}|_1)|\boldsymbol{v}_h|_1 + \|e_{\boldsymbol{\omega}}^{n+\frac{1}{2}}\|_0\|\boldsymbol{v}_h\|_0 \\
&\lesssim (\tau^2 + h^k + h^{k+1} + |e_{\boldsymbol{u}}^{n+\frac{1}{2}}|_1 + \|e_{\boldsymbol{\omega}}^{n+\frac{1}{2}}\|_0 + \|\delta_t e_{\boldsymbol{u}}^{n+1}\|_0)|\boldsymbol{v}_h|_1.
\end{aligned}
\tag{4.37}
$$

Considering the discrete inf-sup condition in Lemma 3.4, we have

$$
\begin{aligned}
\|e_p^{n+\frac{1}{2}}\|_0 &\lesssim \sup_{\boldsymbol{v}_h \in \boldsymbol{V}_h, \boldsymbol{v}_h \neq \boldsymbol{0}} \frac{\mathcal{B}(\boldsymbol{v}_h, e_p^{n+\frac{1}{2}})}{|\boldsymbol{v}_h|_1} \\
&\lesssim \tau^2 + h^k + |e_{\boldsymbol{u}}^{n+\frac{1}{2}}|_1 + \|e_{\boldsymbol{\omega}}^{n+\frac{1}{2}}\|_0 + \|\delta_t e_{\boldsymbol{u}}^{n+1}\|_0.
\end{aligned}
\tag{4.38}
$$

From Theorem 4.1, (4.35) and (4.38), we obtain

$$
\begin{aligned}
\tau\sum_{n=0}^{m}\|e_p^{n+\frac{1}{2}}\|_0^2 &\lesssim \tau\sum_{n=0}^{m}(\tau^4 + h^{2k}) + \tau\sum_{n=0}^{m}(|e_{\boldsymbol{u}}^{n+\frac{1}{2}}|_1^2 + \|e_{\boldsymbol{\omega}}^{n+\frac{1}{2}}\|_0^2 + \|\delta_t e_{\boldsymbol{u}}^{n+1}\|_0^2) \\
&\lesssim \tau^4 + h^{2k}.
\end{aligned}
\tag{4.39}
$$

The proof is finished.

5 Numerical experiments

In this section, we will present the numerical experiments to validate the theories derived in the previous section and demonstrate the accuracy and energy stability of the proposed numerical scheme. Further, we will apply the developed scheme to simulate the defect dynamics in flows of liquid crystals. In the present work, a family of polygonal meshes are generated by PolyMesher [39] and the codes are implemented by using the software package FreeFem++, see [22].

5.1 Accuracy and stability test

We first test the accuracy and stability of the proposed algorithm. The polynomial degree of accuracy for the numerical tests is $k = 2$. The computational domain is set as $\Omega := (0, 1)^2$. And we set the initial conditions as follows

$$\boldsymbol{d}^0 = (\sin(a), \cos(a))^t, \ a := 2.0\pi(\cos(x) - \sin(y)), \ \boldsymbol{u}^0 = \mathbf{0}, \ p^0 = 0,$$

and set the parameters as $\nu = 0.1$, $\lambda = \gamma = 1$ and $\varepsilon = 10^{-3}$.

For the disk Ω we consider the sequences of polygonal meshes:

- Sequence of the distorted quadrilateral meshes with $h = 1/5, 1/10, 1/20, 1/40, 1/80$,
- Sequence of the Voronoi meshes with $h = 1/5, 1/10, 1/20, 1/40, 1/80$.

Figure 1 displays an example of the adopted meshes. Since we do not have the exact solution of the given problem, to verify the optimal convergence rates, the reference solution is taken as the numerical solution, where the time step size τ is required to satisfy $\tau = \mathcal{O}(h^2)$.

To verify the convergence rates of spatial errors, we fix the time step size $\tau = 1.2 \times 10^{-4}$ and choosing the decreasing mesh sizes. Figure 2 shows the errors and convergence rates of the velocity, orientation vector and pressure fields by using the two polygonal meshes. We can see that the obtained spatial convergence rate of both are $\mathcal{O}(h^2)$, which is consistent with our theoretical prediction.

To confirm the temporal error, we take the reference solution corresponding to $\tau = 1 \times 10^{-4}$ and $h = 1/80$. In Fig. 3, we show the L^2 errors of the velocity, orientation vector and pressure fields at $t = 0.5$ by using the two polygonal meshes, where we choose the decreasing temporal step sizes. It can be seen that the convergence rate are both $\mathcal{O}(\tau^2)$ for all variables, which is consistent with the theoretical predictions given in the previous section.

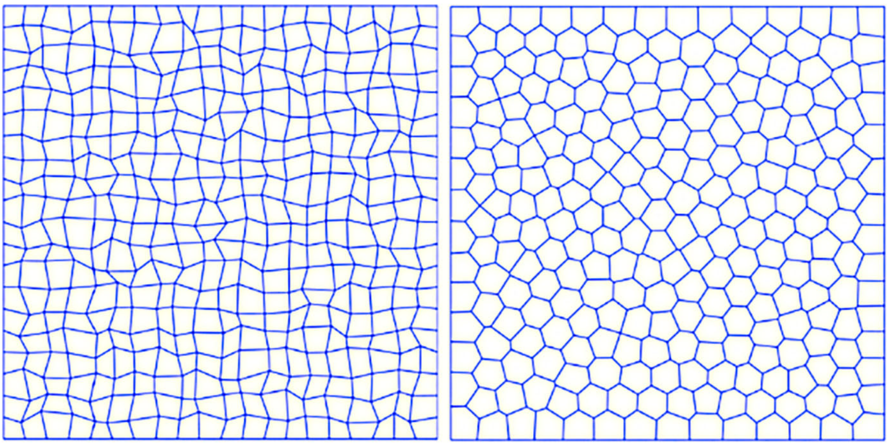

Fig. 1 Sample meshes: The distorted quadrilateral meshes (left) and Voronoi meshes (right)

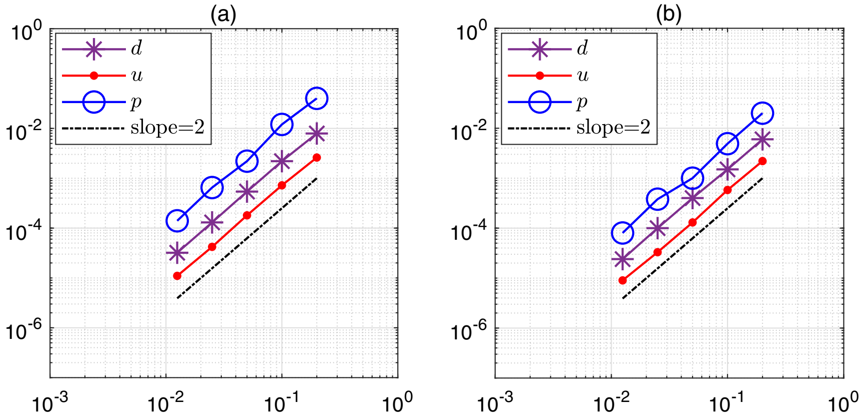

Fig. 2 Convergence tests by refinement computed by using (a) the distorted quadrilateral meshes and (b) Voronoi meshes in spatial direction

In Fig. 4, we plot the time evolution curve of the total energy to test the energy stability of the proposed scheme. It can be seen that the obtained energy evolution curves always show monotonic decays, which means that our scheme is energy stable.

To compare the approaches between the FEM and VEM, the domain Ω is partitioned with a sequence of standard triangular meshes with diameter $h = 1/4, 1/8, 1/16, 1/32$. Table 1 presents the numerical results when $t = 0.6$. It is worth noting that, the value $|\boldsymbol{d}|$ is close to 1 in the theoretical analysis, by contrast, the proposed VEM computes the orientation vector $\boldsymbol{d}$ with higher accuracy than FEM as depicted in Table 1.

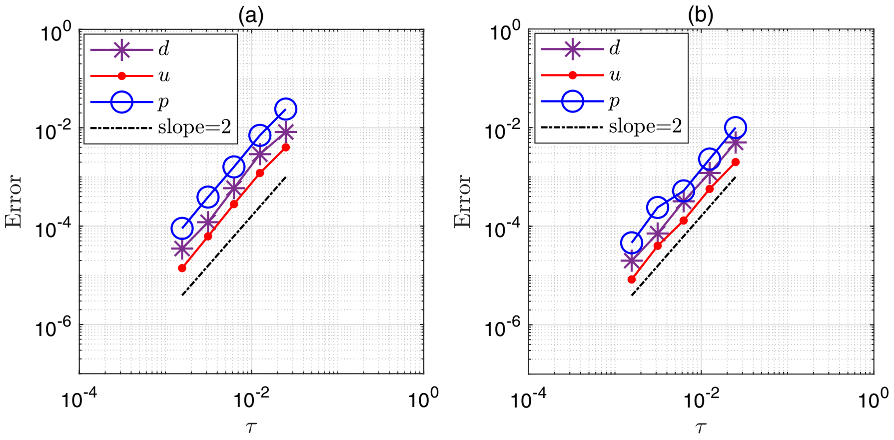

Fig. 3 Convergence tests by refinement computed by using (a) the distorted quadrilateral meshesand (b) Voronoi meshes in temporal direction

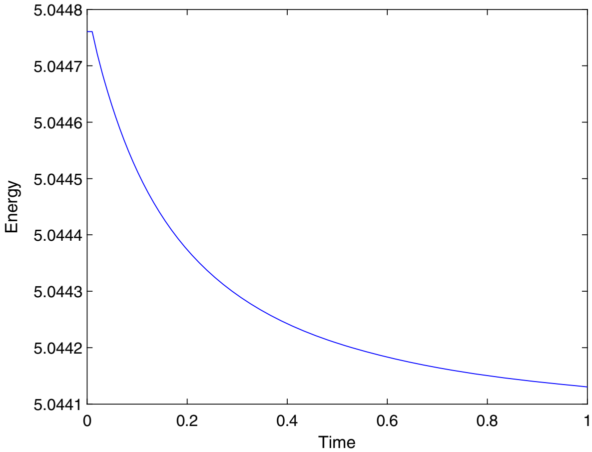

Fig. 4 Time evolution of the total energy functional $\mathcal{E}_h$

5.2 Dynamics of defects in liquid crystals

In this subsection, we study the defect dynamics in flows of liquid crystals numerically using the implemented VEM.

We consider the computational domain as $\Omega := [0, 1]\times[0, 1]$. The initial conditions are set as follows:

$$\boldsymbol{d}^0 = (\cos(a), \sin(a)),\ \ a := \tfrac{1}{2}\arctan 2(y, x),$$
$$\boldsymbol{u}^0 = (0.1 \times \cos 2(\theta_0 + \arctan(\tfrac{y}{x-1})), 0.1 \times \sin 2(\theta_0 + \arctan(\tfrac{y}{x-1}))),\ \ p^0 = 0,$$

where θ_0 denotes the relative orientation, and the homogeneous Dirichlet boundary conditions are enforced over $\boldsymbol{u}$ and $\boldsymbol{d}$, respectively. The parameters are chosen as $\nu = 0.1, \lambda = \gamma = 1, \varepsilon = 10^{-3}, \tau = 0.005, h = 1/100$.

When the orientation of the liquid crystal on the $x - y$ plane is isotropic and dominant, we refer to this state as the defect, which may include an isotropic state or an oblate state. Figures 5 and 6 show the liquid crystal director orientation, flow velocity field and corresponding velocity magnitude with the relative orientation $\theta_0 = 0$ and $\theta_0 = 0.5$, respectively. We observe that the initially imposed $+1$ defect is not stable so that it splits into two $+\frac{1}{2}$ defects over time subject to the Dirichlet boundary condition.

Table 1 Maximal of $(|\mathbf{d}_h^n| - 1)$ (DoFs values) computed by using FEM and VEM

$1/h$	4	8	16	32
FEM	3.78e−01	3.64e−01	2.99e−01	2.05e−01
VEM	6.45e−07	5.84e−07	4.37e−07	3.96e−07

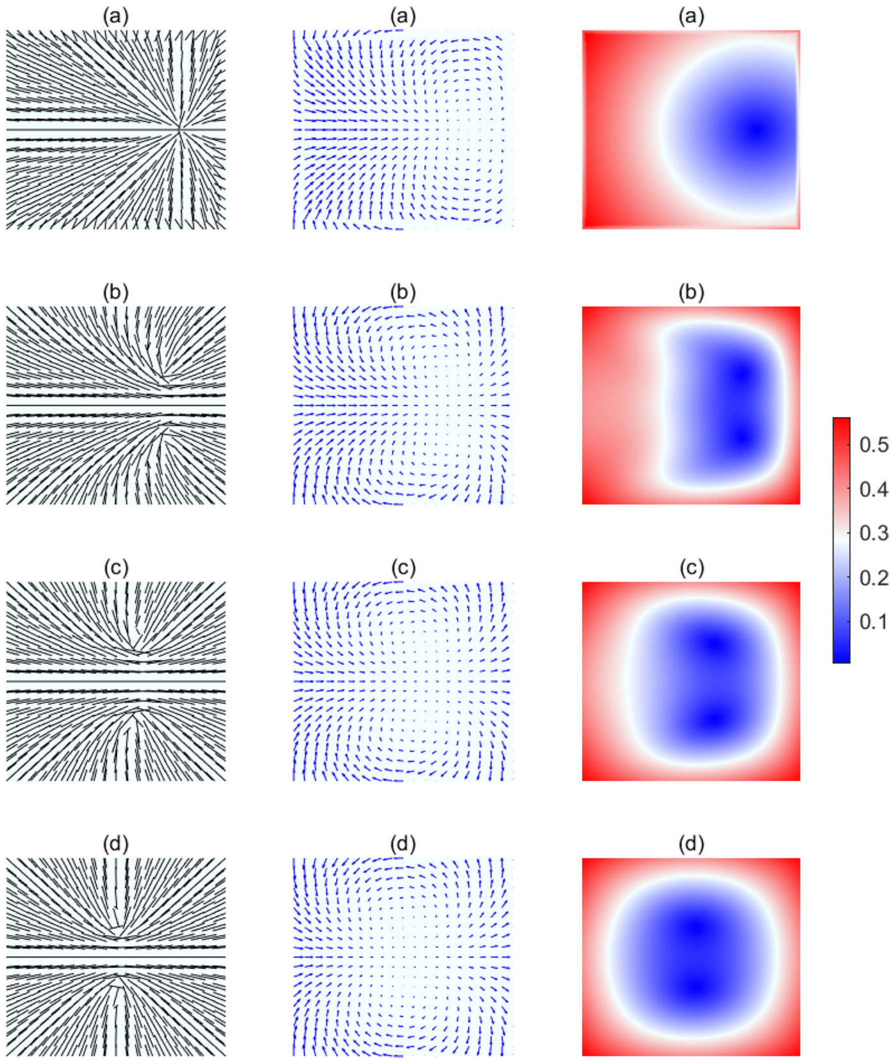

Fig. 5 Defect dynamics. This figure shows that an initially unstable $+1$ defect splits into two $+\frac{1}{2}$ defects and the two defects remain stable subject to the Dirichlet boundary condition with $\theta_0 = 0$. The left column shows the liquid crystal director orientation on the $x - y$ plane at times: (a)-(d) are for $t = 0.005,\ 0.05,\ 0.1,\ 0.2$. The middle column shows the flow velocity field. The right column shows the corresponding magnitude of velocity

The two $+\frac{1}{2}$ defects move away from each other slowly and then evolves to reach a steady state, inducing a weak velocity field shown in the middle column of Figs. 5 and 6, where two pairs of vortices are shown existing around the defects, but the patterns of the defects and vortices are changed with the different relative orientation.

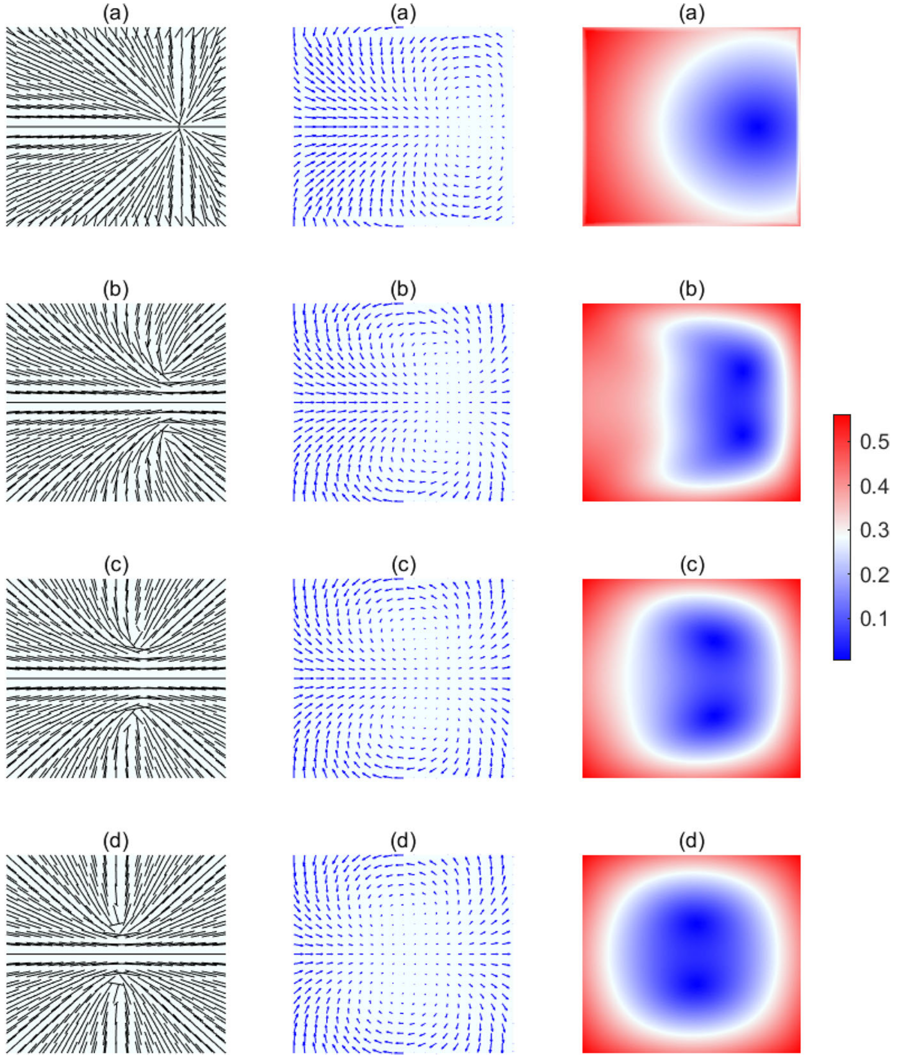

Fig. 6 Defect dynamics. This figure shows that an initially unstable $+1$ defect splits into two $+\frac{1}{2}$ defects and the two defects remain stable subject to the Dirichlet boundary condition with $\theta_0 = 0.5$. The left column shows the liquid crystal director orientation on the $x - y$ plane at times: (a)-(d) are for $t = 0.005,\ 0.05,\ 0.1,\ 0.2$. The middle column shows the flow velocity field. The right column shows the corresponding magnitude of velocity

6 Concluding remarks

In this paper, we consider the virtual element approximations of a hydrodynamics system for modeling the nematic liquid crystal flows, which is obtained by using the L^2-gradient flow approach. In discrete level, we develop an unconditionally energy stable fully discrete numerical scheme, achieved by the convex splitting technique to deal with the strong nonlinearity in the penalty function, and use the extrapolated Crank-Nicolson (C-N) time-stepping scheme for nonlinear terms and coupling terms. In addition, the unique solvability in the discrete level is derived, and we strictly prove the optimal error estimates of the proposed scheme. We also conduct several numerical experiments to demonstrate the accuracy and stability of the scheme, and the numerical results also illustrate the good performance of the proposed scheme. Furthermore, the numerical scheme has been used to simulate the dynamics of defects in liquid crystals.

Acknowledgements The authors are grateful to the reviewers for carefully reading this paper and for their comments and suggestions which have improved the paper.

Funding Guang-an Zou is supported by China Postdoctoral Science Foundation (No. 2019M662476), and the Key Scientific Research Projects of Colleges and Universities in Henan Province, China (23A110006). Jian Li is supported by NSF of China (No. 11771259), Shaanxi Provincial Joint Laboratory of Artificial Intelligence (No. 2022JC-SYS-05), Innovative team project of Shaanxi Provincial Department of Education (No. 21JP013) and 2022 Shaanxi Provincial Social Science Fund Annual Project (No. 2022D332).

Declarations

Conflict of interest The authors declare no competing interests.

References

1. Adak, D., Natarajan, E., Kumar, S.: Convergence analysis of virtual element methods for semilinear parabolic problems on polygonal meshes. Numer. Methods Partial Differ. Equ. **35**, 222–245 (2018)
2. Ahmad, B., Alsaedi, A., Brezzi, F., Marini, L.D., Russo, A.: Equivalent projectors for virtual element methods. Comput. Math. Appl. **66**, 376–391 (2013)
3. Akbas, M., Kaya, S., Rebholz, L.: On the stability at all times of linearly extrapolated BDF2 timestepping for multiphysics incompressible flow problems. Numer. Methods Partial Differ. Equ. **33**, 999–1017 (2017)
4. Akrivis, G.D., Dougalis, V.A., Karakashian, O.A.: On fully discrete Galerkin methods of second-order temporal accuracy for the nonlinear Schrödinger equation. Numer. Math. **59**, 31–53 (1991)
5. Becker, R., Feng, X., Prohl, A.: Finite element approximations of the Ericksen-Leslie model for nematic liquid crystal flow. SIAM J. Numer. Anal. **46**, 1704–1731 (2008)
6. Basic principles of virtual element methods: Beirão da Veiga, L., Brezzi, F., Cangiani, A., Manzini, G., Marini, L.D., Russo, A. Math. Models Methods Appl. Sci. **23**, 199–214 (2013)
7. Beirão da Veiga, L.., Brezzi, F.., Marini, L..D..: Virtual elements for linear elasticity problems. SIAM J. Numer. Anal. **51**, 794–812 (2013)
8. Beirão da Veiga, L.., Brezzi, F.., Marini, L..D.., Russo, A..: The Hitchhiker guide to the virtual element method. Math. Models Methods Appl. Sci. **24**, 1541–1573 (2014)
9. Beirão da Veiga, L., Lovadina, C., Mora, D.: A virtual element method for elastic and inelastic problems on polytope meshes. Comput. Methods Appl. Mech. Eng. **295**, 327–346, (2015)
10. Beirão da Veiga, L., Brezzi, F., Russo, A.: Virtual element method for general second-order elliptic problems on polygonal meshes. Math. Models Methods Appl. Sci. **26**, 729–750, (2016)
11. Beirão da Veiga, L., Lovadina, C., Russo, A.: Stability analysis for the virtual element method. Math. Models Methods Appl. Sci. **27**, 2557–2594 (2017)
12. Beirão da Veiga, L., Lovadina, C., Vacca, G.: Divergence free virtual elements for the Stokes problem on polygonal meshes. ESAIM:M2AN **51**, 509–535, (2017)
13. Beirão da Veiga, L., Lovadina, C., Vacca, G.: Virtual elements for the Navier-Stokes problem on polygonal meshes. SIAM J. Numer. Anal. **56**, 1210–1242, (2018)
14. Beirão da Veiga, L., Russo, A., Vacca, G.: The virtual element method with curved edges. ESAIM:M2AN, **53**, 375–404, (2019)

15. Brezis, H.: The interplay between analysis and topology in some nonlinear PDE problems. Bull. Am. Math. Soc. **40**, 179–202 (2003)
16. Cangiani, A., Gyrya, V., Manzini, G.: The nonconforming virtual element method for the Stokes equations. SIAM J. Numer. Anal. **54**, 3411–3435 (2016)
17. Cangiani, A., Manzini, G., Sutton, O.J.: Conforming and nonconforming virtual element methods for elliptic problems. IMA J. Numer. Anal. **27**, 1317–1354 (2017)
18. Erickson, J.L.: Continuum theory of nematic liquid crystals. Res. Mechanica **21**, 381–392 (1987)
19. Gain, A.L., Talischi, C., Paulino, G.H.: On the virtual element method for three-dimensional linear elasticity problems on arbitrary polyhedral meshes. Comput. Methods Appl. Mech. Eng. **282**, 132–160 (2014)
20. Gatica, G.N., Munar, M., Sequeira, F.A.: A mixed virtual element method for the Navier-Stokes equations. Math. Models Methods Appl. Sci. **28**, 2719–2762 (2018)
21. Guillén-González, F.M., Gutiérrez-Santacreu, J.V.: A linear mixed finite element scheme for a nematic Ericksen-Leslie liquid crystal model. ESAIM:M2AN, **47**, 1433–1464, (2013)
22. Hecht, F., Pironneau, O., Ohtsuka, K.: FreeFEM++, http://www.freefem.org/
23. Leslie, F.M.: Some constitutive equations for anisotropic fluids. Q. J. Mech. Appl. Math. **19**, 357–370 (1966)
24. Leslie, F.M.: Theory of flow phenomena in liquid crystals. Advances in Liquid Crystals, Academic Press, New York **4**, 1–81 (1979)
25. Li, M., Zhao, J., Wang, N., Chen, S.: Conforming and nonconforming conservative virtual element methods for nonlinear Schrödinger equation: A unified framework. Comput. Methods Appl. Mech. Eng. **380**, 113793 (2021)
26. Lin, F.: Nonlinear theory of defects in nematic liquid crystals phase transition and flow phenomena. Commun. Pure Appl. Math. **42**, 789–814 (1989)
27. Lin, F., Liu, C.: Nonparabolic dissipative systems modeling the flow of liquid crystals. Commun. Pure Appl. Math. **48**, 501–537 (1995)
28. Lin, F., Liu, C.: Existence of solutions for the Ericksen-Leslie system. Arch. Ration. Mech. Anal. **154**, 135–156 (2000)
29. Lin, P., Liu, C.: Simulations of singularity dynamics in liquid crystal flows: A C^0 finite element approach. J. Comput. Phys. **37**, 348–362 (2006)
30. Liu, C., Walkington, N.J.: Approximation of liquid crystal flows. SIAM J. Numer. Anal. **37**, 725–741 (2000)
31. Liu, C., Walkington, N.J.: Mixed methods for the approximation of liquid crystal flows. ESAIM:M2AN **37**, 205–222, (2002)
32. Liu, C., Shen, J., Yang, X.: Dynamics of defect motion in nematic liquid crystal flow: modeling and numerical simulation. Commun. Comput. Phys. **2**, 1184–1198 (2007)
33. Liu, X., Li, J., Chen, Z.: A nonconforming virtual element method for the Stokes problem on general meshes. Comput. Methods Appl. Mech. Eng. **320**, 694–711 (2017)
34. Liu, X., Chen, Z.:s The nonconforming virtual element method for the Navier-Stokes equations. Adv. Comput. Math. **45**, 51–74, (2019)
35. Liu, X., He, Z., Chen, Z.: A fully discrete virtual element scheme for the Cahn-Hilliard equation in mixed form. Comput. Phys. Commun. **246**, 106870 (2020)
36. Liu, X., Nie, Y.: A modified nonconforming virtual element with BDM-like reconstruction for the Navier-Stokes equations. Appl. Numer. Math. **167**, 375–388 (2021)
37. Rey, A.D., Denn, M.M.: Dynamical phenomena in liquid-crystalline materials. Annu. Rev. Fluid Mech. **34**, 233–266 (2002)
38. Rivière, B.: Discontinuous Galerkin Methods for Solving Elliptic and Parabolic Equations: Theory and Implementation. SIAM, (2008)
39. Talischi, C., Paulino, G.H., Pereira, A., Menezes, I.F.M.: Polymesher: a general-purpose mesh generator for polygonal elements written in Matlab. Struct. Multidiscip. Optim. **45**(3), 309–328 (2012)
40. Tang, Y., Zou, G., Li, J.: Unconditionally energy-stable finite element scheme for the chemotaxis-fluid system. J. Sci. Comput. **95**, 1, (2023) https://doi.org/10.1007/s10915-023-02118-4
41. Vacca, G., Beirão da Veiga, L.: Virtual element methods for parabolic problems on polygonal meshes. Numer. Methods Partial Differ. Equ. **31**, 2110–2134, (2015)
42. Wang, C., Wang, J., Xia, Z., Xu, L.: Optimal error estimates of a Crank-Nicolson finite element projection method for magnetohydrodynamic equations. ESAIM:M2AN, **56**, 767–789, (2022)

43. Yang, X., Forest, M.G., Liu, C., Shen, J.: Shear cell rupture of nematic liquid crystal droplets in viscous fluids. J. Non-Newtonian Fluid Mech. **166**, 487–499 (2011)
44. Zhang, X., Feng, M.: A projection-based stabilized virtual element method for the unsteady incompressible Brinkman equations. Appl. Math. Comput. **408**, 126325 (2021)
45. Zhao, J., Yang, X., Li, J., Wang, Q.: Energy stable numerical schemes for a hydrodynamic model of nematic liquid crystals. SIAM J. Sci. Comput. **38**, A3264–A3290 (2016)
46. Zhao, J., Yang, X., Shen, J., Wang, Q.: A decoupled energy stable scheme for a hydrodynamic phase-field model of mixtures of nematic liquid crystals and viscous fluids. J. Comput. Phys. **305**, 539–556 (2016)
47. Zhao, J., Wang, Q.: Semi-discrete energy-stable schemes for a tensor-based hydrodynamic model of nematic liquid crystal flows. J. Sci. Comput. **68**, 1241–1266 (2016)
48. Zou, G., Wang, B., Yang, X.: A fully-decoupled discontinuous Galerkin approximation of the Cahn-Hilliard-Brinkman-Ohta-Kawasaki tumor growth model. ESAIM:M2AN **56**, 2141–2180, (2022)
49. Zou, G., Li, Z., Yang, X.: Fully discrete discontinuous Galerkin numerical scheme with second-order temporal accuracy for the hydrodynamically coupled lipid vesicle model. J. Sci. Comput. **95**, 5 (2023). https://doi.org/10.1007/s10915-023-02129-1